Master's thesis

NTNU
Norwegian University of Science and Technology

Fredrik Schwencke

Development of Load Distribution Concept for Cross Country Skis

Master's thesis in Mechanical Engineering
Supervisor: Knut Einar Aasland
June 2019

NTNU
Norwegian University of
Science and Technology

Fredrik Schwencke

Development of Load Distribution Concept for Cross Country Skis

Master's thesis in Mechanical Engineering
Supervisor: Knut Einar Aasland
June 2019

Norwegian University of Science and Technology

NTNU
Norwegian University of
Science and Technology

Abstract

Having top performing skis is critical for a world class cross country skier to be able to fight for the medals in the Olympics, World Championships and other major races. Throughout the last decade, measuring ski properties has become increasingly important. Today, the Norwegian Olympic Foundation is in charge of measuring skis and technology development for the Norwegian national team. The Norwegian Olympic Foundation use pressure mats to measure pressure distribution, which is considered time consuming and costly if the accuracy of the measurements are to be satisfying.

Pressure distribution is important for a skis performance as it has great influence on the friction between the snow and the base of the ski. The aim of this thesis is, therefore, to develop a concept that simplifies and more accurately measures pressure distribution over the length of the ski. The concept developed relies on a load sensor sliding under the length of the ski while the ski is loaded with a set point load in the area around the binding.

The concept developed is based on the load sensor elevating the ski from the surface to get a proper reading. This results in a more concentrated load on the load sensor. With the use of pressure mats, on the other hand, the full contact area of the ski is naturally distributed on the pressure mats, which results in lower pressure compared to the concept developed. Another difference is that the developed concept is dependant on a spring in the loading mechanism to keep the applied load stable. For the pressure mats, a static load is used as no elevation of the ski is necessary.

Test results shows continuous load curves with one peak on the front end and one peak on the back end of the ski. The pressure mats, on the other hand, show several peaks and lows on both ends of the ski. There are clear similarities between the developed concept and the pressure mats when it comes to the location of the peak pressure and how these peaks move with increasing applied load.

The results from the thesis show that the concept has potential for further development as time usage and resolution can be improved compared to the pressure mats used by the Norwegian Olympic Foundation. Since the results cannot be directly compared to the results from the pressure mats, it is necessary to establish a base of measurements to find potential relationships between snow conditions and skis. Further testing is crucial, but it is expected that the concept can contribute to improved understanding of the pressure distribution of a ski.

Abstrakt

Å tilstrebe best mulige ski er kritisk for langrennsløpere hvis man skal ha mulighet til å kjempe om de gjeveste medaljene i de olympiske leker, verdemsmesterskap, eller andre store skirenn. Gjennom de siste tiårene har måling av skiegenskaper blitt stadig viktigere. I dag er det i all hovedsak Olympiatoppen som står for måling av ski og teknologiutvikling for det norske landslaget. Olympiatoppen bruker trykkmatter til å måle trykkfordeling mot underlaget, noe de anser som tidkrevende og kostbar teknologi dersom målenøyaktigheten skal være tilfredsstillende.

Trykkfordeling er viktig for skiens ytelse fordi den påvirker friksjonen mellom snøen og sålen til skien. Målet med denne masteroppgaven er derfor å utvikle et konsept som enklere og mer nøyaktig måler trykkfordeling over skiens lengderetning. Konseptet som er utviklet baserer seg på en lastsensor som føres under skien i skiens lengderetning mens skien er lastet med en bestemt punktlast i området rundt bindingen.

Konseptet som er utviklet baserer seg på at lastsensoren hever skien fra underlaget for at den skal kunne lese av lasten. Dette gjør at lasten blir mer konsentrert på lastsensoren. Ved bruk av trykkmatter derimot, ligger hele skiens kontaktflate fordelt naturlig på trykkmattene, noe som gjør at det måles lavere trykk enn for konseptet. En annen forskjell er at konseptet er avhengig av å bruke en fjær i lastmekanismen for å holde den påførte lasten stabil. For trykkmattene brukes det en statisk last fordi skien ikke må heves.

Testresultater fra konseptet viser sammenhengende lastkurver med ett topppunkt på fremski og ett på bakski, i motsetning til trykkmattene som viser flere topp- og bunnpunkter. Det er klare likhetstrekk mellom trykkmattene og konseptet med tanke på lokasjonen av det høyeste trykket og hvordan dette trykket beveger seg med økende last.

Resultatene viser at konseptet har potensiale til videreutvikling da tidsbruk og nøyaktighet vil kunne forbedres i forhold til Olympiatoppens trykkmatter. Siden resultatene ikke kan sammenlignes direkte med resultatene fra trykkmattene er det nødvendig å etablere en base med målinger for å finne potensielle sammenhenger mellom snøforhold og ski. Ytterligere testing er derfor avgjørende, men det er forventetet at teknologien kan bistå til å bedre forståelsen av skiens trykkfordelingsegenskaper.

Preface

This master thesis was written during the spring semester of 2019 and concludes my degree in Mechanical Engineering at the Norwegian University of Science and Technology. The thesis was carried out for the Norwegian Olympic Foundation. Dr. Felix Breitschädel presented several different ideas on technology that could be developed to benefit their project towards the upcoming Olympic Games. Together we agreed on a suitable and interesting project. Dr. Breitschädel was of solid help with his expertise within cross country skiing technology.

It is assumed that the reader has basic knowledge on mechanics and mechatronics.

Acknowledgement

I would like to thank supervisor Knut Einar Aasland who helped me throughout the semester and always was available for questions. I would also like to thank Felix Breitschädel who, with his relevant knowledge, helped me in the right direction and was available whenever I needed to ask questions or discuss the thesis. I would also like to thank Dr. Breitschädel for the two opportunities I had to join The Norwegian Olympic Foundation and the Norwegian wax team to learn more about skis and relevant technology. Lastly, I would like to thank Sindre Tungesvik who helped with the initial testing to assure the best possible results.

Contents

List of Figures

List of Tables

List of Symbols

$\Delta\frac{l}{l}$	fractional change in length
$\Delta\frac{R}{R}$	fractional change in gauge resistance because of strain
μ	coefficient of friction
ω	angle of which force is applied, Nm
$\Phi(x)$	total nominal pressure distribution function for a ski
$\Phi_1(x)$	total nominal pressure distribution function for the forebody of a ski
$\Phi_2(x)$	total nominal pressure distribution function for the backbody of a ski
ρ	sample resistivity, $\Omega * m$
A_0	cross-sectional area, m^2
D	distance, m
EI	flexural stiffness at the position x
F	force, N
F_F	friction force
F_N	normal force
$h''(x)$	the second derivative of the deformation at the position x
l_0	length, m
l_1	half nominal contact length on the forebody of the ski (l_1-$l_f/2$), m
l_2	half nominal contact length on the forebody of the ski (l_2-$l_b/2$), m
l_b	nominal contact length on the back end of the ski, m
l_f	nominal contact length on the front end of the ski, m
m	acceleration, $\frac{m}{s^2}$
m	mass, kg
$M(x)$	bending moment at the position x

N normal load on the ski from skier, N

R_0 sample resistance, Ω

W work, Nm

w_b nominal contact width on the back end of the ski, m

w_f nominal contact width on the front end of the ski, m

1 Introduction

1.1 Background

Having top performing skis is critical for world class skiers. To find the best possible skis, it is necessary to measure and find ski properties that suit the skier and the conditions optimally. Norway is one of the pioneers within cross country skiing and significant time and resources is spent on development and testing.

For maximum gliding capabilities, the pressure distribution on the snow is crucial. Even though this property is important, only the fundamental characteristics are known, not the precise relationship. It is desirable to find this relationship. Different ski manufacturers typically have their own setup measuring important ski properties. This is also true for the biggest nations within cross country skiing. The Norwegian Olympic Foundation (hereafter OLT), known as "Olympiatoppen" in Norway, has a setup using pressure mats. This setup gives usable results on pressure distribution, but there are several limitations this setup possesses that are desirable to improve/eliminate.

This master thesis is aiming to develop a load distribution concept that potentially eliminates the drawbacks of the current setup. Dynamic loading and angled skis are not taken into consideration. A simplification, measuring a loaded static ski on a plane surface is considered sufficient at this point.

The master thesis is written in cooperation with Olympiatoppen. OLT is responsible for the development in Norwegian elite sports and has the full responsibility for the Norwegian results. OLT is also responsible for the Norwegian participation in the Olympic and Paralympic games [20].

OLTs ultimate goal is to be able to measure the important properties of a new pair of skis and based on the results, decide which weight and which conditions this pair of skis will perform best in.

1.2 Objectives

The main objective of this Master's thesis is to develop and test a pressure distribution concept for cross country skis and compare it to the technology used by OLT today. Additionally, looking into possible new valuable measurements to complement the concept, and thereby achieve a greater understanding of what characterizes a top level ski, is desireable.

1.3 Approach

Thorough testing was performed on a physical concept prototype and then compared to a test performed on the OLT setup. To get a fuller understanding of the potential of the concept, a single ski was tested in many different setups. Thereafter, a ski with different properties was tested to look into the concepts' ability to differentiate between skis.

1.4 Limitations

The greatest limitation of this thesis is that analysis of ski construction and technology is often kept within a company or team because of a competitive market. Therefore, technology that could potentially be useful is not available. Measuring and finding top level skis is by many considered craftsmanship, meaning that technology is often not integrated sufficiently into the phases of testing and finding top skis. Today, some ski properties have not been possible to categorize and compare. This emphasizes the challenge of categorizing skis.

1.5 Outline

- Chapter 2 presents necessary theory for the thesis. This includes the construction and properties of a cross country ski and relevant sensor technology.
- Chapter 3 describes OLTs existing technology and its drawbacks. Other existing technology on the topic is also discussed.
- Chapter 4 describes the methodology used through the master thesis including development and testing of the concept.
- Chapter 5 discusses the developed concept in detail, with its theoretical challenges, construction, use of sensors, developed software, and testing.
- Chapter 6 presents and discusses the results from the testing by looking into advantages and limitations of the concept, and comparing the results to OLTs pressure distribution measurements.
- Chapter 7 concludes the master thesis and discusses recommended further work.

2 Theoretical Background

2.1 Introduction to Cross Country Skiing

Cross country skiing was originally used as a means of transport. Archaeologists believe skis have been used for more than 5000 years, similar to the timeline of the wheel. Skis were originally made out of wood and the poles out of bamboo. From a means of transport, cross country skiing developed into a competitive sport in the 1900s. Cross country ski races has been organized in Norway as far back as the 1840s[21]. In 1974, Thomas Magnusson was the first ever to win a World Championship title on glass fiber skis[22]. In the end of the 1970s, the American Bill Koch introduced the skating technique[23], which is a great part of skiing today.

Today, skiers compete almost every week throughout the winter season in varying events such as sprint races, distance races, and team relays. Throughout the competitive period the Olympic Games has been considered the most prestigious event to win, and still is. The Olympic Games are held every fourth year.

2.1.1 Classic and Skating Technique

There are two main techniques of cross country skiing today, namely classic and skate. Figure 2.1 and 2.2 shows an illustration of classic and skate, respectively. As seen in the figure, the classic technique relies on straight forward motion where the forward motion comes from kick wax under the ski, which sticks to the snow when kicking, in combination with arm power using the poles. The skating technique, on the other hand, relies on pushing the ski in a combination of straight forward and sideways. Skating does not require kick wax and is typically faster than classic skiing.

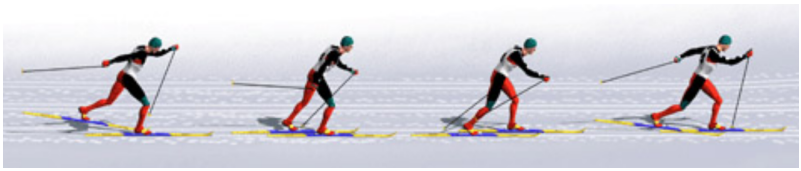

Figure 2.1: Illustration of the classic technique[1]

Figure 2.2: Illustration of the skating technique[1]

2.2 Basics of a Cross Country Ski

To be able to construct a well functioning measuring concept and device, it is crucial to understand the properties of a ski and how it is constructed. The different properties discussed in the following sections are all important for a ski to perform as well as possible. Still, as mentioned, there are different ski manufacturers making skis. This means that a top performing ski from one manufacturer with a certain set of properties would not necessarily be a top performing ski from a different manufacturer with the exact same properties. It is to be noted that a significant amount of the theory describing the properties of the ski is from the project report.

Classic skis are typically 180-210cm long, while skate skis are 160-195cm long, depending on the height of the skier. Classic skis are longer as they are only moving straight forward, as mentioned above. Skate skis are shorter to be able to ski with proper technique without stumbling.

Figure 2.3: Classic skis (top) and skate skis (bottom)[2]

Figure 2.3 shows a pair of top racing skis for the two different techniques, classic and skate. As seen in the figure, the skis are thinner towards the front and back of the ski. The bindings, where the ski boot is attached, is located towards the center of the ski, close to the balance point. Standing up and down on both legs means that the center of mass is approximately 14cm behind the tip of the toe. A racing ski weighs in the range of 900 to 1100 grams, depending on the length and manufacturer of the ski.

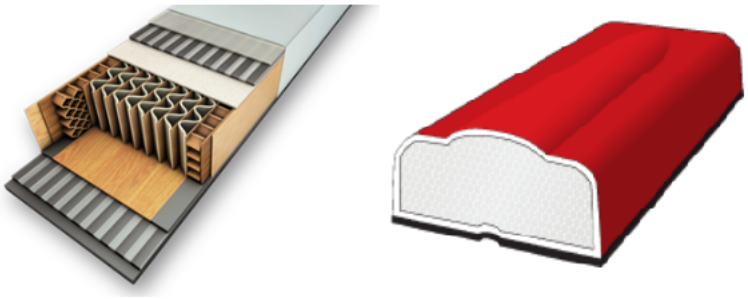

Figure 2.4: Ski core construction - Fischer (left) and Madshus (right) [3][4]

Figure 2.4 shows how the core of a Fischer and Madshus racing-ski is constructed. For the Fischer ski, a ski core "with over 80% air content for extremely light weight combined with highly molecular carbon fibres"[3] creates a light and strong construction. The Madshus core "is a high-performance Rohacell foam core that was developed for extreme strength-to-weight applications in aeronautics that helps provide dampening properties and adds strength and stiffness to the ski without extra weight"[4].

Although different ski manufacturers construct their skis differently, they all aim to provide the skiers the ultimate ski with focus on the same properties. It is crucial to have the right

balance between weight and stability on the snow when constructing a ski. Therefore, an extremely light ski is not preferable. Fischer skis, as the most commonly used brand, are used throughout the rest of the thesis for figures and testing for simplification.

2.3 Ski Properties

2.3.1 Curvature and Camber

The curvature and camber of a cross-country ski varies depending on the conditions it is supposed to be used in. Figure 2.5 shows a simplified comparison between skis used in three different conditions.

Figure 2.5: Ski curvature for cold conditions (blue), medium conditions (red), and warm/soft conditions (yellow)[5]

The ski represented in yellow shows a typical ski curvature for warm conditions when the ski is loaded. For a classic ski, the higher peak curvature, also known as ”pocket”, is present because kick wax for warm conditions is thicker than for cold conditions, hence it needs a higher pocket. Kick wax is used to get grip on the snow when classic skiing. The differences in the curvature of the tip of the ski comes from the fact that warmer conditions means softer snow. For the ski to travel as smooth as possible over the snow it is therefore important that the tip is soft in soft snow. This is relevant for both classic and skate skis. Using a stiff tip in warm conditions will result in the tip digging into the snow when skiing.

As seen in Figure 2.5 the surface contact area for the ski is longer for the colder skis. This is discussed further in section 2.3.3.

2.3.2 Stiffness and Flex

Stiffness is the capacity of a mechanical system to sustain loads without excessive changes to its geometry [24]. Stiffness is important in skiing as it influences the properties of a ski significantly. The stiffness is distributed over the full length of the ski. This distribution varies depending on what type of conditions the ski is intended to be used in.

As mentioned, a ski is thicker towards the center of the length of the ski. Therefore, the stiffness of a ski is significantly higher in this area. Figure 2.6 shows representation of a typical stiffness curve of a ski. As seen, the stiffness has a bell-curved shape with the peak stiffness towards the center of the ski.

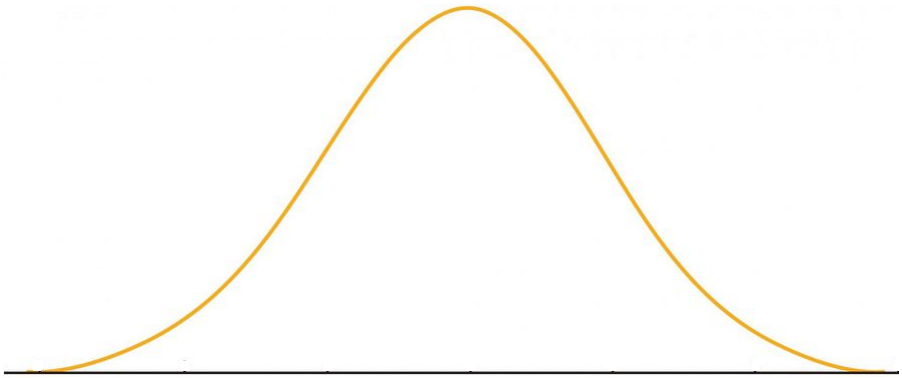

Figure 2.6: Simplified illustration of the stiffness of a ski with the length of the ski on the x-axis and the stiffness on the y-axis

Flex and flex height go hand in hand with stiffness. The flex without any load is similar for skate and classic skis. Typically the skis have a contact zone approximately ten centimeters behind the tip and in front of the tail of the ski, both approximately 5cm long. This flex is a result of how the ski was originally made.

As discussed earlier, classic skis have kick wax on them to ensure the possibility of forward motion on uphills. To be able to get grip on the snow, it is necessary to push the kick wax in contact with the snow. Still, to assure maximal glide, it is crucial that the kick wax is not in contact with the snow on the downhills. Figure 2.7 shows a typical flex height of a classic ski. The zero on the x-axis represents where the ski boot is attached to the binding. As seen in the figure, the maximum flex height is approximately 1mm at half weight. Kick wax is typically applied from flex height of 0.1mm at half weight to right under the heel of the athlete. A ski is typically marked at 0.1, 0.2, and 0.3mm flex heights to allow for kick wax of different thickness to be applied. The length and height of the 'pocket', the area under the middle of the ski not in contact with the snow, influences pressure distribution and contact areas, properties that will be further discussed in the next section.

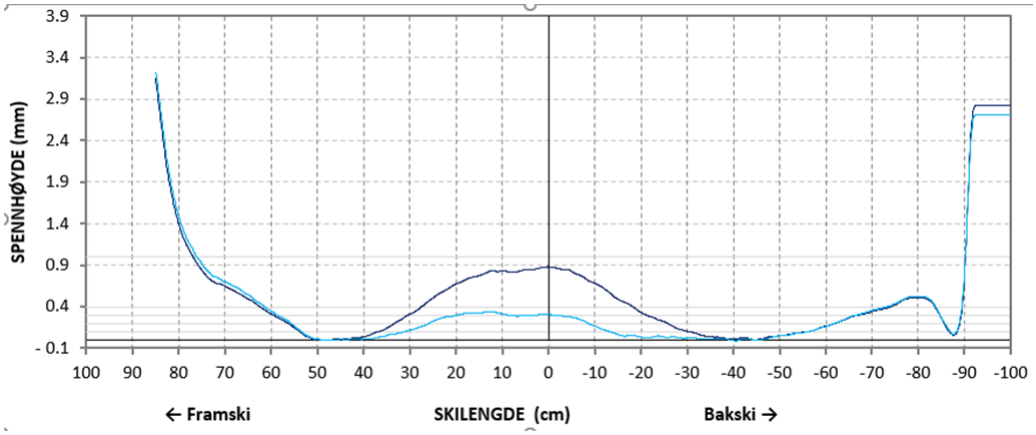

Figure 2.7: Flex height with half and full weight - classic ski, with ski length on the x-axis and flex height on the y-axis[6]

Figure 2.8 shows the height of the flex for a skate ski. As seen in the figure, the flex height is significantly higher for both half and full weight. As opposed to a classic ski, the flex height of a skate ski only affects how the ski feels and behaves on the snow as kick wax is irrelevant.

Similarly as for classic skis, it also affects the pressure distribution and contact areas. It is to be noticed that the ”pocket” and its peak height is located slightly in front of the binding.

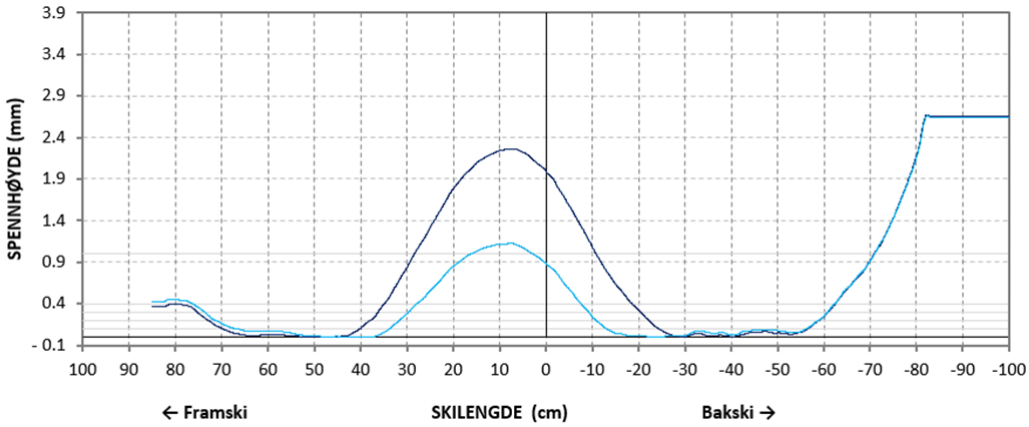

Figure 2.8: Flex height with half and full weight - skate ski, with ski length on the x-axis and flex height on the y-axis[6]

2.3.3 Pressure Distribution

Friction

To understand the importance of pressure distribution and contact areas, it is necessary to get a brief introduction to the role of friction. Friction can be defined as dissipation of energy between sliding bodies [25]. Haaland[26] explains this well by stating that “the energy loss can be transferred into heat or it can result in wear or deformation on the softest of the sliding surfaces. When skis are sliding on snow, the friction heat may result in a phase change, this is ice or snow transforming into water. The occurring water will be used as lubrication source that smooths the surface and lowers the coefficient of friction.” Friction is given by:

$$F_F = \mu F_N \tag{2.1}$$

From equation 2.1 it is shown that a low coefficient of friction results in low friction force and thereby improved glide[26].

There are three different friction mechanisms for snow, namely dry plouging, lubricated, and capillary suction[7], as shown in Figure 2.9. Dry plouging typically occur at low temperatures and slow speed, and does not have a water film between the ski base and the snow. This means higher friction as the ski must overcome the asperities in the snow[26][8]. The lubricated friction phase is the most ideal. In this phase the film thickness is sufficient to avoid the asperities in the snow, and still thin enough to avoid capillary suction. Capillary suction typically happens at temperatures around 0°C and warmer, and means that “a continuous connection between the ski base and the snow surface via a liquid film causes adhesion”[8].

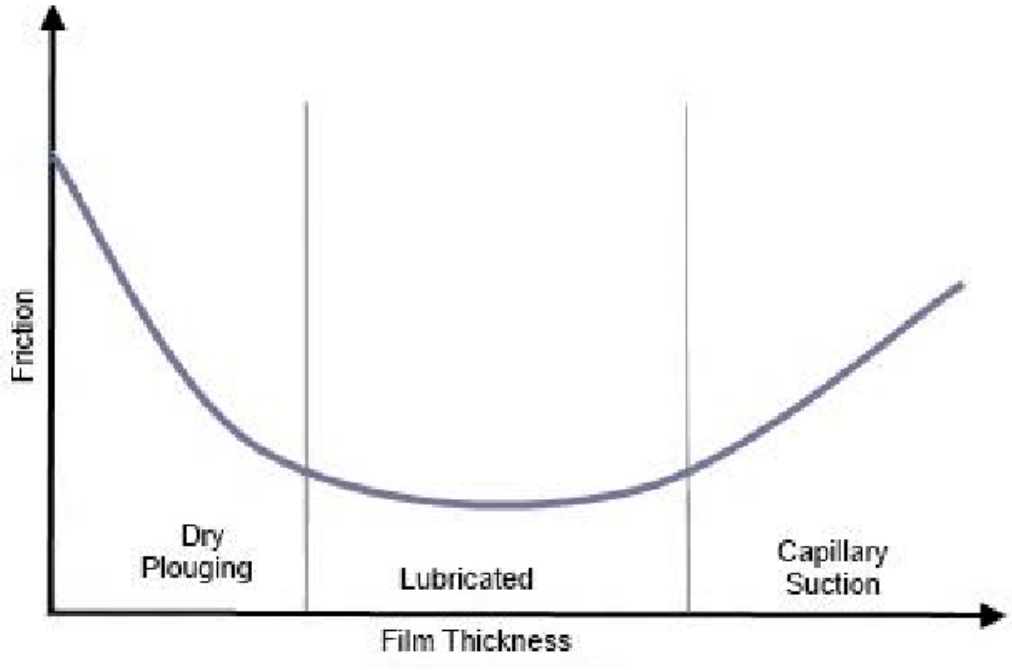

Figure 2.9: The three main friction mechanisms on snow [7]

Naturally, the lowest possible friction is desired for a ski to maximize the gliding capabilities and a significant contributor to this is the pressure distribution. Skis for cold conditions typically have a long contact area. Theoretically, for cold conditions, it is preferable to have the contact areas as close to each other as possible because of more heating of the snow, but since contact areas further apart mean more stable skis, this is not ideal. Skis for warmer conditions, on the other hand, often have shorter contact areas.

Pressure Distribution

As shown in Figure 2.5 there are two main areas throughout the length of the ski in contact with the snow, located in front of and behind the binding. Looking at this theoretically, the nominal area of contact between ski and snow, A_n, can be defined as[27]:

$$A_n = l_f w_f + l_b w_b \tag{2.2}$$

From this, the nominal pressure distribution $p_n(x)$ along the ski in the x-direction can then be defined as:

$$p_n(x) = \frac{N}{A_n}\Phi(x),$$

$$\frac{1}{2(l_1 + l_2)}\left[\int_{-l_1}^{l_1} \Phi_1(x)dx + \int_{-l_2}^{l_2} \Phi_2(x)dx\right] = 1 \tag{2.3}$$

It is the length of the contact area and the pressure distribution function on this area that influences the gliding capabilities of the ski. The percentage distribution of pressure between the front end and back end of the ski varies depending on the ski and where the load is applied, but in general a significant amount of the pressure is located on the back part of the ski.

Contact Area

As discussed, there are two contact areas. Figure 2.10 shows the contact areas for five different pairs of skis with both half weight and full weight load, which in this case is 36 and 72kg, respectively. It is clear from the figure that there is a significant gap between the contact areas.

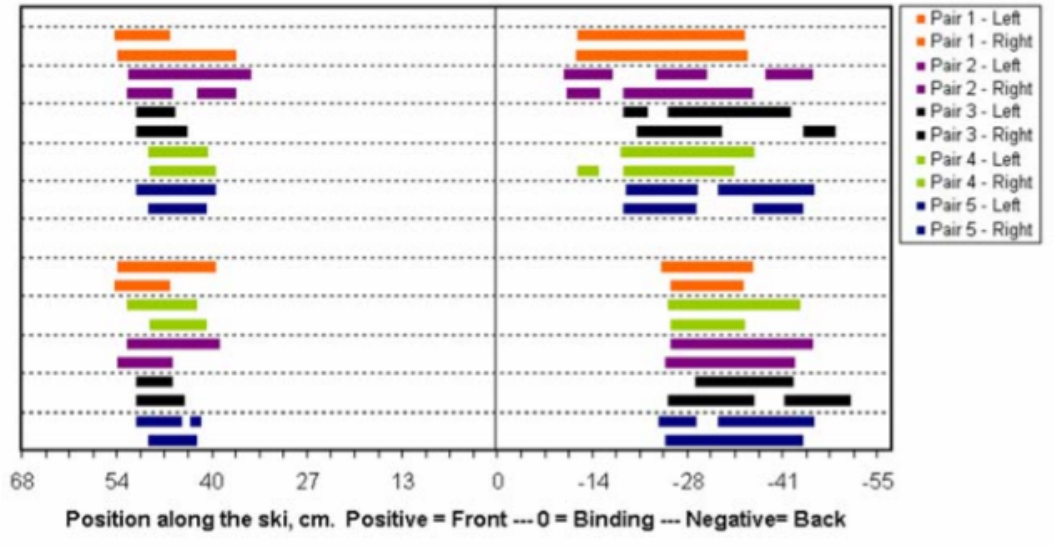

Figure 2.10: Contact areas for five different skis loaded with 36 kg (lower five pairs) and 72 kg (upper five pairs). The coloured bars represent the contact areas.[8]

Figure 2.11 can be used to get a better understanding of how an overload affects the ski and its contact zones. Looking at the plots labeled "flat," it is clear that it takes extensive overweight to narrow the gap. From this, theoretically, there is no need to measure pressure distribution in this area.

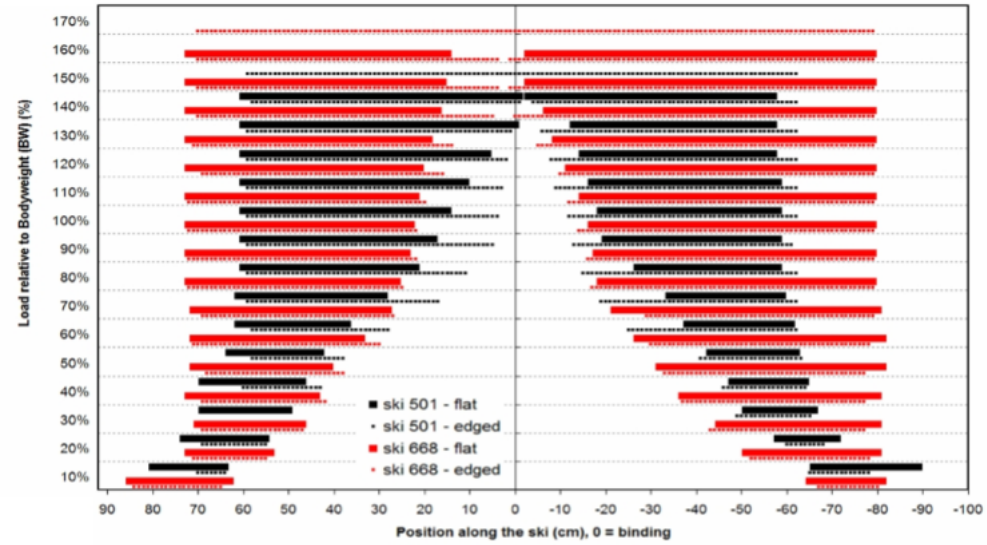

Figure 2.11: Comparison of contact length between warm ski and intermediate cold ski with loads up to 170% of body weight.[8]

Affects from Base and Grind

Another significant contributor to the gliding performance of the ski is the base and its grind. The base of the ski, which is the part of the ski in contact with the snow, is primarily made out of Ultra High Molecular Weight Polyethylene (UHMWPE). Other elements, such as carbon, flour particles, and graphite, are added for improved performance depending on the snow conditions the base is made for[14].

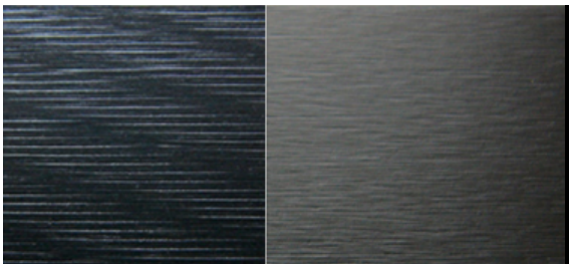

Figure 2.12: Examples of grinds for warm and cold conditions, respectively[9]

For maximal gliding, the base is grinded. Figure 2.12 shows typical grinds for warm and cold conditions. A structure is applied to the base to create the lowest possible friction on the snow. Explained with simplicity, in cold conditions finer structure is used to heat up the contact area between the snow and the ski to reduce the friction, which again improves the gliding. For warmer conditions, a coarser structure is used to drain water away from the base, also reducing friction. Although the base and the grind is not directly relevant for this master thesis, it is important to understand that the quality of the base and the grind can influence the performance of the ski significantly. This is one of the aspects that increases the difficulty of categorizing properties of a top ski. Two identically constructed skis can perform significantly different with different grinds and base material composition when tested.

2.4 Relevant Sensor Technology

Strain gauge principles

Strain gauges are sensors whose resistance change with the applied force. This is due to the fact that strain converts directly into a resistance change, which can be derived by the following equations [28]:
The resistance of a metal sample is given by

$$R_0 = \rho \frac{l_0}{A_0} \tag{2.4}$$

As the sample is subjected to a tensile load, the length will increase and the area will decrease, which means that:

$$V = l_0 A_0 = (l_0 + \Delta l)(A_0 - \Delta A) \tag{2.5}$$

Since both the length and area of the sample has changed, the resistance will also change:

$$R = \rho \frac{l_0 + \Delta l}{A_0 - \Delta A} \tag{2.6}$$

With the use of Equation 2.5 and 2.6, the new resistance is given by:

$$R \simeq \rho \frac{l_0}{A_0}(1 + 2\frac{\Delta l}{l_0}) \tag{2.7}$$

which means that the change in resistance is given by:

$$\Delta R \simeq 2R_0 \frac{\Delta l}{l_0} \tag{2.8}$$

Equation 2.8 shows how metal strain gauges convert strain directly into resistance change. Equation 2.8 is only approximately true. Factors such as impurities and type of metal can affect the relation. Therefore, a gauge factor is necessary to indicate the correct relation [28]. The gauge factor is given as:

$$GF = \frac{\Delta R/R}{\Delta l/l} \tag{2.9}$$

Figure 2.13 shows an illustration of a strain gauge, where either a metal wire or foil is used, which is typically 0.05mm thick and can be glued to a surface much like a postage stamp [29]. The connection leads are in the figure located to the right on the strain gauge, which are where the resistance is measured.

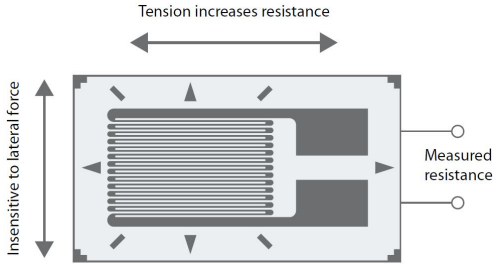

Figure 2.13: Strain gauge illustration [10]

Load Cells

Typically, load cells have the strain gauges arranged in a bridge configuration as shown in Figure 2.14, where

- $R_1 - R_4$ are resistors
- V_s is the excitation voltage
- V_out is the bridge output voltage

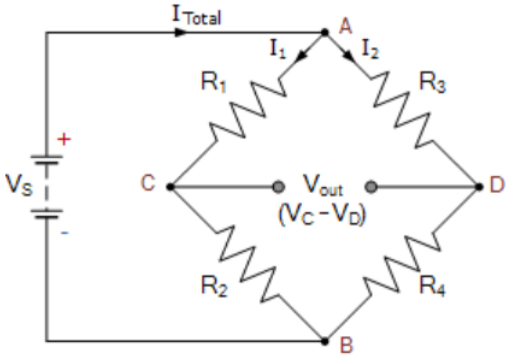

Figure 2.14: Wheatstone bridge

Load cells are typically found in three different strain gauge configurations, namely quarter-bridge, half-bridge and full-bridge circuits, illustrated in Figure 2.15. The bridges are always complete, despite what the naming says, only depending on the extent of which the bridge is completed by strain gauges or fixed resistors[30].

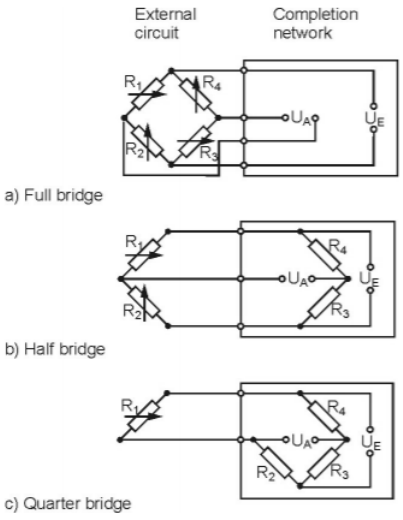

Figure 2.15: Quarter, half, and full-bridge illustration [11]

Temperature can have an impact on the strain gauges. A single strain gauge is prone to temperature effects. Therefore, in a quarter-bridge circuit, a ”dummy” strain gauge is often used to compensate for this. The ”dummy” strain gauge is positioned where there will be no strain applied to it. This means that with no force applied, the strain gauges will both be

equally affected by temperature, keeping the bridge in balance. For a half-bridge circuit, with its two strain gauges, the temperature effect is cancelled as the bridge is balanced. This is also true for a full-bridge configuration.

Figure 2.16 shows how two strain gauges are typically attached to the specimen. When the resistance of R_1 and R_2 is equal, the resistance of R_3 and R_4 is equal, and no strain is applied, the voltage drop across each arm is equal. Hence, the bridge is balanced and the measured bridge output voltage is zero. When a bending load is applied to the specimen one of the strain gauges will compressed and one will be in tension, resulting in decrease and increase in resistance, respectively. This means that the voltage drop across R_1 will change, resulting in a bridge output voltage different from zero. This value is used to calculate the applied load on the load cell. A full-bridge load cell would be twice as accurate as four strain gauges would double the bridge output voltage with the same load. It is to be noted that the two strain gauges in compression in a full-bridge configuration would have to be R_1 and R_3 and the strain gauges in tension R_2 and R_4, or the other way around.

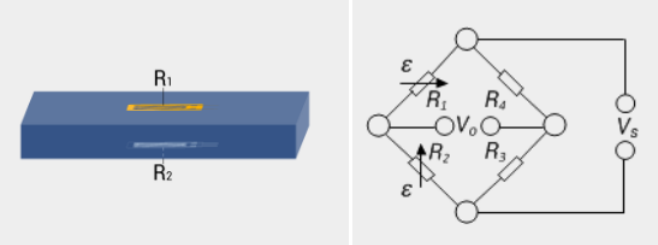

Figure 2.16: Half-bridge illustration and rhombus representation

3 | OLTs Existing Technology

OLTs measuring device measures three different properties in three different setups on the same device. The properties are flex and flex height, surface pressure distribution, and the stiffness of the ski. The original fixture measures the camber height only. As the need to measure other properties was presented, setups for measuring pressure distribution and stiffness were added by OLT. Standing up and down on a pair of skis on both legs means that the center of mass is around 14cm behind the tip of the toe. When skiing and standing on one ski, the pressure is typically applied 8cm behind the tip of the toe. Consequently, 14 and 8 centimeters is used as a measurement standard by OLT and is used for loading in this setup.

Even though the pressure distribution is the setup and the measurement of interest in this project, it is important to look into how flex height and stiffness are measured also, as the goal is a concept that potentially allows for integration of these measurements in the setup.

3.1 Setup and Procedure

3.1.1 Flex Height

The flex height is measured under two different loads, half weight and full weight of the skier. This is because these are the loads distributed on the skis when skiing. Obviously, there is a fluctuation in load as the skier moves, but this variation is not taken into consideration for simplification. When the ski is loaded, as shown in Figure 3.1b, a laser is moved under the full length of the ski. The laser can be seen in Figure 3.1a. The laser is calibrated before measuring. The laser measurement is then plotted on a graph in excel.

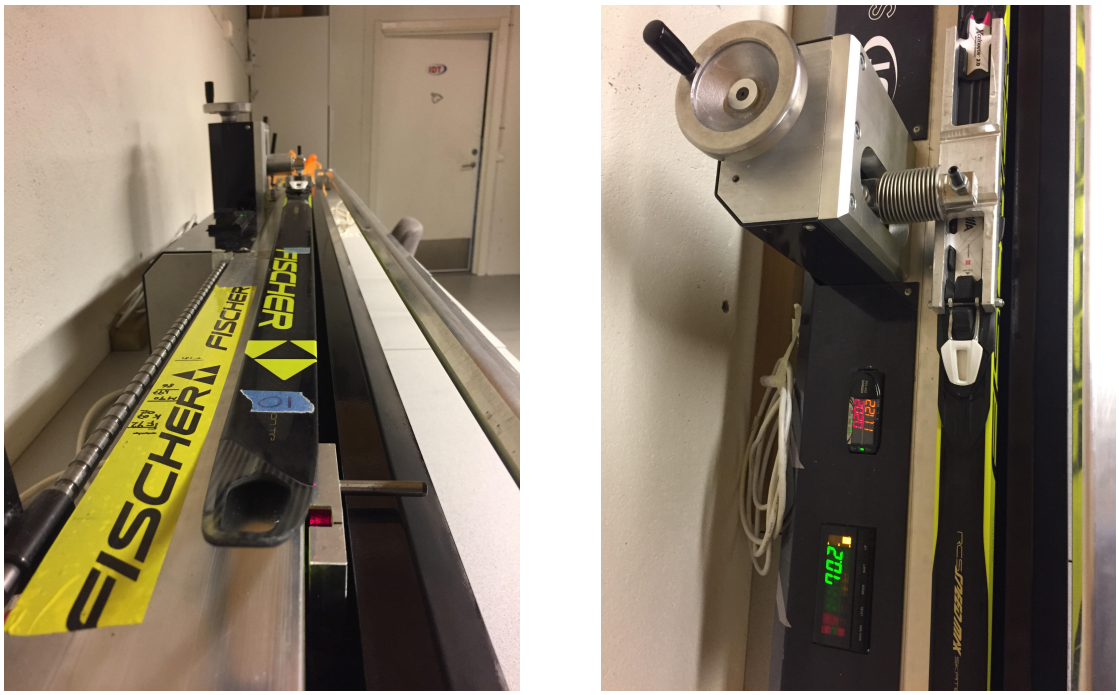

(a) (b)

Figure 3.1: Loaded ski with the laser ready to slide along the edge of the ski (a), and the loading mechanism (b)

3.1.2 Stiffness

The stiffness is found by first measuring the zero flex of the ski. Thereafter, the ski is placed on two metal bars with a known distance from the tip of the ski to the bar and from the end of the ski to the bar, as shown in Figure 3.2. This is done in two different setups. First, the metal bar is placed near the tip of the ski and loaded with 3kg. This results in significant bending in the front and back of the ski. The laser is then used to measure the deflection. Then the metal bars are moved closer to the loading mechanism and the ski is loaded with 30kg. The laser is again used to measure the deflection. This results in greater deflection in the center of the ski length. A balance of the forces and bending moment distribution is then calculated. The difference in bending between zero flex and the loaded ski is then taken into consideration. The following formula is used to calculate the flexural stiffness from the measured deformation[31]:

$$EI(x) = \frac{M(x)}{h''(x)} \tag{3.1}$$

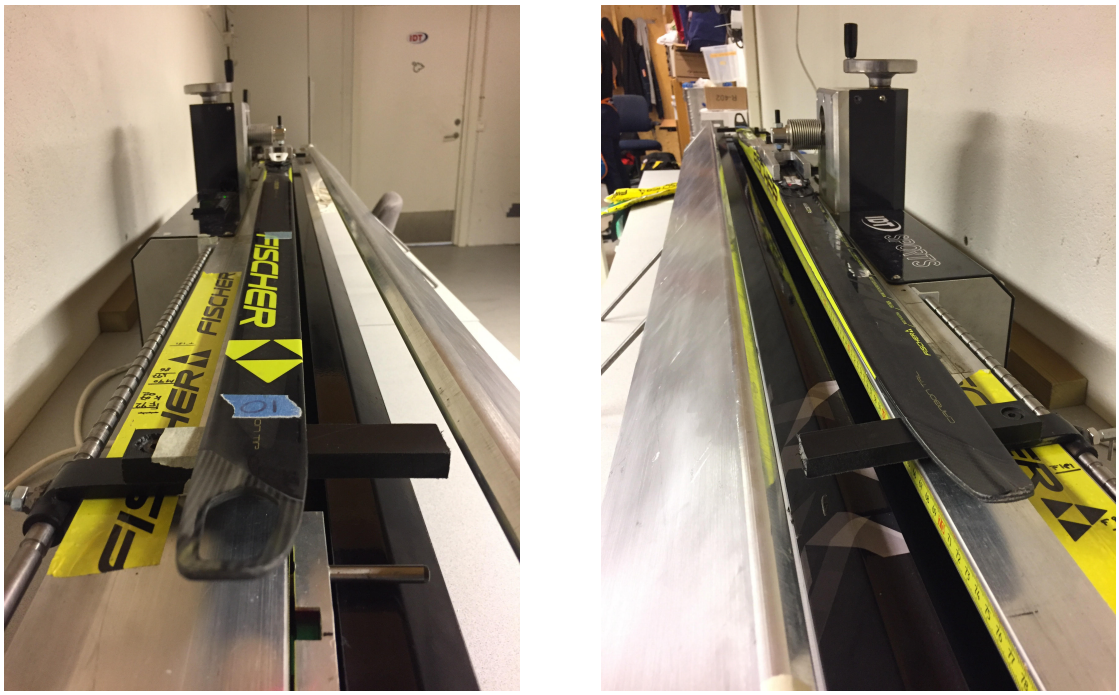

(a) (b)

Figure 3.2: Front (a) and back (b) view of stiffness setup

3.1.3 Pressure Distribution

To measure the pressure distribution, the ski has to be removed from the measuring device. Then a metal plate is flipped to lay on top of the original surface. A black rubber mat is used between the pressure mat and the surface, as shown in Figure 3.3, to represent snow and to avoid point wise pressure distribution. Although the rubber mats cannot represent snow perfectly, they do so sufficiently. The pressure mats are placed in the same spot every time to assure comparable results. The mats are then connected to the data acquisition device, which is connected to a computer with the supporting software. The ski is then placed on the mats and loaded.

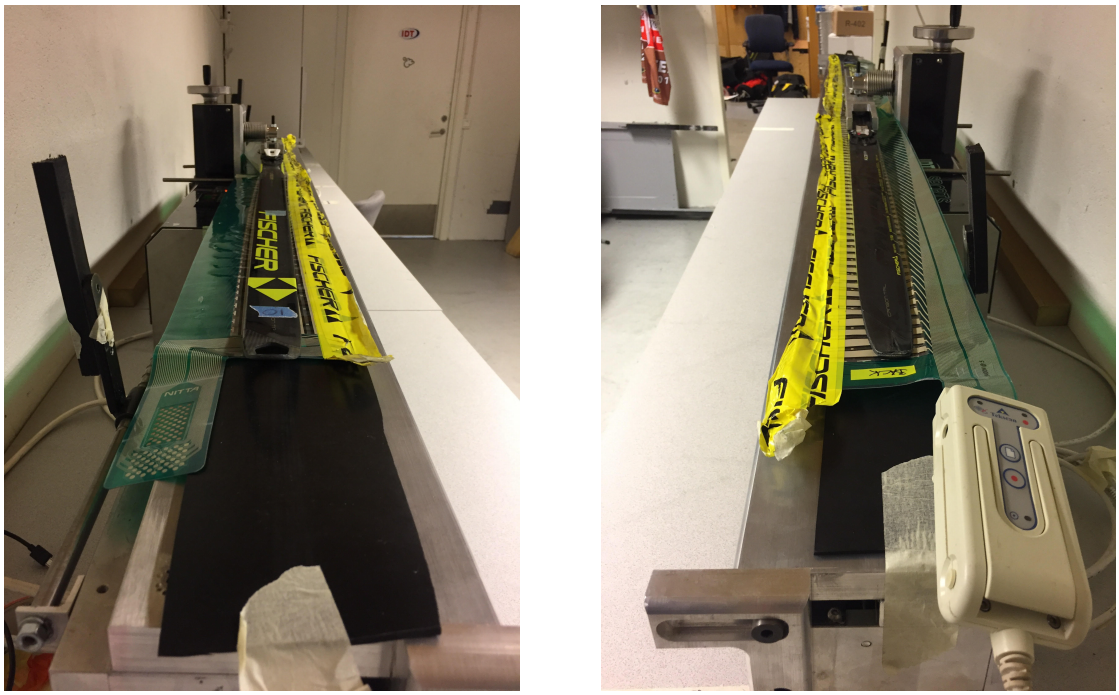

(a) (b)

Figure 3.3: Pressure distribution setup front view (a) and back view (b)

Pressure Mats

The pressure mats used by OLT comes from Tekscan, a company delivering pressure mapping, force measurement and tactile sensors. The 5400N mat, which is the one used by OLT, has a pressure range of 0-4psi. The original size of the matrix is 884x578mm, but as seen in Figure 3.4, the mat is modified to better fit both measuring device and skis.

Figure 3.4: Pressure mat used by OLT

The mat is constructed as a matrix of force sensing resistors, as shown in Figure 3.5, with

resolution of a sensor every 17.0mm in both directions, to measure length and width. The mats have a sampling rate of 100Hz. This allows for dynamic analysis if desired. The data from the mats is transferred via USB to the computer software. The mats have 40 different sensitivity levels with eight bits resolution, which means that the mat can resolve the measurement into 256 levels. Setting the resolution to its maximum therefore results in a lower maximum pressure capacity. For example, if the highest sensitivity allows for a 10 grams or 100 grams accuracy, the maximum capacity would be 10g*256=2560g and 100g*256=25600g, respectively. OLT uses the lowest resolution to allow for the highest possible load on each sensor, otherwise, most of the sensors would be saturated.

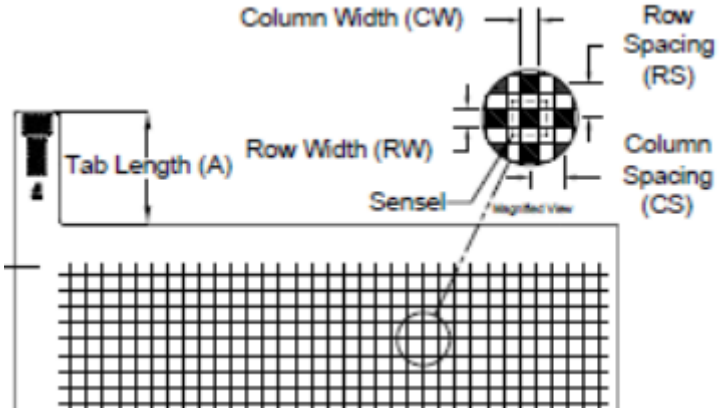

Figure 3.5: Pressure mat used by OLT[12]

The responses of individual elements may vary slightly, therefore, the mats must be calibrated regularly to deal with this. To assure accurate calibration, the mat are supposed to be placed within a vacuum pressure calibration device where it is subject to different pressures at fixed time intervals. Multiple calibration points are necessary to create a calibration curve [8]. OLT does not have this equipment available so an alternative solution for calibration is used. OLT uses quadratic wooden bars, with 5kg increase in weight, which are placed on the mat. It is necessary to load at least 40 % of the mat to calibrate the mat accurately. Therefore, as the mat is adjusted size wise to fit the setup, this is not possible.

3.2 OLT Measurement Data

3.2.1 Flex Height

Figure 3.6 shows the resulting plot using the laser to measure the flex height of a pair of classic skis. The grey horizontal lines on the bottom half of the plot represent the position of the flex heights at 0.1, 0.2, 0.3, 0.4, and 1.0mm, which are the flex heights of interest when it comes to kick wax, as discussed in Chapter 2, section 2.2.2.

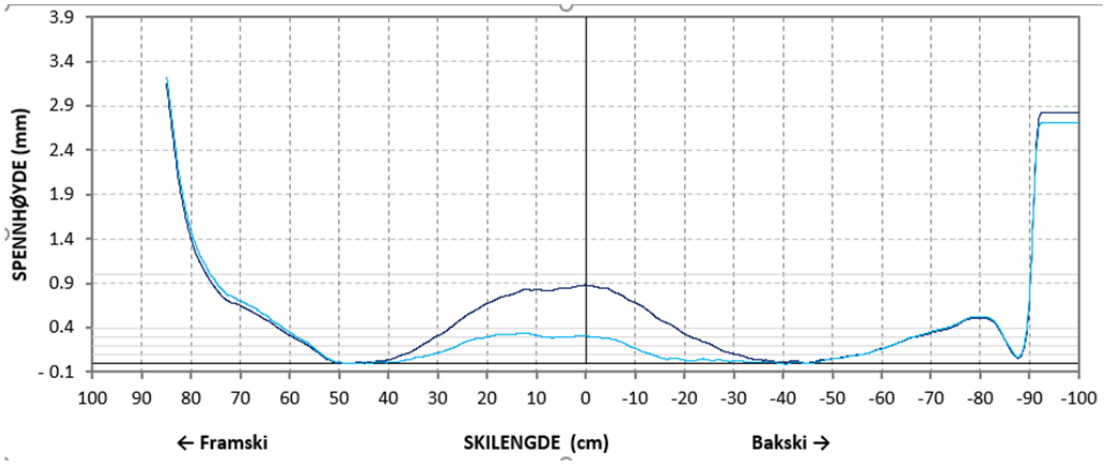

Figure 3.6: Resulting graph using the laser with ski length on the x-axis and flex height on the y-axis[6]

3.2.2 Stiffness

Figure 3.7 shows the interpolated bending stiffness graph of a pair of skis using the method of OLT. In this case the stiffness is measured and calculated every 10cm.

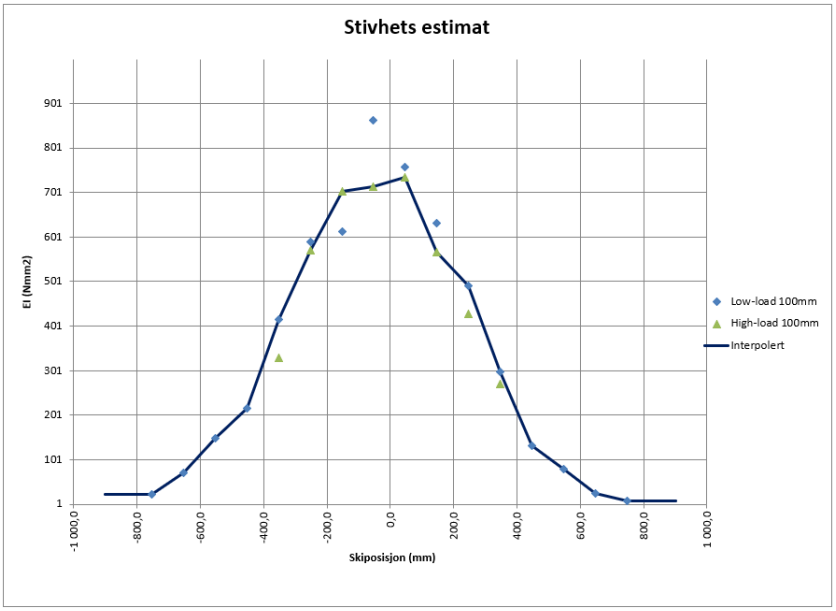

Figure 3.7: Interpolated stiffness of a ski with ski position on the x-axis and flexural stiffness on the y-axis[6]

Figure 3.8 shows a comparison of three different skis. It shows the difference in bending stiffness throughout the length of the ski. The numbers represented in the legend entry (812, 685, 49) are simply the identification number for the relevant ski. Currently, it is not known if this data can be useful or whether the method is sufficient or not.

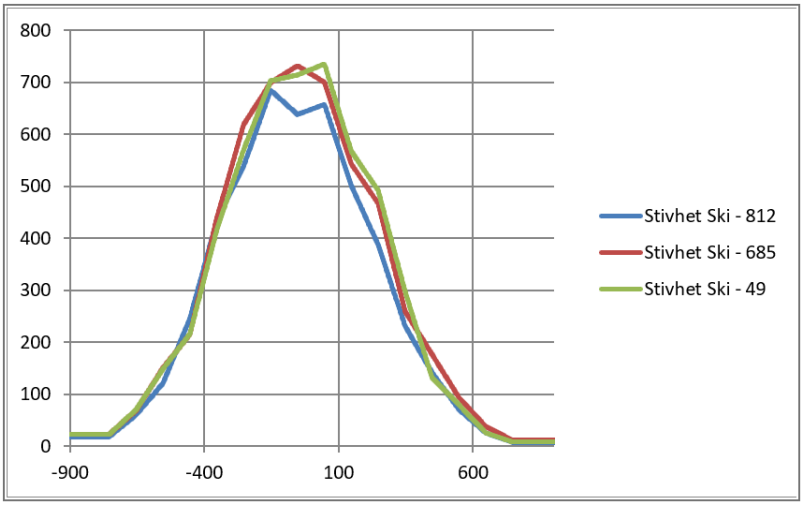

Figure 3.8: Comparison of stiffness of three different skis, where the x-axis is the ski position in cm and the y-axis in flexural stiffness in $EI(mm^2)$[6]

3.2.3 Pressure Distribution

Figure 3.9 and Figure 3.10 show the plotting from the pressure mats with half weight and full weight, respectively. The white screen shows the 3D pressure distribution with a top view, while the black screen shows a 2D representation with force in N on the y-axis and distance in cm on the x-axis. Comparing the results from the half and full weight, it is clear that the pressure distribution changes significantly.

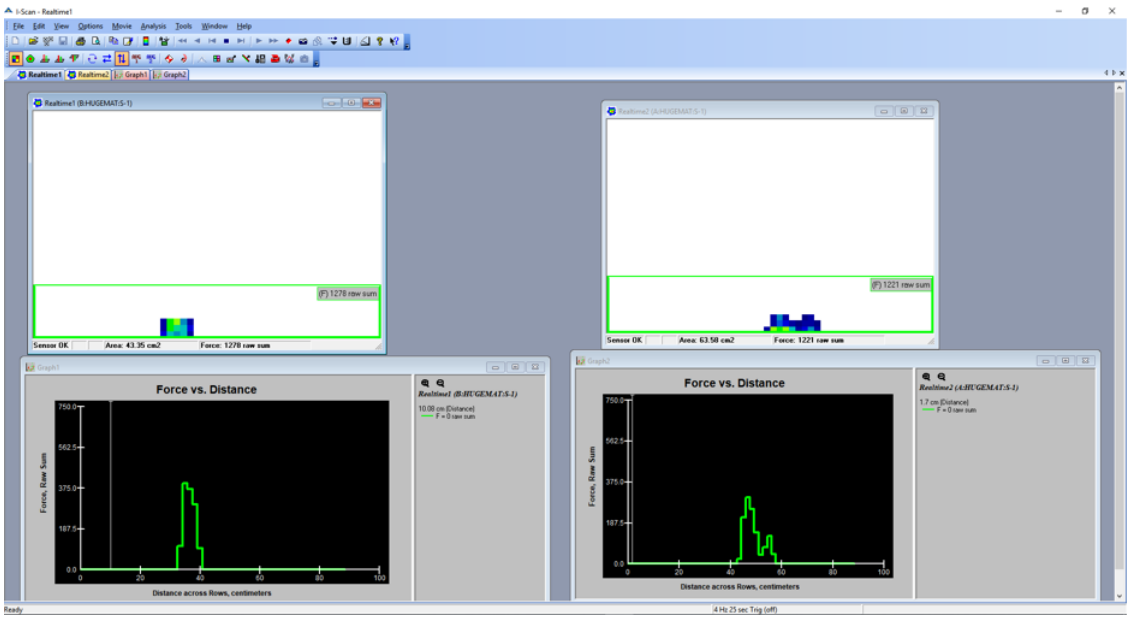

Figure 3.9: Pressure distribution half weight - Fischer ski[6]

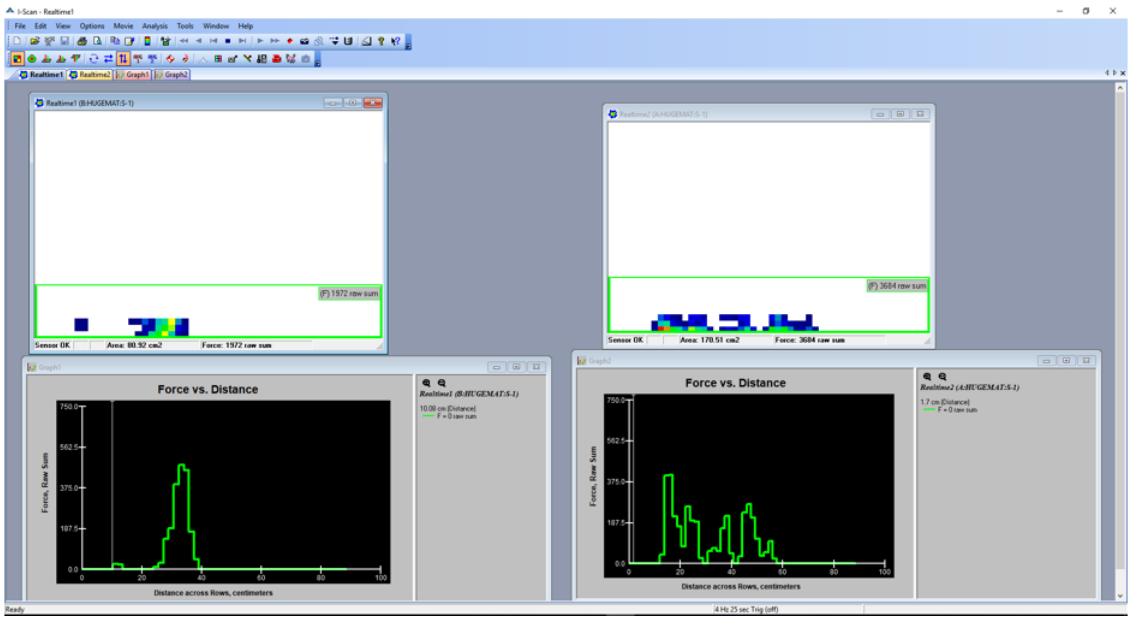

Figure 3.10: Pressure distribution full weight - Fischer ski[6]

3.3 Drawbacks and Limitations with Pressure Distribution Measurement

One of the main drawbacks with this setup is the time aspect. Professional skiers have multiples of ten pairs of skis each that need to be measured and if measuring one ski takes five minutes or more, the overall time spent measuring skis for many skiers will be way too long with just one measuring device.

Another important aspect is the price of the pressure distribution mats. The mats currently used cost approximately 25 000 NOK each, and the data acquisition device costs significantly more. This means that if multiple measuring fixtures are wanted, this adds on a notable cost. It is important to realize that acquiring equipment that measures the ski properties extremely well is possible, but requires a lot of money to be spent, which is not desirable. This is emphasized by that it is far from guaranteed that it will be able to categorize a top ski.

The mats are prone to saturation, which means that the peak pressure is not obtainable. In other words, a possibly important value is not registered. This means that the correct percentage pressure distribution between the front and the back of the ski is not obtained.

The resolution of the mats can be improved significantly. As mentioned, the mats measure pressure every 17.0mm. Figure 3.9 and Figure 3.10 show how the graph has a step change that represents this resolution. This means that potentially important information from a higher resolution is not obtained. The mats have the same resolution in the direction of the width of the ski. This is most likely not necessary as one measurement should be sufficient.

3.4 Other Existing Technology

Different ski manufacturers typically have their own means of measuring and characterizing skis. But, as mentioned, the willingness to share technology is limited. Still, some technology is available and therefore presented in the following sections.

3.4.1 Swedish Ski Team

Back in 2008, Backström, Dahlen, and Tinnsten presented a concept where a sliding load cell was moved underneath the length of the ski to measure the pressure distribution. This setup was used by the Swedish ski team for two and a half years up until the paper called "Essential ski characteristics for cross-country skis performance"[13] was written for the ISEA Conference in 2008. Figure 3.11 shows plots of two different classic skis measured by the setup. Figure 3.12 shows a plot of a skate ski together with a flex height measurement. The flex height measurement is integrated in the setup. The skis have been measured with a load of 40kg for men and 25 and 35kg for women, 14cm behind the binding. [13]

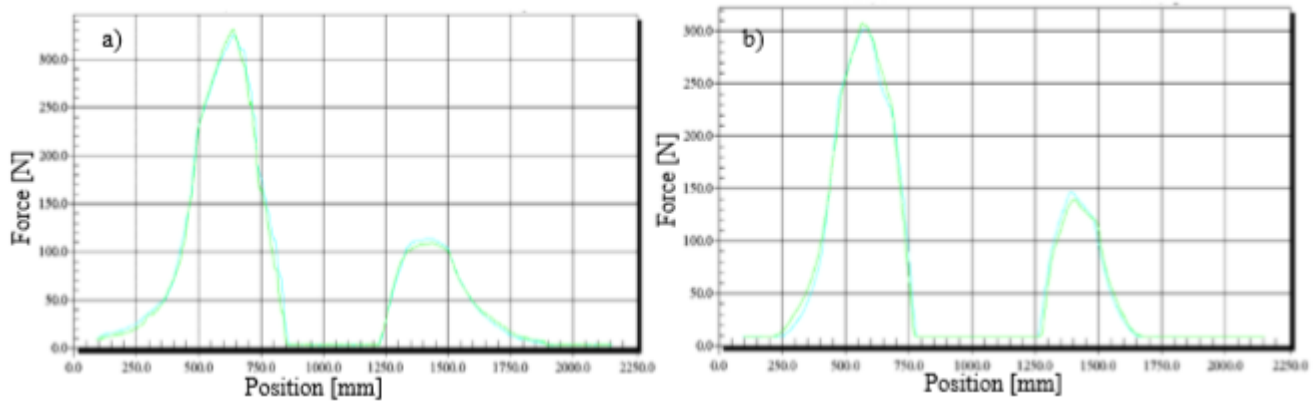

Figure 3.11: Pressure distribution of two different classic skis [13]

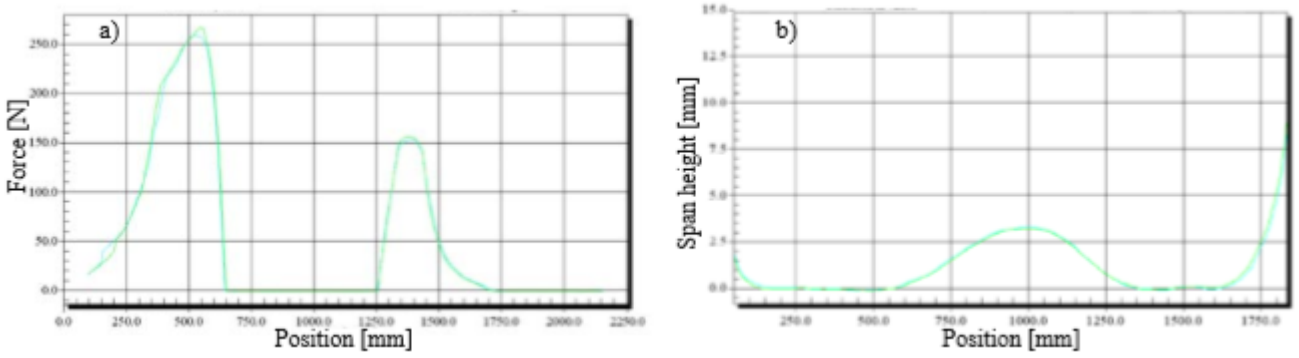

Figure 3.12: Pressure distribution and flex height for skate ski [13]

3.4.2 Madshus Technology

Madshus measures pressure distribution with a stationary sensor by sliding the ski over it, producing a pressure distribution curve. This system is called Compuflex. Figure 3.13 shows

the resulting pressure distribution curve when measuring a ski. It is important to notice that this figure is from 1999, meaning that significant improvements could have been made since then. Still, it is a solid representation of the results from the system and newer data has not yet become obtainable.

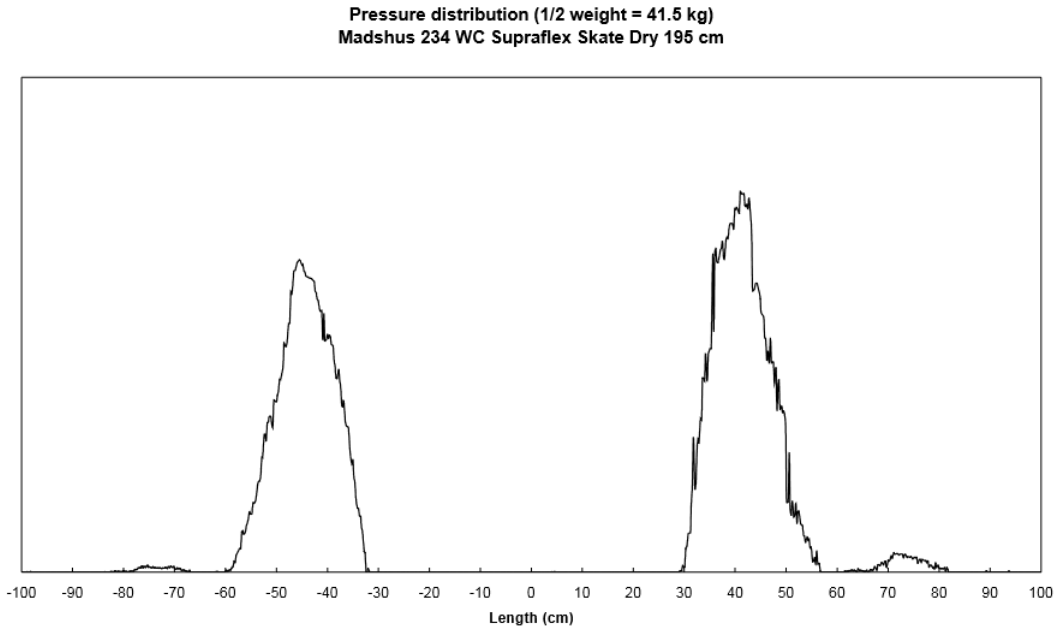

Figure 3.13: Pressure (or load) distribution from Madshus Compuflex [14]. The y-axis values and units are unknown.

3.4.3 Pioneer Midwest

Mr. Matthew Liebsch from the sports store Pioneer Midwest, in Minnesota, developed a device that measures the load distribution of a ski by utilizing multiple load cells in the direction of the length of the ski. According to Mr. Liebsch, the resolution of the device is a load cell every 2.5cm. When measuring the ski, the results are plotted in a graph on a connected screen. A Raspberry Pi is used for data acquisition. Mr. Liebsch points to keeping the load cells on the same level as the biggest challenge.

3.4.4 Eagle River Nordic

Eagle River Nordic developed a setup, shown in Figure 3.14, with 15 transducers with a 10cm distance between to test the pressure distribution. The testing was performed by loading skate skis from half body weight to full body weight, and classic skis the same as well to represent the kick. There is no data obtainable on this concept[8].

Figure 3.14: Setup used by Eagle River Nordic[8]

4 | Methodology

Ulrich and Eppinger present a solid and detailed description of the different stages of product development in their book, "Product Design and Development"[15]. The book serves as a great tool when developing a product and the methodology of this thesis is, therefore, significantly based on it.

4.1 Development Approach

Figure 4.1 shows a front-end process and its activities. This approach corresponds well to the nature of this master thesis. The first two, partly three, activities presented in Figure 4.1 were investigated through the project report. Therefore, the main focus throughout the mater thesis is the next three stages, namely concept generation, concept selection and concept testing. The approach to these stages will be discussed in the following sections.

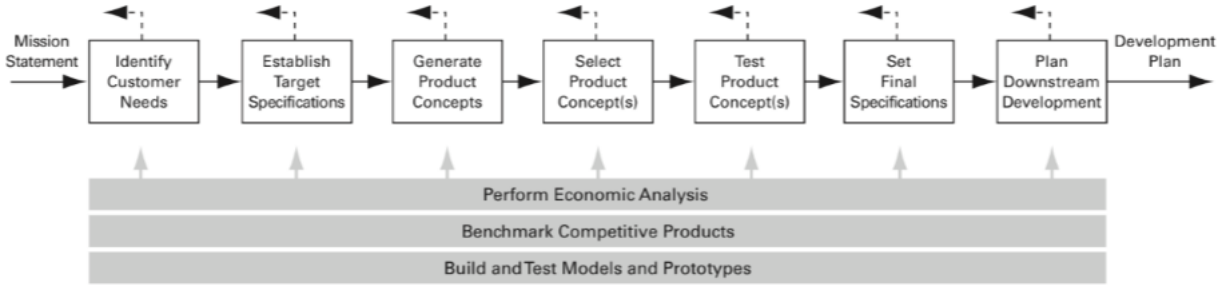

Figure 4.1: Front-end activities [15]

4.1.1 Concept Generation

To be able to explore the space of solutions, it is necessary to dig into and come up with a variety of possible solutions. Benchmarking, which is applied to a wide variety of activities that organizations undertake to compare their performance level with others [32], was used in this concept generation part of the master thesis. Throughout the project report, several concepts were generated to challenge the set requirements. The feasibility of the solutions varied significantly to push the solution space. According to Ulrich and Eppinger, this is a healthy approach.

4.1.2 Concept Selection

Ulrich and Eppinger [15] mentions several product development challenges, one of them being "time pressure". This challenge explains how decisions are often made quickly and without complete information. Deciding on a concept for the master thesis represents this challenge.

Without the knowledge of the expected time usage on a proof-of-concept prototype, it was necessary to make a decision on which concept to work with. Ulrich and Eppinger [15] point at different methods on how to choose among concepts. Ideally, the ”prototype and test” method would be used to get a better understanding of the concepts. Knowing the constrains on the thesis and to avoid excessive time use, two other methods were used instead; ”intuition” and ”pros and cons”. These methods were used to decide which of the concepts generated to develop. With the use of these methods, the concept considered to be the best and possibly benefit the customer (OLT) the most, was decided. A similar concept was developed approximately 15 years ago, which produced usable results, though limited details on the setup. This was considered a great advantage as it was reasonable to believe that the concept would work and that the measurements would be comparable to the technology used by OLT today.

When the concept to develop was decided upon, a streamlined product development approach was used. This approach has similarities to the much used waterfall approach. Figure 4.2 shows the characteristics of this approach.

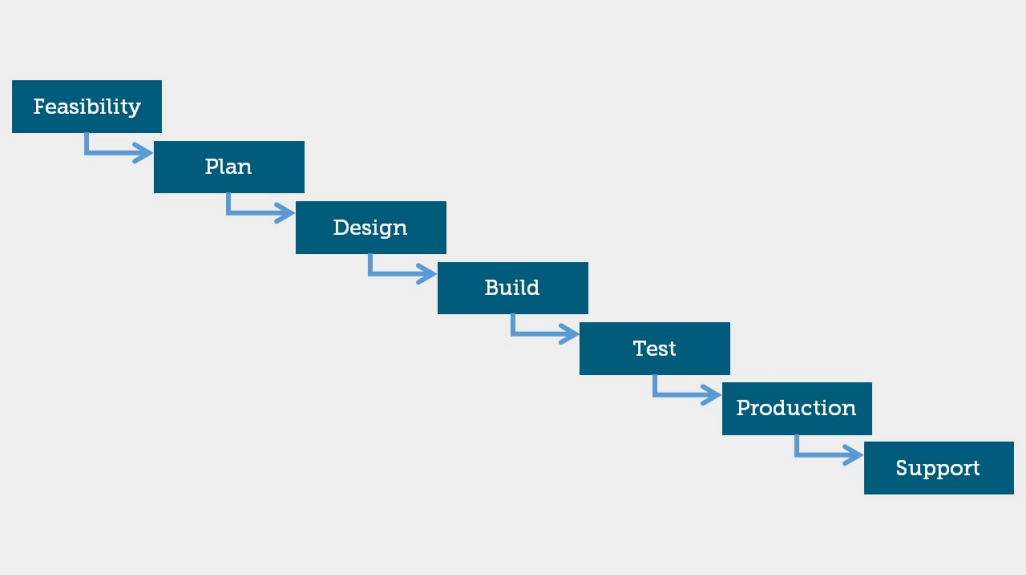

Figure 4.2: Waterfall product development approach [16]

The waterfall approach relies on a linear phase sequential where the next phase is dependent on the deliverables from the last one. One of the main criticisms of this approach is that customers do not know their exact requirements and change these as the project runs, typically causing redesign and redevelopment, which can be costly.

In real world product development environments, the waterfall approach is considered inadequate as it does not allow for flexibility. In the development process of this master thesis, this agility is not crucial after a decision on which concept to work with is made. The reason for this is that a concept that does not fulfill the requirements is a result, just as much as a concept that is proven to work. The idea is to test a concept that is considered to have the potential to outdo or supplement the existing technology. Therefore, a waterfall approach was considered solid and trustworthy considering the circumstances of this thesis.

4.1.3 Concept Testing

Prototyping

Developing a prototype able to prove and sufficiently test the concept was necessary. There are three purposes of a prototype that relates to this thesis: learning, integration, and milestones [15]. Learning involves questions like "Will it work?", which is what this master thesis is focusing on. Integration refers to ensuring that "components and subsystems of the product work together as expected"[15]. Lastly, milestones refers to that "prototypes are used to demonstrate that the product has achieved the desired level of functionality"[15]. These three aspects are directly relatable to this master thesis and were, therefore, in focus.

There are two ways to test a concept; analytical or physical prototypes. An analytical prototype is generally more flexible than a physical prototype [15]. The reason for this is that parameters can be varied to represent design alternatives. Naturally, changing a variable in an analytical prototype is most often easier than in a physical one, and the variable can be varied on a larger scale. Throughout this master thesis period, a great portion of time was spent building and developing a physical prototype. An analytical prototype was considered unsuitable as the complexity of ski construction and theoretical challenges that were present resulted in a decision to focus on a physical approach that could give a fuller understanding of the concept. A physical prototype has all the laws of physics present, which means that unanticipated phenomenons will be encountered, if present[15]. Additionally, as the setup used by OLT is physical, a results from a physical prototype would be better suited for comparison.

One of the main challenges of this master thesis was to avoid what Clausing[33] calls "hardware swamp". "The swamp is caused by misguided prototyping efforts, that is, the building and debugging of prototypes that do not substantially contribute to the goals of the overall product development project"[15]. To avoid this, it was necessary to plan out the prototype. This was done by following four steps presented by Ulrich and Eppinger[15]:

- Define the purpose of the prototype
- Establish the level of approximation of the prototype
- Outline an experimental plan
- Create a schedule for procurement, construction, and testing

Prototyping was used to construct a product somewhere in between an alpha and beta prototype. A comprehensive prototype was considered the best approach as all the attributes were related to each other and needed to work sufficiently. Consequently, the complexity of the prototype increased.

4.1.4 3D-printing

The master thesis has heavily relied on 3D-printing. 3D-printing can be a great tool when creating prototypes. 3D-printing can be time consuming, but is still often considered a rapid prototyping tool. One of the reasons why 3D-printing was heavily used throughout this master thesis is that a significant amount of time was spent on developing a sufficient software. This, together with writing on the thesis itself, made it possible to transition between the tasks, eliminating some of the potential time waste. Another important aspect of 3D-printing that

made it suitable is that it is possible to achieve desired structures and shapes with solid accuracy. In a normal product development environment, it would be preferable to find more efficient tools for prototyping.

5 | Developed Concept

From gained knowledge on ski construction, properties and drawbacks of OLTs existing technology, the following requirements were established:

- High resolution in the direction of the length of the ski, preferably with millimeter precision
- Deviation of no more than 5-10%
- Capacity of measuring peak pressure
- Time-frame of less than five minutes per ski
- Keeping the costs as low as possible
- Great repeatability
- Integration of stiffness and camber height measurement setup
- Maximum length of 220cm

5.1 Concept Decision

From the requirements presented above, it was decided to develop and test a concept where a load cell is slid under the length of the ski to further explore the possibilities of the concept. Several concepts were considered, but this concept was chosen as it has the potential to fulfill most of the requirements. As discussed, a similar product has been developed earlier. An attempt was made to get in touch with the creator, but this was unsuccessful. Therefore, it was decided explore the concept and the possibilities that comes with. The following list presents aspects of the concept not mentioned investigated:

- Testing skis with an increasing load from 10kg up to full body weight
- Test skis with different load locations
- Test different lifting heights
- Look into the area under the graph to find potential trends and correlations
- Compare the concept to the current technology used by OLT, measuring the same property
- Look into the possibility of adding new useful measurements

Figure 5.1 shows the final developed concept with the ski loaded.

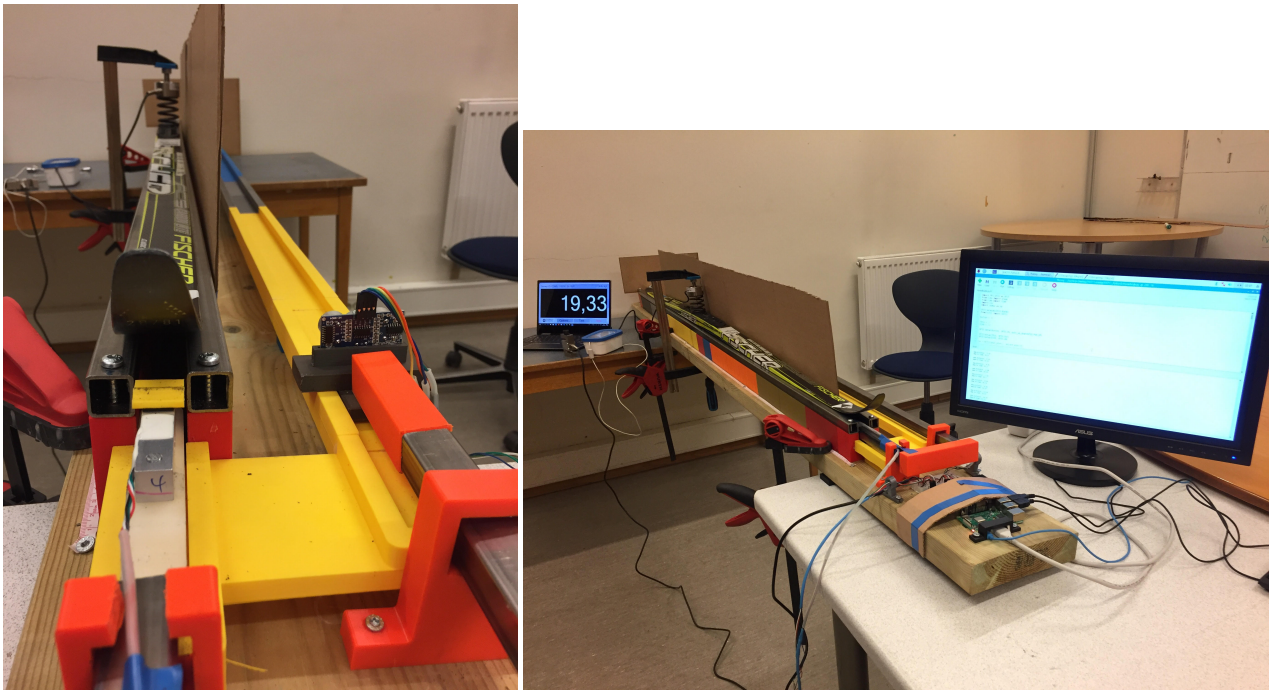

(a) (b)

Figure 5.1: Front view (a) and full overview (b) of loaded final concept

Possibility of Integration of Other Property Measurements

Integrating the laser sensor to measure the flex height of the ski will be possible as shown by Backström [13]. As mentioned, measuring the flex height is a standardized and common practice. Including the stiffness setup discussed in Chapter 3 is doable. Although, it seems reasonable to assume that it involves reloading the ski on the setup.

5.2 Theoretical Concept Challenges

There are two main theoretical challenges that come with the chosen concept. The first one is that it is necessary to elevate the ski slightly for the load cell to get a sufficient reading. Figure 5.2 shows a simplification and exaggeration of the problem, where the front part of the ski is entirely lifted from the surface. The red rectangle represents the load cell and the blue represents the loading mechanism. In this case, the load distribution on the front ski is fully concentrated on the load cell. It is to be noted that this is a simplification as there would be a transition of load, in regards to the back end of the ski, when the ski is lifted this significantly in the front end. In this case, the load distribution of the ski would not be represented correctly.

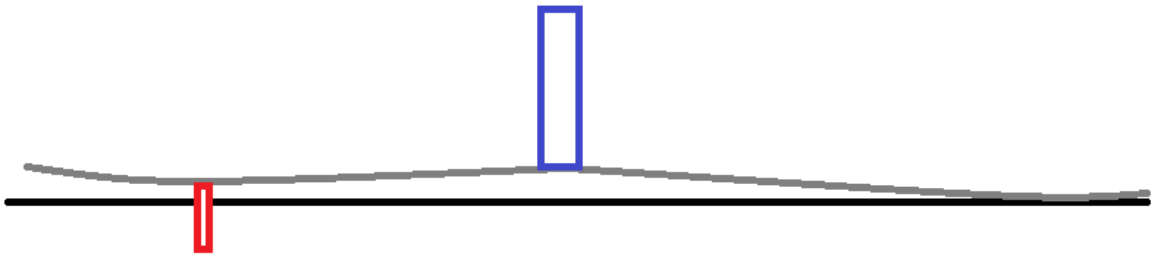

Figure 5.2: Load concentrated on load cell

The second challenge is also related to the elevation of the ski. At higher loads, closer to full body weight, a significant part of the ski is close to the ground, including the area close to where the load is applied. With the current loading situation, the ski is locked in position by the static load, which means that lifting the ski right under the load is not possible. If the system is considered infinitely stiff and the sliding load cell is higher above the surface than the distance between the surface and the base of the ski directly under where the ski is loaded, it is impossible to slide the load cell under the ski. In reality, it would be the ski and its base that would be plastically deformed.

The lifting of the ski close to the loading point will also increase the load if it is locked in place. Figure 5.3 shows an illustration with the sliding load cell in two different positions, one of the right under the loading mechanism and one closer to the tip of the ski. As discussed in chapter 2.3.2, the stiffness increases towards the center of the ski. As the load cell slides towards the center of the ski, the ski will resist bending, increasingly. Consequently, as the ski is lifted and the ski is locked in position, there will be an increase in the applied load on the ski. This means that measuring the ski at a certain applied load is not possible, as the load will vary depending on where the sliding load cell is located during measurement.

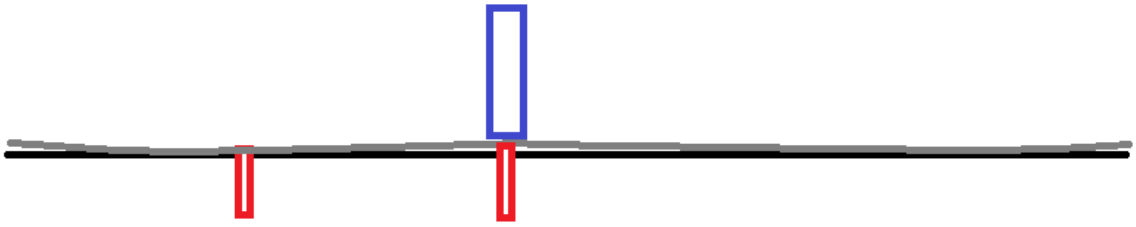

Figure 5.3: Static load not possible to lift

It is, therefore, critical that the load cell is minimally higher than the surface the ski is resting on so that it can slide under the whole length of the ski with minimum influence on the applied load and load distribution. An option is to use a spring to allow for slight lifting. The testing and analysis of these challenges are discussed in Chapter 6.

5.2.1 Construction

Materials

The prototype is mainly constructed of polylactic acid(PLA) and steel bars. The PLA parts are 3D-printed with an infill of 5% to avoid excessive use of plastic, except for the parts where screws are used, or where the part is expected to be loaded significantly. The parts are screwed or glued to a 48x198x220mm timber plank.

Width of Gap

It is important to find the right gap between the surfaces the ski is resting on. Since the ski is loaded with up to 80 kilograms, it is important that it has a big enough area as support to avoid damage to the ski and its base. It is also important that the sliding part in contact with the ski is wide enough to avoid a load concentration damaging the base of the ski. This was simply tested by 3D-printing a part and resting the ski on it with a person standing on the ski. Another 3D-printed part was then pulled under the ski with a wire to see whether the ski was damaged.

5.2.2 Sensors

Load Cells

To be able to use sensors for the prototype, it is necessary to use a computer that allows the control of electrical components for physical computing. Therefore, a Raspberry Pi is ideal. This cheap and small-sized computer provides a set of GPIO (general purpose input/output) pins that allows this. The wiring schematic can be found in Appendix D.

Two load cells were used with the Raspberry Pi, an S-type and a single point load cell, shown in Figure 5.4a and 5.4b, respectively. Both these load cells have a half-bridge configuration, a configuration discussed in Section 2.4. The S-type load cell has a capacity of 100kg and the single point load cell a capacity of 50kg. Test results that verify the use of these sensors can be found in Appendix E.

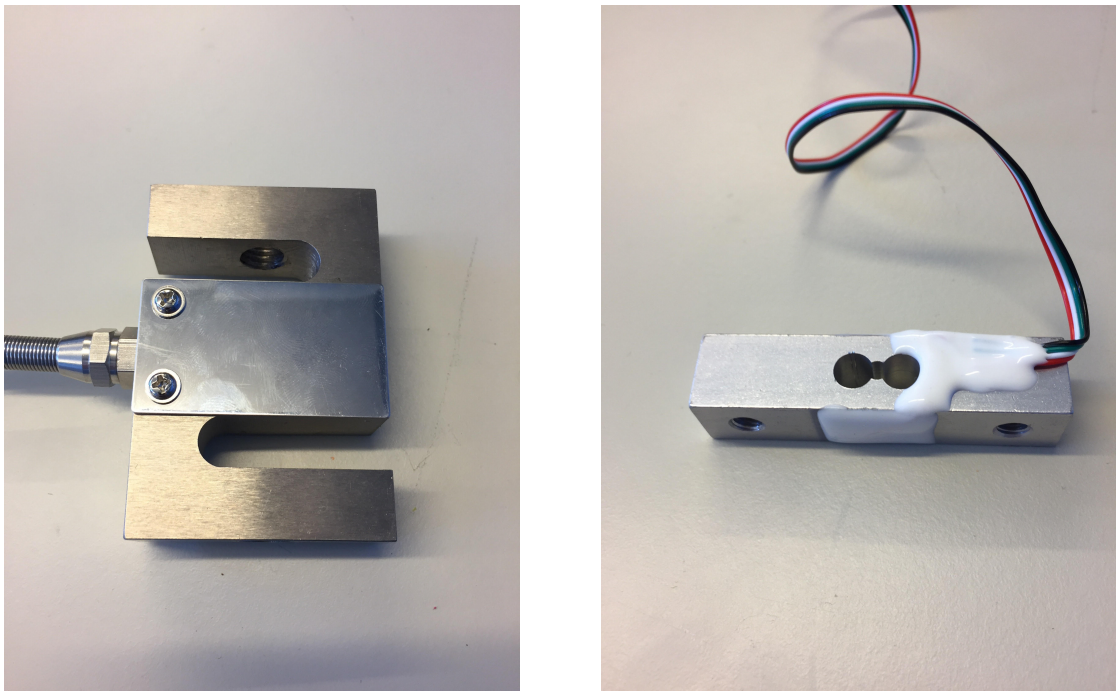

(a) (b)

Figure 5.4: S-type (a) and single point (b) load cell

The single point load cell was chosen due to the fact that it is small in size, meaning that it can slide through a narrow gap. The S-type load cell was chosen because it is suitable for clamping down on the ski. It is also only two centimeters wide in one direction, which results in great accuracy when it comes to position on the ski and where the ski is to be loaded for optimal results.

In addition to these two sensors, a 100kg disc load cell borrowed from OLT was used. This load cell comes with software, which is simple to use. Figure 5.5 shows the disc load cell with the load cell and software.

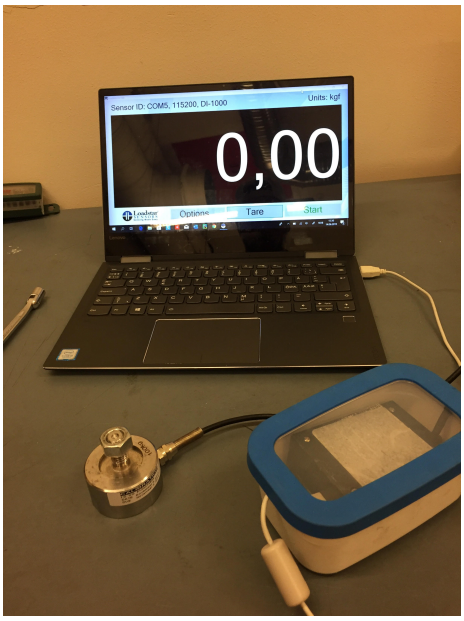

Figure 5.5: Loadstar disc load cell with software

Analog-to-Digital Converter

The load cells used with the Raspberry Pi outputs an analog signal in the millivolt range. It is, therefore, necessary to amplify the signal. This is done by using an analog-to-digital converter, in this case an HX711 [34], which is specifically designed for weight scale operations. This amplifier has a resolution of 24 bits.

Distance Sensor

The distance sensor used for the prototype is a HC-SR04, which is an ultrasonic sensor that sends a high frequency sound of 40Hz, which is reflected off an object and received by the transmitter, as shown in Figure 5.6. The properties of the sensor are shown in Table 5.1.

Table 5.1: Distance sensor properties[19]

HC_SR04	
Minimum range	2cm
Maximum range	4m
Accuracy	3mm
Effectual angle	15°
Working frequenzy	40Hz
Working voltage	5V

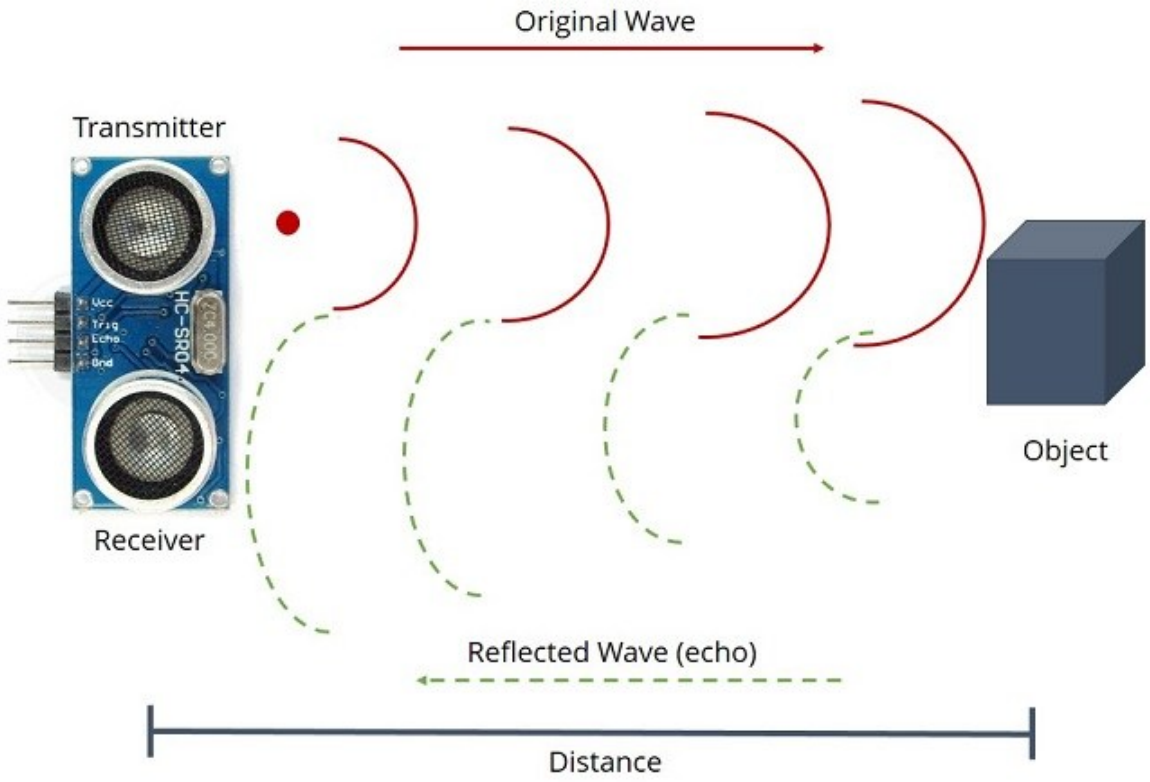

Figure 5.6: Distance sensor, how it works [17]

This sensor was chosen as it is simple to use and program and also has a resolution that is sufficient in proving this particular concept. Test results that verify the use of this sensor can be found in Appendix E.

5.2.3 Software

To use the sensors, it is necessary to write a code that sufficiently collects and processes the sensor readings. A python program was, therefore, developed. The full code can be found in Appendix A. The Pi.GPIO package was used, which allows for communication between the GPIO pins on the Raspberry Pi and the sensors.

A library for the HX711[35] exists and was used throughout the code. The code allows for the possibility to calibrate both load cells every time the code is run. Depending on the type of test to be carried out, the user can choose whether or not both sensors shall be used.

To improve the accuracy of the load sensor, the number of measurements averaged can be adjusted. With fewer data values averaged, less time is spent per loop in the code. Consequently, the rate of data values saved to the lists increases. Therefore, if a similar resolution is wanted, it is necessary to decrease the speed of which the sensors travel.

The data collected through running the code is saved to a CSV-file. The code asks for a file name that identifies the ski, the load, and the type of test carried out.

5.3 Test of Concept

Before a full length prototype was built, it was necessary to test if the prototype was able to provide adequate results with well working sensors. Therefore, a shorter version was built as shown in Figure 5.7. The distance the sensors can slide in this setup is approximately 60cm. Figure 5.8a and 5.8b shows the setup with a loaded ski.

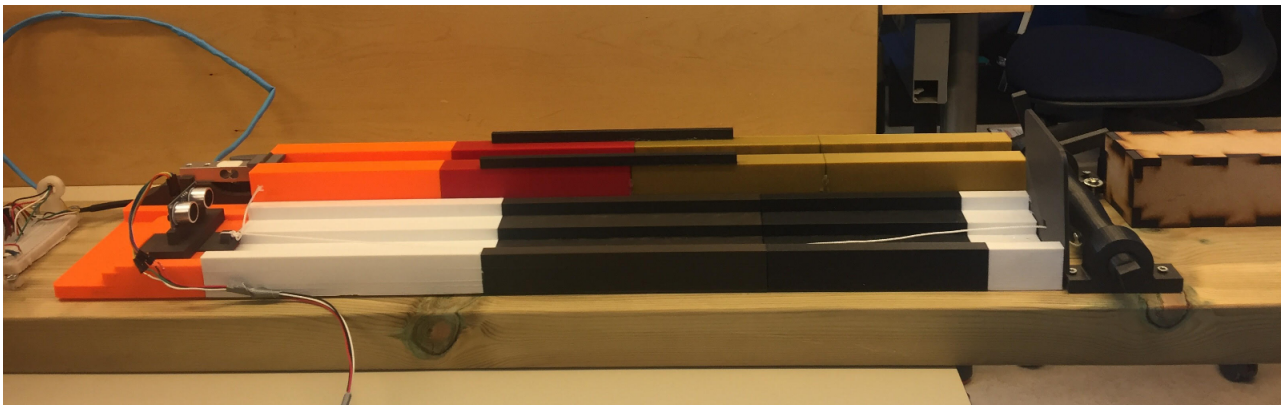

Figure 5.7: Side view of test setup

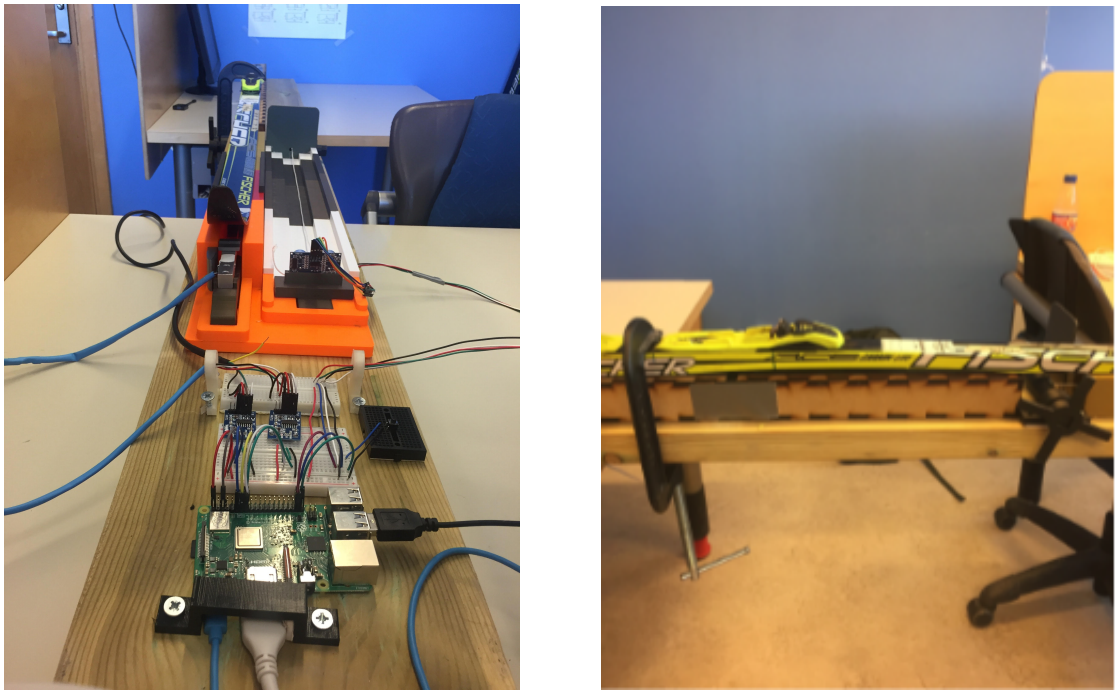

(a) (b)

Figure 5.8: Loaded ski on the concept test with front view (a) and side view (b)

The ski was loaded with the use of a clamp. The load was not measured, but the clamp was tightened sufficiently, meaning that the ski was pressed to the ground with a decent amount of force. The ski was loaded in the correct position, 14cm behind the binding locking mechanism. Figure 5.9a and 5.9b show the plot of the data achieved from the prototype test.

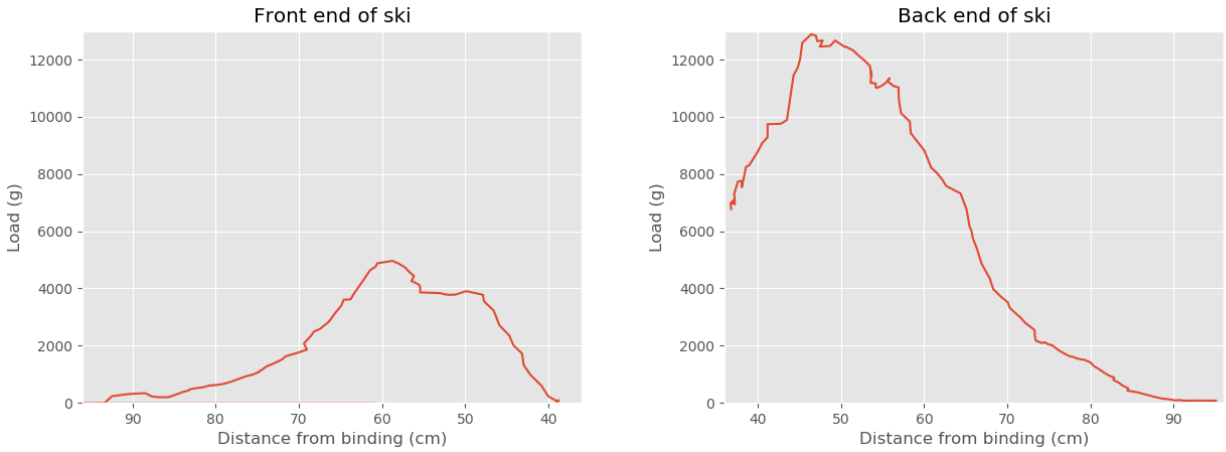

(a) (b)

Figure 5.9: Load distribution front end (a) and back end (b) of ski

The graphs show a solid representation of the load distribution, with a curvature that seems reasonable compared to what was discussed in Section 3.2.3. It is important to understand that the area under the graph does not have a direct relationship to the load applied to the ski, as it does for the OLT pressure distribution setup. In this case, the area under the graph is related to work, which is given by:

$$W = F * D * cos(\omega) \tag{5.1}$$

where

$$F = ma \tag{5.2}$$

The area under the graph will not represent the work necessary to slide the load cell under the length of the ski. This would be related to the friction from both the sliding surface and the friction from the contact between the ski and the load cell. In this case the force on the wire would be the force of interest. The resulting work of interest in this thesis, on the other hand, is the load on the load cell along the length of the ski.

It is to be noted that the back end of the ski was tested by sliding the sensor from the back towards the center of the ski as the setup required the ski to be turned 180 degrees to measure this end. This means that this measurement is not representative of a full length setup, but it is sufficient for testing the concept. Reasonable graphs, well working sensors, and the fact that it is necessary to test the setup closer to and under the load, meant that building a full length prototype was justifiable.

5.4 Test of Final Concept

Two skis were used in the test of the final developed concept. One was from a pair of medium classic skis with a length of 202cm, and one was from a pair of stiffer skate skis with a length of 191cm . The classic ski was measured at the OLT setup beforehand to assure the possibility of comparison. The bindings on both pairs of skis were removed to assure a plane surface for the load cell. The load was applied 14cm behind the binding if no specified otherwise.

Clamp Load

In the first loading setup, the ski was loaded with a clamp only. This means that the ski does not have the ability to be lifted further from the surface. Figure 5.10 shows the loading of the ski with the S-type and disc load cell.

(a) (b)

Figure 5.10: Clamp load setup with S-type (a) and disc (b) load cell

Spring Load

In the second loading setup, a spring was used in series with the load cell loading the ski. Since the spring is in series with the load cell, it does not matter whether the load cell is under or on top of the spring. This setup allows for the ski to be lifted, as the load does not lock the ski in position. The properties of the spring used, shown in Figure 5.11, is presented in Table 5.2.

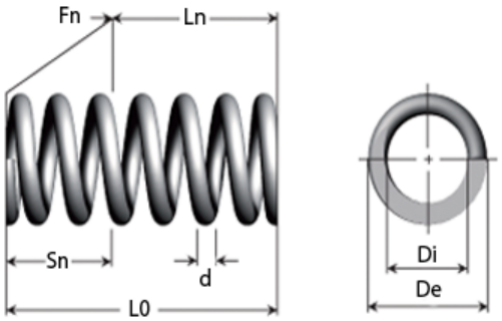

Figure 5.11: Spring properties [18]

Table 5.2: Spring properties[18]

Property	Abbreviation	Value
Wire diameter (mm)	d	5
External diameter (mm)	De	45
Internal diameter (mm)	Di	35
Unloaded length (mm)	L0	64
Max. loaded length (mm)	Ln	29.6
Maximum travel (mm)	Sn	34.4
Maximum load at Ln (N)	Fn	980.67
Spring constant (N/mm)	R	28.34

Several factors influenced the choice of spring. The maximum spring load had to be sufficient when knowing the maximum load to be applied to the ski. Additionally, a low spring constant was desired to allow the ski to be lifted. With this spring, less than a 3kg load is required to result in a 1mm travel. The spring had to be short enough to be able to fit under the clamp mechanism. A longer spring would also be harder to handle when loading the ski. The diameter of the spring had to be small enough to fit the load cell and the ski. Figure 5.12 shows the loading of the ski with the spring.

Figure 5.12: Clamp load setup with spring

5.4.1 Test Procedure and Experimental Aspects

To understand the nature of the results, it is necessary to have an understanding on how the tests were performed.

The environment for which the tests were performed is shown in Figure 5.13. When the ski is placed on the setup, the appropriate load cell, with or without the spring, is placed on top of the ski at the desired position for loading. Thereafter, a clamp is used to load the ski with the desired load. When the clamp is tightened to the correct load, the load distribution of

the ski can be measured. The button is pressed to start collecting data from sensors in use. The moving sensors are then pushed throughout the length of the ski. When the two sensors have moved the full length of the setup, the button is pressed again and the data is saved to a CSV-file. The ski is then removed from the setup and the sensors are moved back in starting position. Once all the tests were completed, the data was plotted and the area under the curves were calculated. The stiffness of the tip and the tail of the ski was tested by pushed the load cell a set distance under the ski and then loading the ski increasingly up to 80kg. More images of the prototype can be found in Appendix F. The following tests were performed following the above procedure:

- Three identical tests of the classic ski to test repeatability
- Tests with three different lifting heights on the classic ski
- 10-80kg applied load with a 10kg step increase for both a classic and a skate ski with the clamp setup
- 10-60kg applied load with a 10kg step increase for the classic ski with the spring setup
- 10-70kg applied load with a 10kg step increase for both a classic and a skate ski with the spring setup and an increased lifting height of 0.5mm
- Relocation of the applied load 10cm in front of and behind the load location used for the other tests for both skis
- 10-70kg applied load with a 10kg step increase for the classic ski with a load location 8cm behind the binding
- 10-80kg applied load for two different classic and two different skate skis with a 1.5cm lifter and a 1cm lifter for the tip and tail of the ski, respectively

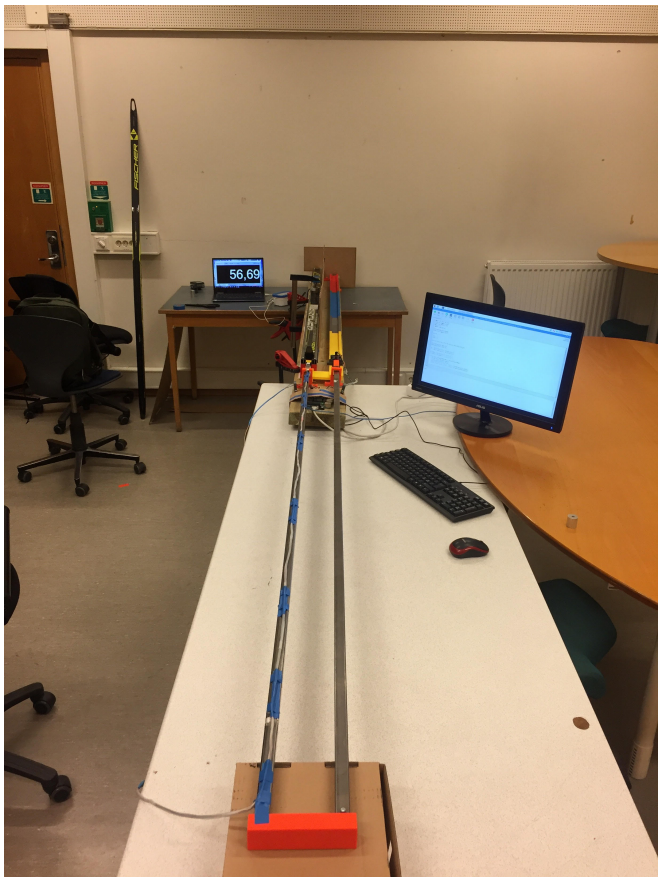

Figure 5.13: Test setup and environment

The different loading setups were tested over a period of two weeks. The reason for the time span was the presence of variation in the load cell. After a certain amount of testing, it became evident that the load cell showed a lower load, even though there was no load applied. Consequently, loading the load cell with a known mass resulted in an incorrect increase in the output from the load cell. Since the load cell was subjected to this problem, the output from the load cell was checked often to make sure the results were reliable. Calibration was tried to overcome this, but it did not work sufficiently. The reason for this is most likely that some of the strain resulting from the applied load did not fully recover fast enough after extensive use. Therefore, the test was stopped once the load cell did not output the correct values. A break was used to let the load cell recover. It was then observed that the load cell was back to normal when returning to testing the next day.

Since the setup has some unevenness present, the ski was placed on the setup in the same position for every test run. The same was done with the load cell loading the ski. Still, it was impossible to load the ski in the exact same position every test. Hence, there is a small potential error as a result of this. Another aspect of the loading was the clamping mechanism.

When the ski was placed on the setup and loaded, the sliding sensors were pushed throughout the length of the ski. An effort was made to make the speed of which the sensors were pushed as even and similar as possible throughout the run for all the tests performed. A small twist possible in the pushing mechanism, shown in the bottom of Figure 5.13, made it impossible to keep the sensors exactly side by side throughout the measurement. Therefore, a small potential error was present here as well.

6 Results and Discussion

6.1 Repeatability

To assure that the setup provides sufficient results, it was necessary to test the repeatability of the setup. Figure 6.1 shows the data from three different tests with the clamp setup and 40kg load. The plot shows that the three tests correspond well, with some variation in the peak load as shown in Table 6.1. The peak locations vary by approximately 1.8cm at the maximum, which is considered acceptable. Looking at the integral values in the table, there is a 14 percent difference between the two extremes. Hence, the integral values can only be used as an approximation when looking at the development when it comes to the different loads applied to the ski. The integrals are calculated using the trapezoidal rule. The code used to calculate the integrals can be found in Appendix A.

It is to be noted that a minor adjustment to the setup was made after these tests were run that resulted in a slight increase in load distribution. Therefore, the results presented in the table below do not correspond to the test with similar load and test setup. Still, this is considered not to influence the validity of the repeatability test. Additionally, the raw data achieved from the tests contained outliers, varying in the amount. These outliers were adjusted to smooth the curves. The raw data can be found in Appendix C.

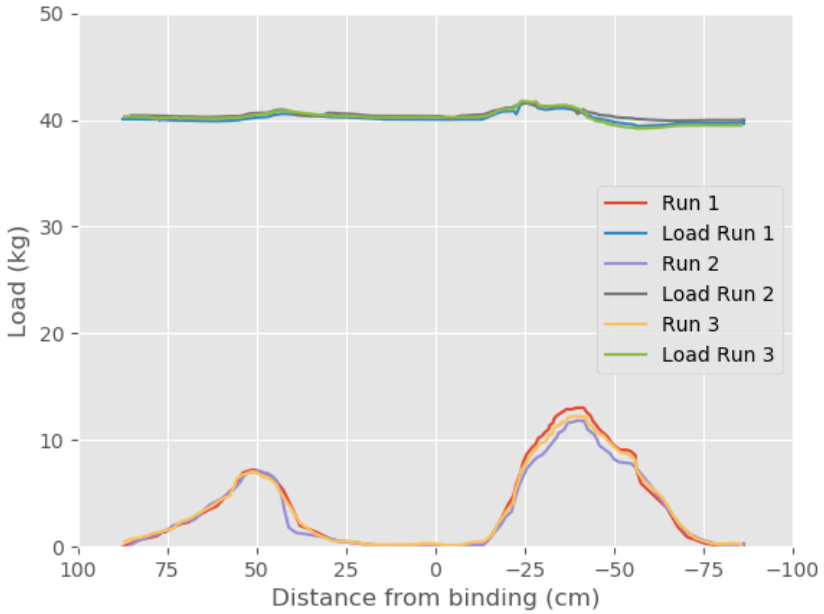

Figure 6.1: Test of repeatability of setup

Table 6.1: Data for repeatability test

Run	Peak front end		Peak back end		Integral	Percent difference
	Load(kg)	Position(cm)	Load(kg)	Position(cm)		
1	7.21	51.33	13.04	-40.12	632.4	-
2	7.08	49.70	11.84	-39.8	544.1	14.0
3	7.04	51.49	12.25	-40.38	576.4	8.9

6.2 Comparison of Different Lifting Heights

As discussed in Section 5.2 , the minor lifting of the ski influences the load distribution. Therefore, to get a better understanding of the extent of this influence, the setup was tested with three different heights of lifting with a 40kg load. Figure 6.2 shows the ”lifters” used. It is to be noted that this test was performed with the same setup as the repeatability test, with the clamp setup where a small adjustment was made afterwards that increased the lifting height slightly. The clamp setup was used to be able to see the development in applied load. This means that the results from this test are not comparable to the other tests, but they are equally reliable.

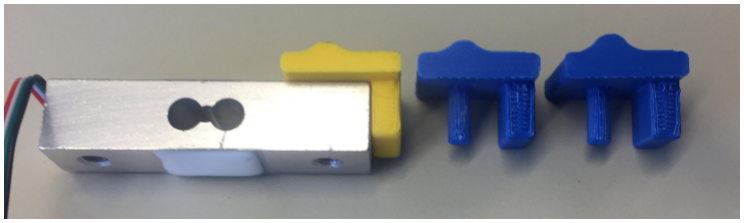

Figure 6.2: The three different ”lifters” used

It was expected that an increase in lifting height would result in an increase in both applied ski load and load distribution. Looking at the results in Figure 6.3, where a 40kg load was used, the plot shows a significant increase in both, as expected. The +0mm plot represents the same ”lifter” as used in the previous section, while the others represent a 1 and 2mm increase in lifting height, relative to the first one. As seen in Figure 6.3, both the +1mm and the +2mm test resulted in constant contact between the ski and the ”lifter” throughout the length of the ski, even though it is known that there is a pocket underneath the center of the ski not in contact with the surface. As this test was performed with a 40kg load, an increase in load would affect this trend significantly. The results emphasizes the importance of minimizing lifting height. It is to be noted that the peak of applied load for the +2mm test is not present as the ski started sliding off the setup where the peak is located, about 12cm behind the binding. This is also the reason why the load decreased significantly more than expected. Furthermore, it is expected that the use of a spring would decrease the trends seen in Figure 6.3 significantly, but would not fully eliminate them.

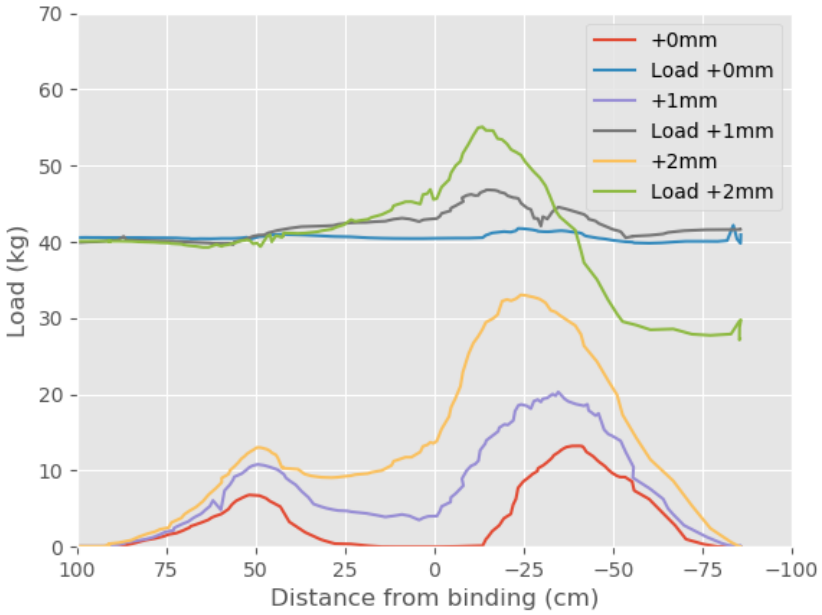

Figure 6.3: Plot of the three different lifting heights with a 40kg load

6.3 Analysis of Classic Ski

6.3.1 Clamp Setup

Figure 6.4 shows the results from the test with the clamp setup. The step load increase of 10kg shows a gradual increase of load. Additionally, the peak load moves towards the center of the ski, as predicted. The peak loads for the tests with 40 and 50kg seem to be outliers as they are too close to the 60kg measurement, as seen in Table 6.2. This is underlined by the peak load of the front end of the ski, which exceeds the value from the 60kg test.

With an applied load of 40kg or more, the sliding load cell is in contact with the ski where the ”pocket” of the ski is located. As the ski is pressed closer to the ground with increasing load applied, the extent of this contact increases. The area under the curves increases gradually with the increase of applied load. As seen in Table 6.2, the percentage increase of the integral value decreases significantly at higher loads. This is further discussed in Section 6.6. It is to be noted that the percentage increase columns represent the increase in percentage compared to the load represented in the row above in the tables. This is true for all the tables in this chapter.

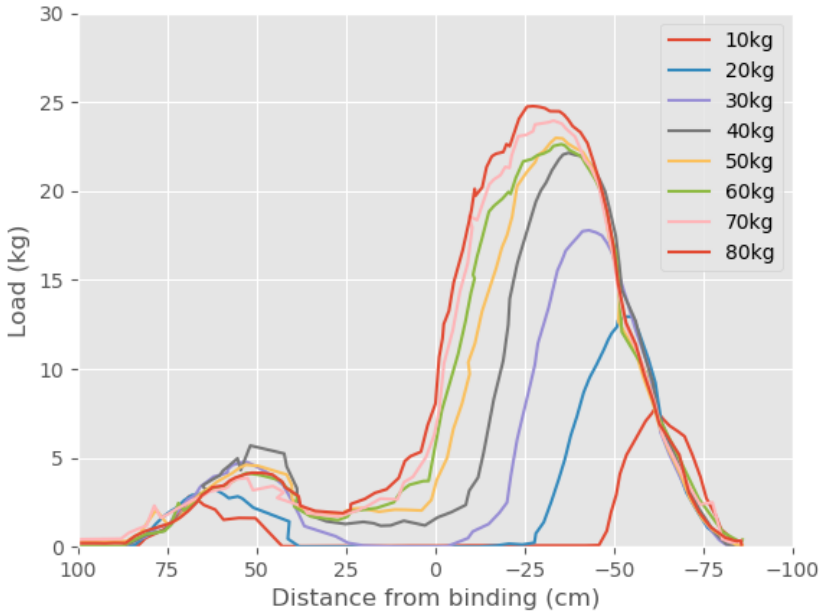

Figure 6.4: Plots of tests 10-80kg with clamp setup

Table 6.2: Data for 10-80kg load for classic ski with original lifting height

Load(kg)	Peak front end		Peak back end		Integral	% increase
	Load(kg)	Position(cm)	Load(kg)	Position(cm)		
10	2.87	67.98	7.68	-61.09	222.5	-
20	3.24	61.76	12.94	-53.13	443.6	99.4
30	4.75	52.61	17.79	-42.95	777.6	75.3
40	5.69	51.84	22.15	-37.24	1105.6	42.2
50	4.61	53.05	22.99	-33.68	1219.9	10.3
60	4.14	52.92	22.63	-35.21	1307.6	7.2
70	3.87	52.63	23.96	-33.02	1381.9	5.7
80	4.16	51.44	24.77	-27.28	1482.0	7.2

Comparison to Skate Ski

An in depth analysis of all the different aspects regarding one specific ski is important. Still, it is necessary to compare this to a different type of ski to see if the results are only valid for the ski tested thoroughly, or if the results can be validated by a different ski. Therefore, a skate ski with different properties was tested. Figure **??** shows the plots from the test of the skate ski with the clamp setup.

An important difference between the classic and skate ski tested is that the skate ski has a section underneath the center of the ski where the sensor is not in contact with the ski, as seen in Figure 6.5. This is true even with a 80kg load. As seen in Figure 6.4, there is contact with the sliding sensor throughout the entire center part of the ski when the load on the ski is 40kg or more. As discussed earlier, this contact influences the resulting integral values significantly, which is not desireable. Comparing the values in Table 6.2 and 6.3 shows this issue clearly when

looking at an applied load of 40kg or more. In Section 2.3.2, the ”pocket” difference between skate skis and classic skis was discussed. This discussion corresponds well with what is seen in the results. The fact that the prototype developed is not accurate enough to provide minimum lifting of the ski makes it seem reasonable that the contact between the classic ski and the sliding load cell can be eliminated, at least partly, with a more accurate setup that allows for the lifting to be 0.3mm or less.

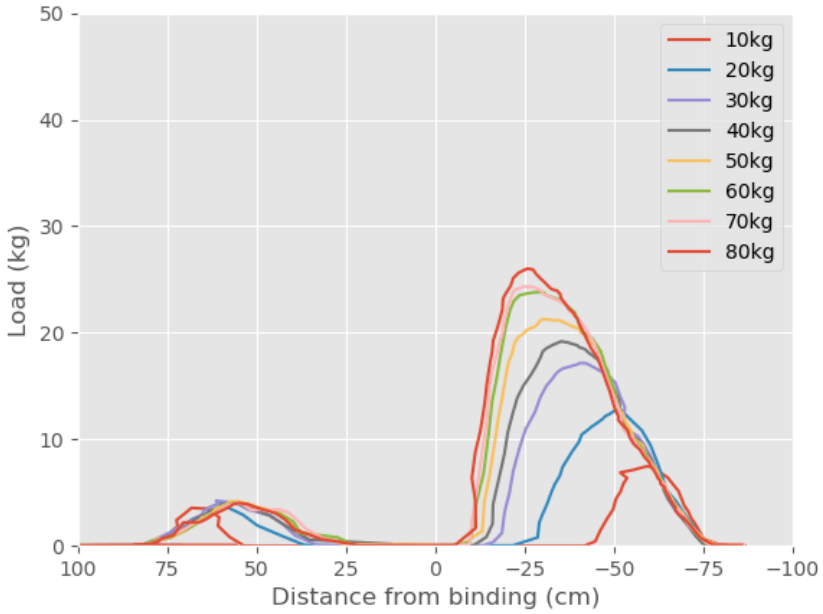

Figure 6.5: Plots for skate ski with 10-80kg load, clamp setup

Table 6.3: Data for 10-80kg load for skate ski with clamp setup

Load(kg)	Peak front end		Peak back end		Integral	% increase
	Load(kg)	Position(cm)	Load(kg)	Position(cm)		
10	3.56	68.3	7.45	-59.1	200.7	-
20	4.08	58.5	12.81	-51.7	449.3	123.9
30	4.24	59.4	16.93	-43.33	710.2	58.1
40	4.05	57.3	19.19	-35.19	814.1	14.6
50	4.18	55.5	21.27	-30.5	939.6	15.4
60	4.01	54.8	23.82	-29.0	1036.2	10.3
70	3.99	54.2	24.33	-24.5	1048.5	1.2
80	4.02	54.8	26.02	-25.7	1080.1	3.0

6.3.2 Development of Applied Load

An interesting aspect revealed itself during testing. Figure 6.6 shows the increase in load with the clamp setup for four different loads, starting at 20kg, with a 20kg increase for each test.

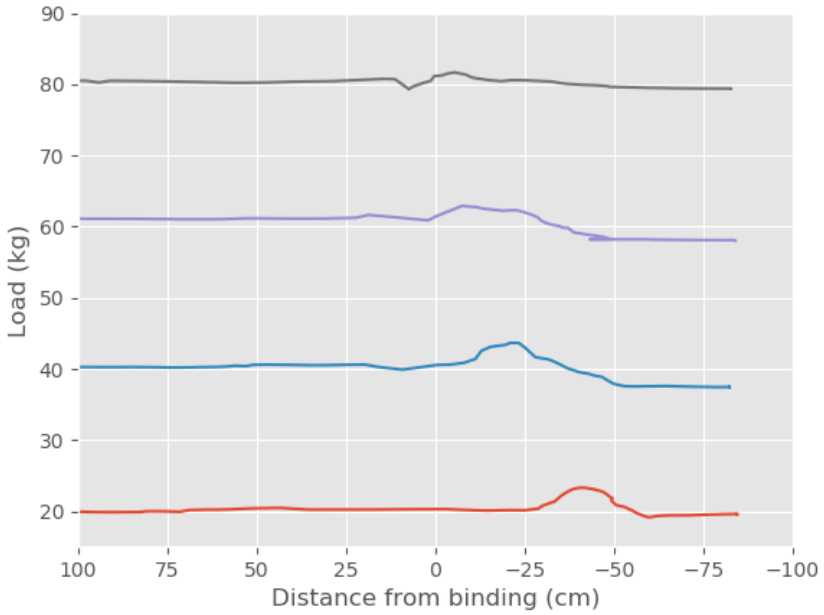

Figure 6.6: Development of applied load

As seen in the figure, there is a greater increase of applied load for the lower loads. With 20 and 40kg loads, the increase in applied load is significant. Contradictory, the increase in applied load increases much less with higher loads applied before the load cell was slid under the ski. There is a chance that the sliding load cell is loaded by an amount that pushes it down to the level of which the ski is resting on. The part the sliding load cell is attached to is 3D-printed with 100% fill. A metal part was considered, but since there is a present unevenness of the surface the ski is resting on, it was decided that it was necessary to allow the load cell setup a minor compression to avoid potential damage to the ski. That being said, the load distribution in Figure 6.4 shows a clear increase in load for all measurements. Still, the increase decreases significantly when the load is increased from 40 to 50kg, as seen in Table 6.2. Whether this change in percentage increase comes from this, or that the load is distributed over a greater length of the ski, is uncertain.

Further testing with a step increase in lifting height of 0.2mm showed that the applied load kept increasing for applied loads higher than 40kg. From this, it is then concluded that only the results up to and including 40kg are trustworthy in Figure 6.4 and 6.5. Since an increased lifting height resulted in great resistance when pushing the load cell underneath the length of the ski, it was concluded that a spring setup was necessary when testing.

6.3.3 Comparing to Spring Setup

Even though it was concluded that the use of a spring with an increased lifting height was necessary, a test of the classic ski with the same lifting height as in Figure 6.4 and 6.5 was run to look into the differences in load measured by the sliding load cell. Figure 6.7 shows the results from the test. It is to be noted that the test is performed up to a 60kg applied load. As seen in Table 6.4, the loads are lower than for the clamp setup, as expected. Still, for loads higher than 40kg, the same development is registered, where the change in the increase in load decreases significantly. In other words, a higher lifting height is confirmed necessary.

This is also emphasized by that the peak load on the front end of the ski is on a consistent level throughout the measurements as seen in Table 6.2, Table 6.3, and Table 6.4. Even though the resolution of the setup is not optimal and the peak might not get registered for that reason, this consistency of low loads seem to show invalid results in this area. This is further discussed in Section 6.3.4.

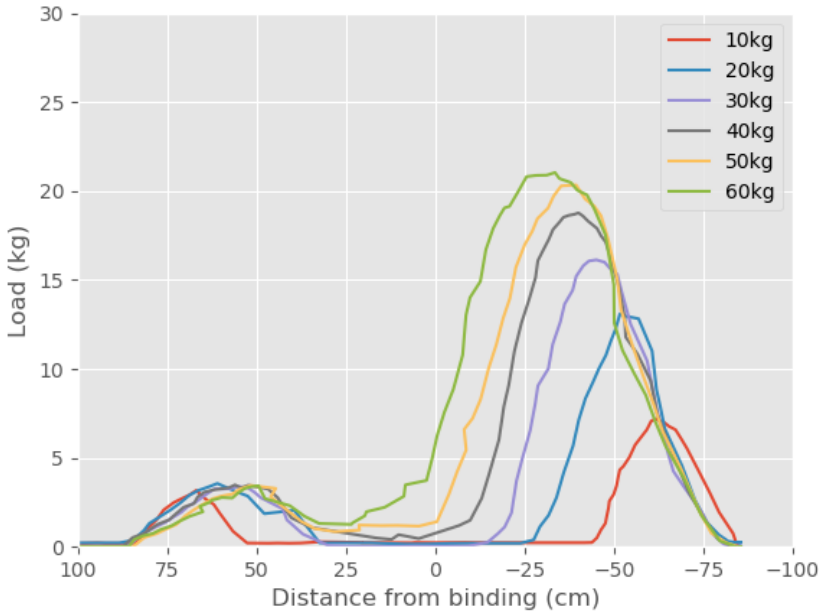

Figure 6.7: Plots of tests 10-60kg with spring setup

Table 6.4: Data for 10-60kg load for classic ski with original lifting height

Load(kg)	Peak front end		Peak back end		Integral	% increase
	Load(kg)	Position(cm)	Load(kg)	Position(cm)		
10	3.17	66.99	7.19	-61.7	215.2	-
20	3.56	61.06	13.1	-51.64	439.0	104.0
30	3.39	55.22	16.13	-45.05	648.1	47.6
40	3.48	56.11	18.77	-40.01	879.2	35.7
50	3.45	51.7	20.34	-39.35	1026.8	16.8
60	3.43	49.54	21.04	-33.44	1213.2	18.2

6.3.4 Tests with Increased Lifting Height

Increasing the lifting height by approximately 0.5mm changed the results significantly. Firstly, the development of the peak load for the front end of the ski, changed significantly. As discussed in Section 6.3.3, the load on the front end of the ski was consistent even though the applied load increased. With the increased lifting height, on the other hand, this load increased as the applied load increased, as expected. Table 6.6 looks into the load distribution for the first three measurements, with 10, 20, and 30kg applied load. As seen in Figure 6.8 the base of the ski is in contact with the sliding sensor under the 'pocket' of the ski. Therefore, it is not possible to compare the load distribution. Still, it is easy to see from the plots that the load distribution

is transitioning to the back end of the ski. As seen in Table 6.6, the load distribution is consistent for the 10 and 20kg applied load, but for the 30kg load the distribution starts to shift significantly. Looking at the data in Table 6.5 the increased lifting height makes the peaks move slightly towards the center of the ski if compared with Table 6.4.

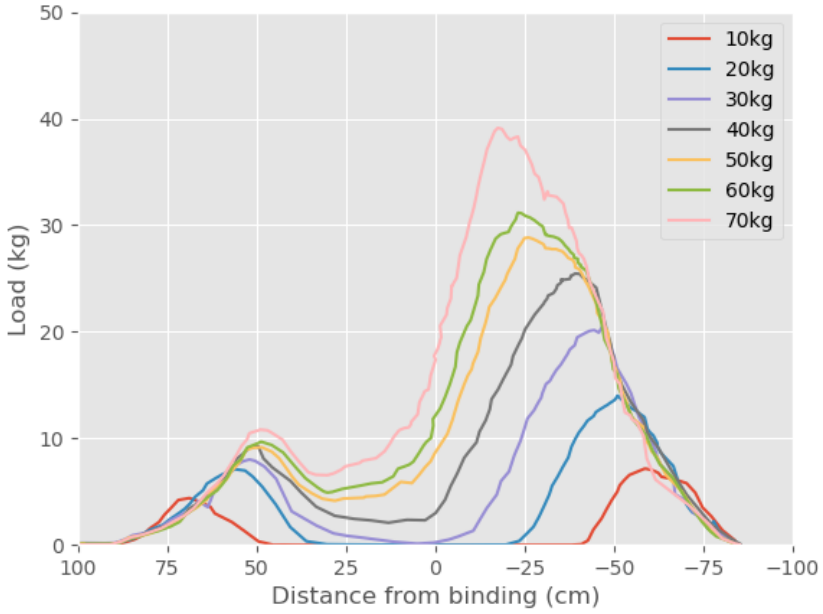

Figure 6.8: Plots of tests 10-70kg with increased lifting height

Table 6.5: Data for 10-70kg load for classic ski with increased lifting height

Load(kg)	Peak front end		Peak back end		Integral	% increase
	Load(kg)	Position(cm)	Load(kg)	Position(cm)		
10	4.39	68.88	7.15	-58.51	270.4	-
20	7.1	56.13	13.98	-50.96	610.3	125.7
30	8.01	52.04	20.53	-46.76	968.2	58.6
40	9.25	49.61	25.46	-39.09	1425.5	47.2
50	9.16	48.63	28.84	-26.0	1753.0	23.0
60	9.68	48.77	31.16	-23.11	1939.0	10.7
70	10.81	49.03	39.12	-17.44	2334.4	20.3

Table 6.6: Data for load distribution for classic ski with increased lifting height

Load(kg)	Front end	Back end	% Distribution
10	90.6	179.9	33/67
20	197.6	423.2	32/68
30	223.7	746.1	23/77

Comparison to Skate ski

As mentioned earlier, it is important to see whether the setup is able to seperate the skis. Figure 6.9 shows how the load for the skate ski increases significantly faster for the back end of the ski, especially for higher applied loads. Additionally, the peak load on the back end of the ski is higher than for the classic ski, except for the 70kg load, which seems to be an outlier in the results for the classic ski. Because of the constant contact between the base of the classic ski and the sliding load cell, it is difficult to compare where the contact zones begin compared to where they do for the skate ski. Also, the skate ski is shorter, which emphasizes the difficulty. Looking at the integral values, it is hard to make a comparison for the same reason. This is also underlined by Section 6.1, where there was a significant variation in integral values for the same exact test. It is to be noted that the tests with the spring setup only have measurements up to 70kg. The reason for this is that it was too difficult to tighten the spring to 80kg.

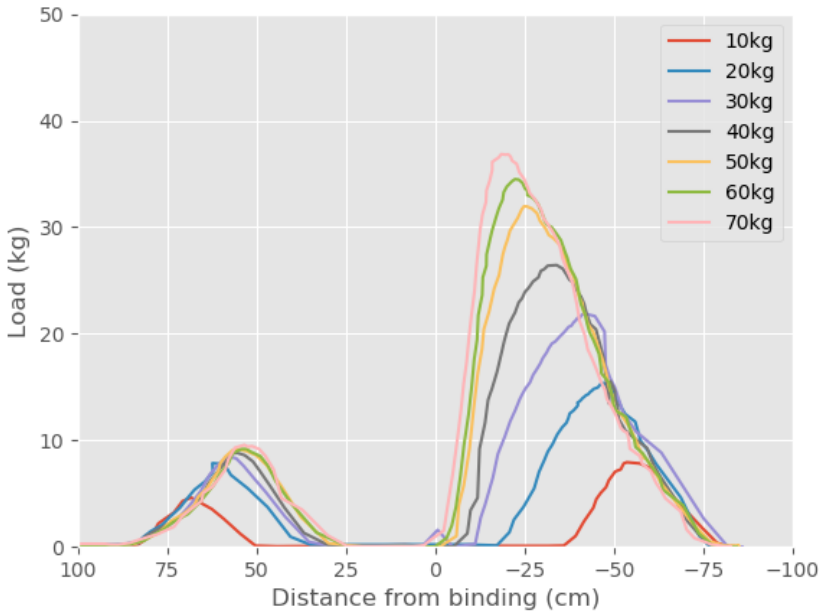

Figure 6.9: Plots of 10-70kg loads with increased lifting height

Table 6.7: Data for 10-70kg load for skate ski with increased lifting height

Load(kg)	Peak front end		Peak back end		Integral	% increase
	Load(kg)	Position(cm)	Load(kg)	Position(cm)		
10	4.62	68.39	7.94	-53.56	278.1	-
20	7.85	62.45	15.37	-47.27	666.7	139.7
30	8.48	58.05	21.87	-41.75	1035.9	55.4
40	8.83	55.57	26.44	-33.92	1208.0	16.6
50	9.16	55.29	31.95	-24.76	1430.5	18.4
60	9.18	52.92	34.5	-22.23	1527.6	6.8
70	9.57	53.49	36.85	-18.41	1570.9	2.8

Since the sliding load cell is not in contact underneath the center of the skate ski, it is possible to look into the aspect of load distribution between the front and back end of the

ski, as briefly discussed in Section 6.3.4. Table 6.8 shows these distributions, using the area under the curve. Looking at data, the distribution transitions over to the back end. The lowest applied loads has a more balanced distribution, while the mid and higher applied loads develop into a less balanced distribution. This trend was also seen for the classic ski even though only three load distributions were calculated. Further testing of others skis has to be conducted to get a better understanding of these trends.

Table 6.8: Data for load distribution for skate ski with increased lifting height

Load(kg)	Front end	Back end	% Distribution
10	84.8	228.4	27/73
20	175.1	513.7	25/75
30	221.1	824.4	21/79
40	259.0	999.2	21/79
50	258.2	1184.1	18/82
60	278.6	1287.8	18/82
70	258.5	1339.1	16/84

6.3.5 Relocation of Load

To see how the load distribution varies depending on where the ski is loaded, the load was moved 10cm in front of and behind where the load has been applied. Figure 6.10 shows significantly different results for the different locations. The test with the load location 10cm closer to the tip of the ski stands out. From the plot, one can see that the sliding load cell is in contact with the ski throughout the length of the ski. As discussed in Section 2.3.2, the pocket under the ski is located slightly in front of the binding. Moving the load forward means that the load is located closer to the peak of the pocket. Therefore, the pocket is closer to the surface, which results in contact between the ski base and the sliding sensor. Hence, there is a significant increase in applied load in this area.

Naturally, the load with the applied load further forward is distributed more evenly between the front and the back of the ski, with lower peak loads, as seen in Table 6.9. The plot for the test with the load 10cm closer to the tail, on the other hand, has an increase in load on the back end of the ski and a decrease on the front end. The peak on the back end of the ski seems to stay in the same place. This is not the case for the front end of the ski. In this case, the peak moves towards the center of the ski, as expected. The peak load on the back end of the ski with the load in the standard position seems like an outlier with a peak 4-5cm closer to the center of the ski than the other tests.

It is important to keep in mind that these test are performed with a 40kg load. Loading the ski with an 80kg load would emphasize these trends significantly.

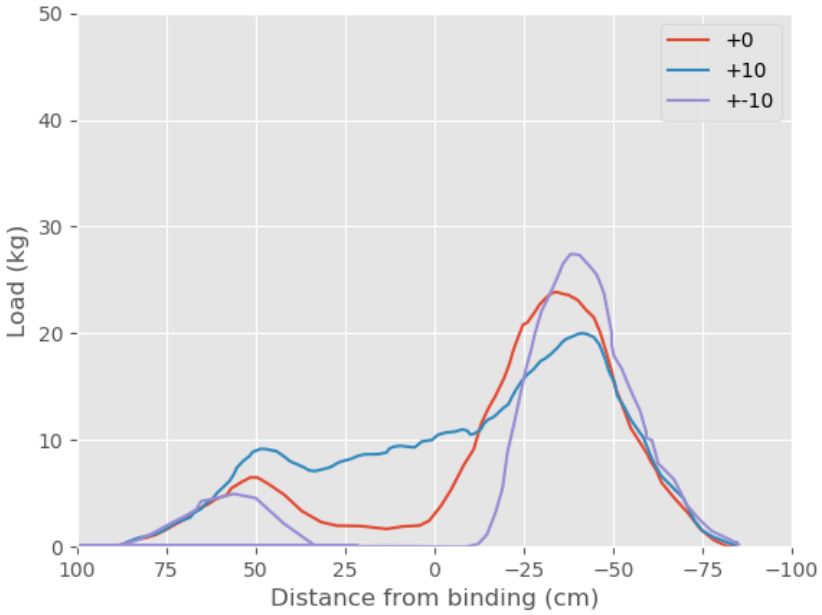

Figure 6.10: Plots for classic ski with varying load location

Table 6.9: Data for relocation of load for classic ski

Location	Peak front end		Peak back end		Integral	% difference
	Load(kg)	Position(cm)	Load(kg)	Position(cm)		
0	6.49	50.59	23.87	-34.13	1272.2	-
+10	9.17	48.73	20.01	-41.13	1490.2	17.1
-10	4.96	56.17	27.43	-38.13	1043.7	18.0

Comparison to Skate Ski

This test looks into the same aspect as Section 6.3.5, but for the skate ski. Comparing the classic ski to the skate ski, it is clear that the sliding load cell is still not in contact under the center of the skate ski, as seen in Figure 6.11. This results in closer integral values than for the classic ski. Even though, theoretically, the pressure distribution for a perfect setup should equal the load applied this is not the case for the concept developed. Moving the load results in the highest integral value for the test where the ski was loaded 10cm closer to the tip of the ski, as seen in Table 6.10. The reason for this is most likely that more of the ski is close enough to the surface of which it is resting on that the sliding load cell is in contact with the ski base for a longer distance. This would increase the area under the curve.

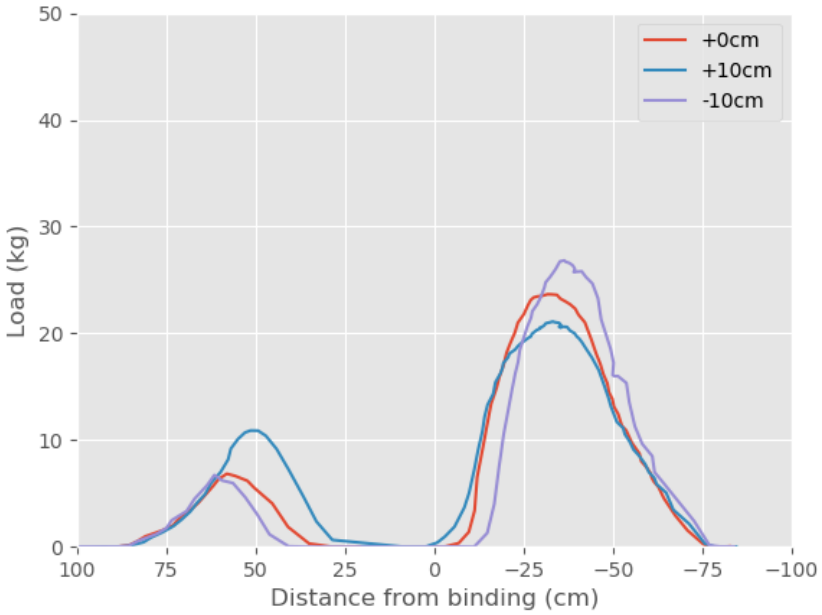

Figure 6.11: Plots for skate ski with varying load location

Table 6.10: Data for relocation of load for skate ski

Location	Peak front end		Peak back end		Integral	% difference
	Load(kg)	Position(cm)	Load(kg)	Position(cm)		
0	6.84	58.14	23.66	-31.66	1065.5	-
+10	10.89	51.51	21.10	-33.08	1164.8	9.3
-10	6.72	61.61	26.83	-36.33	1043.3	2.1

Table 6.11 shows the calculated pressure distribution for the three loading locations. As expected, and seen from the plots in Figure 6.11, the pressure distribution moves in the same direction as the location of the load. Furthermore, the change in distribution is more significant between the load location closer to the tip and and the original location, than for the location closer to the tail and the original location. The reason for this is uncertain.

Table 6.11: Data for load distribution for relocation of load

Location	Front end	Back End	% Distribution
+10	299.7	865.0	26/74
0	173.3	892.2	16/84
-10	134.4	908.9	13/87

6.3.6 Test with Load Located 8cm Behind Binding

To see how the plots change for the classic ski with a change in location and an increase in applied load of 10kg from 10 to 70kg, a test was performed with the applied load 8cm behind the binding. This is approximately where the load is applied while gliding on one ski, as mentioned

in Chapter 3. As seen in Figure 6.12, the contact between the base of the ski and the sliding load cell is even more significant underneath the center of the ski, with the load closing up to the front end peak load as the applied load increases. In other words, for this load location, it is necessary with a decreased lifting height for the results to be usable. It is to be noted that for the test with 70kg applied load, the loading setup failed, which can be seen in the plot.

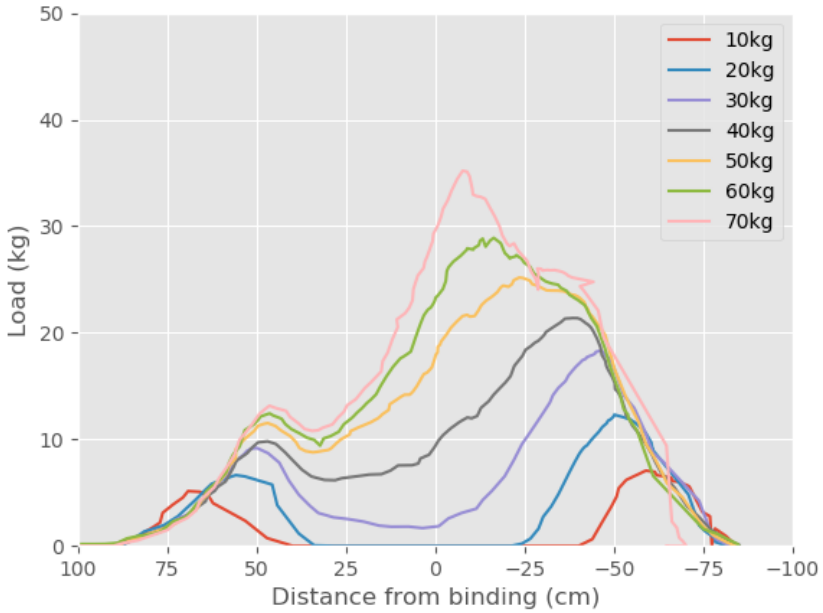

Figure 6.12

6.3.7 Comparison to OLT Data

It is important to compare the results with measurements from the OLT setup. Therefore, the classic ski analyzed in this chapter was measured on the OLT setup as well. The lifting of the ski is proved to influence the load measured by the sliding load cell significantly. Since the setup used by OLT relies on pressure mats, as discussed in Chapter 3, it is reasonable to assume that the peak pressure is significantly lower than for the concept tested in this thesis. The plots from the OLT measurements only can be found in Appendix B.

The plots presented in Figure 6.13 to Figure 6.16 shows the related plots for the OLT setup, the classic ski with the first lifting height and the increased lifting height, both with the spring setup. Three aspects of the plots stand out. Firstly, the peak loads on the front and back end of the ski is significantly higher for the concept developed. Secondly, the pressure mats used by OLT show clearly the variation in load. The tests from this thesis, on the other hand, has a smooth curvature with two clear peaks. This means that the sliding load cell is not capable of revealing these small changes. Still, this was expected. As seen in Figure 2.8, the back end of the ski has a couple of spots not in contact with the surface. The height of these tiny ”pockets” is less than 0.2mm, which means that the lifter will not detect them. Theoretically, with a minimal lifting height, these could be shown on the plots. Lastly, the contact zones are significantly longer for the concept tested. This is expected as the lifter will be in contact with the ski for a longer section than the actual contact zone. This also increases the are under the curve compared to a setup not lifting the ski.

The peaks in the different plots seem to correspond well throughout all the loads. All the plots have their peaks move towards the center of the ski, as expected. Still , there are some differences. This could come from the fact that the setup developed is subject to some measurement errors. For example, it was difficult to slide the sensors side by side exactly. It is expected that, with a quality setup with minimum lifting height, these differences will disappear.

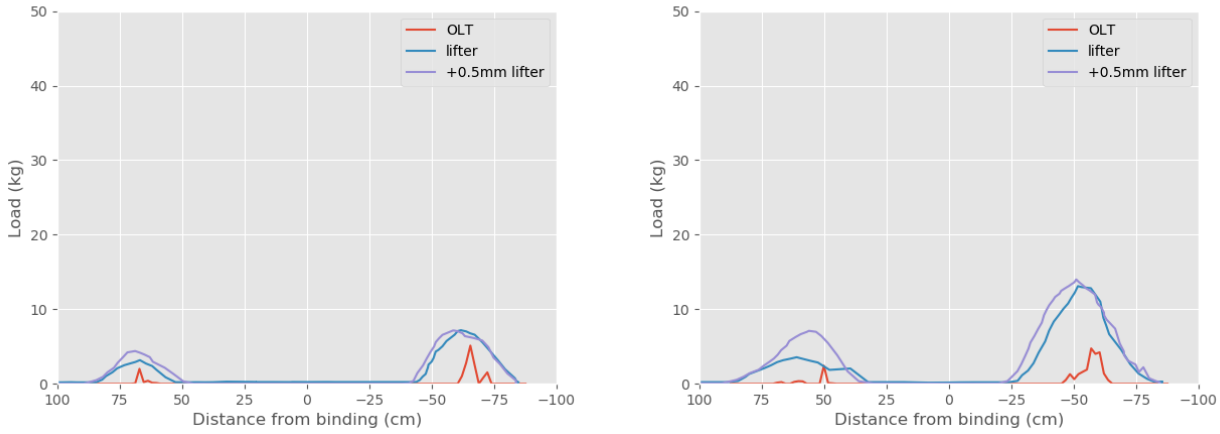

(a) (b)

Figure 6.13: Plot with 10 (a) and 20 (b) kg load

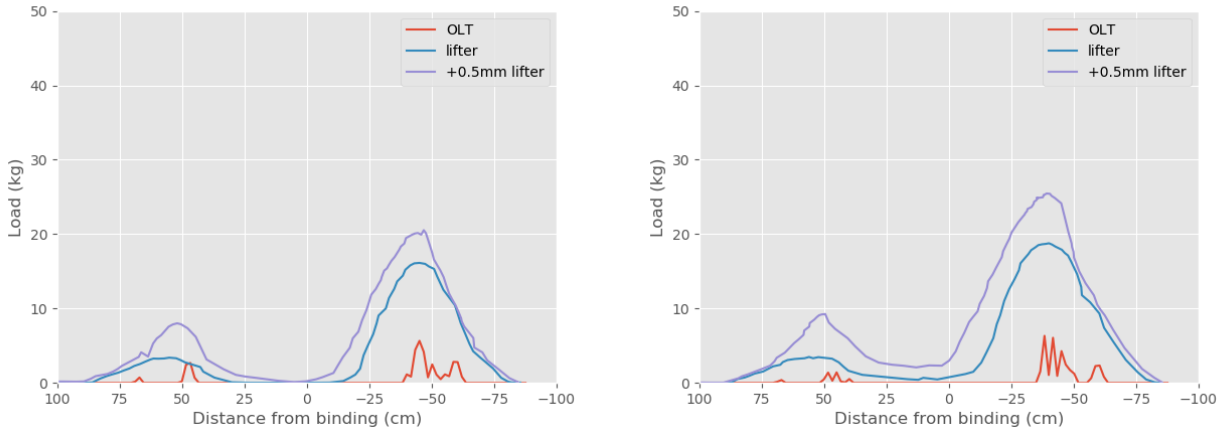

(a) (b)

Figure 6.14: Plot with 30 (a) and 40 (b) kg load

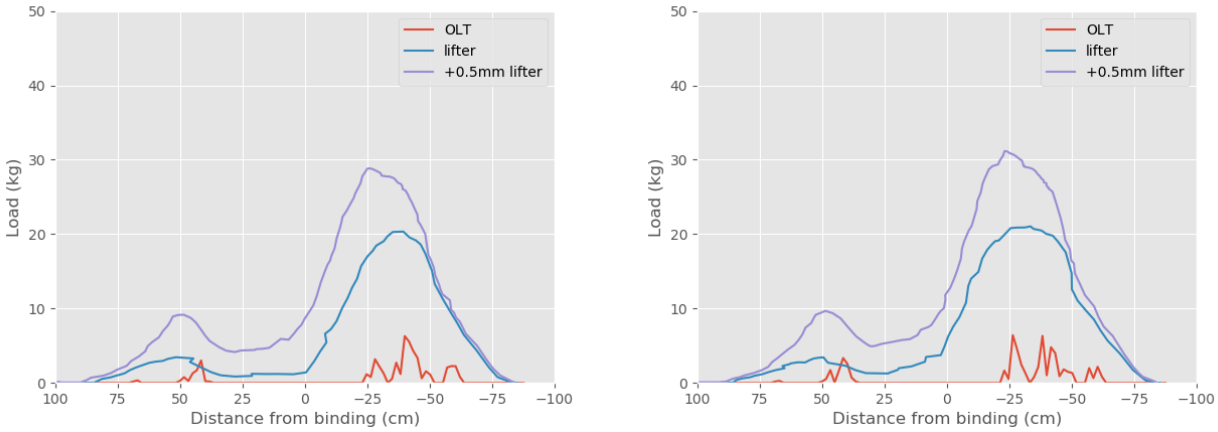

(a) (b)

Figure 6.15: Plot with 50 (a) and 60 (b) kg load

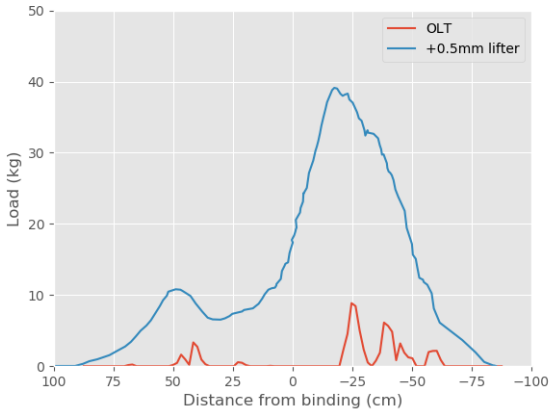

Figure 6.16: Plot with 70kg load

Table 6.12 shows the data from the three tests plotted in the figures above, looking into the pressure and load distribution. The difference between the values presented in the OLT pressure and integral column is simply a multiplication by 1.7, as this is the resolution of the pressure mats. One of the disadvantages of the pressure mats reveals itself looking at Table 6.12. Theoretically, the value of the sum of the pressures should equal the load applied, but this is far from the case. Looking at the values for the 10kg load, the pressure adds up to 16.7kg. In other words, there is a 67% error. Therefore, the percentage increase column is useless and cannot be used for comparison. Consequently, the only trustworthy information gained from the pressure mats is the areas of contact and how they move with different loads. This is supported by the calibration issues discussed in Chapter 3. It is also reasonable to assume that the peaks are closer to the actual peak pressure compared to the developed setup that lifts the ski slightly.

Table 6.12: Data for comparison of integrals to OLT data

		OLT		lifter		+0.5mm lifter	
Load (kg)	$\sum$ pressure	Integral	% increase	Integral	% change	Integral	% change
10	16.7	28.4	-	215.2	-	270.4	-
20	25.9	44.1	55.3	439.0	104.0	610.3	125.7
30	36.4	61.9	40.4	648.1	47.6	968.2	58.6
40	36.5	62.1	0.5	879.2	35.7	1425.5	47.2
50	51.5	87.5	40.9	1026.8	16.8	1753.0	23.0
60	58.4	99.2	13.4	1213.2	18.2	1939.7	10.7
70	79.1	134.5	35.6	-	-	2334.4	20.3

Table 6.13 shows the distributions between the front and the back end of the ski. Since the classic ski is in contact with the sliding load cell for applied loads of 40kg or higher, these distributions are not calculated. Still, it is clear from Figure 6.8 that the distribution moves towards the back part of the ski. Interestingly, the load distributions from the measurements with the OLT setup is more extreme than the distribution from the concept developed. The data below shows a percentage between 13 and 19 on the front end of the ski. Comparing this to the distribution from the test on the developed setup, it is clear that the test developed resulted in a more balanced distribution. Still, as discussed, this distribution transitions towards the distribution from the OLT setup as the applied load increases, if using the skate ski data from Table 6.8 as a reference. Of course, the skate ski possesses different properties than the classic ski, but it is still reasonable to assume that the development of load distribution is somewhat similar.

Table 6.13: Data for pressure/load distribution

Load	OLT Pressure/Integral			Classic ski spring setup		
	Front end	Back end	Distribution	Front end	Back End	Distribution
10	2.91/4.95	13.78/23.43	17/83	90.6	179.9	33/67
20	3.87/6.85	22.05/37.48	15/85	197.6	423.2	32/68
30	6.9/11.73	29.54/50.22	19/81	223.7	746.1	23/77
40	4.85/8.24	31.66/53.82	13/87	-	-	-
50	8.16/13.87	43.3/73.61	16/84	-	-	-
60	11.32/19.24	47.04/79.97	19/81	-	-	-
70	12.31/20.93	66.79/113.54	16/84	-	-	-

6.4 Comparison to Backströms Technology

As discussed, Backström developed a concept with similar features. In his paper, Backström presented measurements from the setup. The load applied is known. Therefore, it is possible to make a simple comparison to see to what extent the results match and, thereby, understand Backström's results thorougher. It is to be noted that the ski tested by Backström is not available. The same applies to the details of the setup. The main aspect of interest is the details on how the load cell moving under the ski is used when it comes to contact with the ski, but this was, as mentioned, not obtainable. This means that only a general comparison can be done. Figure 6.17 shows the results from the test of the classic ski with a 40kg applied load from this

thesis and a test of a classic ski with Backström's setup with a 40kg load. It is to be noted that the y-axis in Backström's plot is force in N. Therefore, it is necessary to divide this number by the acceleration, as seen in Equation 5.2. Both setups load the ski 14cm behind the binding, which increases the validity of the comparison.

The peak load on the back end of the ski is significantly higher for Backström's setup. The value is approximately 33kg, compared to just over 25kg for the measurement from the developed setup. As mentioned, the plots represent two different skis, so there will be differences. But with a 40kg load, a 33kg peak load seems high. The red plot in Figure 6.17a represents the test with the original lifting height, where the results for loads higher than 40kg were considered uncertain. Still, the results representing the back end of the ski with 40kg were considered valid. The peak from this plot is at approximately 17kg, which is half of Backström's setup. As mentioned, the details on the lifting height were not obtainable, but it is reasonable to assume that it is higher than the ones used producing the plots in Figure 6.17a. Another aspect of interest is that Backström's plot shows no sign of contact under the center of the ski, as it does in Figure 6.17a. Considering the lifting height is assumed to be higher than the ones used in Figure 6.17a, this is a contradiction.

The peak of the front end of the ski corresponds well to Backström's plot, except for that the peak is sharper. Still, this is potentially an outlier as all the other peaks in Figure 6.13 to Figure 6.16 are more rounded.

Overall, it seems reasonable to assume that a more accurate setup than the one presented by Backström is possible. The most important factor is minimizing the lifting height. Also, the reason why Backströms meausrements are done with only 40kg and not full body weight is uncertain. The properties of a ski with full body weight is just as important. One reason could be that the load cell would be in contact with the ski base under the full length of the ski, as it was for several of the classic ski tests in this thesis. A last reason could be to prevent damage to the ski base as the ski is pressed to the ground with significant force. But, since the loading mechanism (whether or not a spring was used) and the lifting height is unknown, it is not possible to conclude.

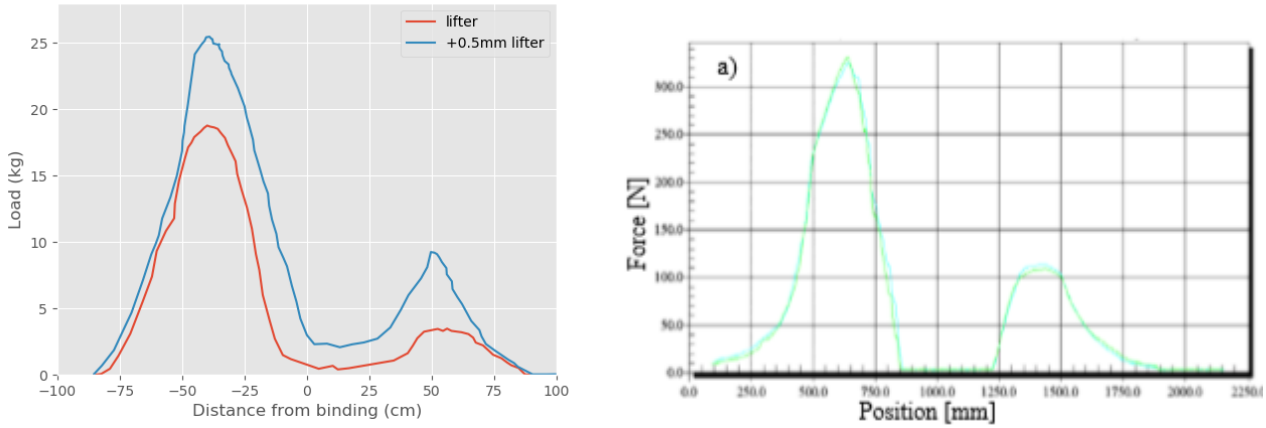

(a) (b)

Figure 6.17: Plot with 40kg load (a) and Backström plot for a mens ski with 40kg load (b)[13]

6.5 Stiffness of Tip and Tail

A new measurement was introduced to complement the setup. The stiffness of the tip of the ski varies depending on the snow, as discussed in Section 2.3. By using a lifter with a height of 1.5cm, the load cell was moved under the tip of the ski. A 1cm lifter was used to perform the same test on the tail of the ski. Images showing the setup are found in Appendix F.

Table 6.14 shows the results from the test of two different classic and skate skis. The "original" skis represent the skis used for testing in the previous sections while the "new" skis are introduced in this section for this specific testing. The biggest variation is shown between the classic skis. The new ski introduced is constructed for soft conditions, while, as mentioned, the ski used throughout the previous testing is supposed to be a medium ski with a medium tip stiffness. From the results, it is confirmed that the new ski has a softer tip. As seen in Table 6.14, the load on the load cell is decreasing as the applied load increases. This comes from that with low loads the contact zone is closer to the tip. As the applied load increases, the contact zone moves closer to the center of the skis, as discussed earlier, which means that the tip is naturally lifted from the ground, increasingly. A stiffer ski would resist this more than a softer ski.

Table 6.14: Data for stiffness test of tip

Load(kg)	Original classic ski	New classic ski	Original skate ski	New skate ski
10	3.72	3.26	3.78	3.85
20	3.13	2.59	3.40	3.48
30	2.88	2.42	3.20	3.27
40	2.79	2.28	3.09	3.18
50	2.73	2.20	3.02	3.09
60	2.67	2.16	3.04	3.07
70	2.65	2.13	2.94	3.02
80	2.62	2.11	2.91	3.01

Table 6.15 shows the results for the same test performed on the tail of the ski. Since the load on the back end of a ski is significantly higher than on the front end, the tail is pressed to the ground with a greater force. Therefore, a 1cm lifter was used instead of the 1.5cm lifter used for the tip of the ski. The results show an interesting aspect regarding the classic ski. The original classic ski decreases the load as the applied load increases until 40kg, then the load increases. All three other skis tested had a continuous decrease in load. The reason for the increase for the classic ski is uncertain, and a high number of skis have to be tested before potentially seeing a trend.

Table 6.15: Data for stiffness test of tail

Load(kg)	Original classic ski	New classic ski	Original skate ski	New skate ski
10	4.04	4.07	5.02	4.60
20	3.37	3.21	4.20	3.86
30	3.06	2.90	3.94	3.57
40	3.00	2.71	3.91	3.55
50	3.03	2.67	3.93	3.51
60	3.07	2.67	3.94	3.52
70	3.11	2.68	3.91	3.49
80	3.12	2.68	3.86	3.49

The results presented in Table 6.14 and 6.15 are directly relatable to the load distribution measurements discussed in the previous sections. For example, a soft tip would decrease the pressure on the surface closer to the tip. Looking at the results from this test in relationship to the load distribution it is reasonable to assume that the skate ski has a steeper pressure curvature on the front end of the ski. Looking at the results from Figure 6.8 and 6.9 the distance from the contact between the sliding sensor and the base of the ski starts, to the peak load on the front end of the ski is approximately 39 and 29cm for the classic and skate ski, respectively. This is with a 40kg load. Hence, the hypothesis is confirmed. It is to be noted that these are two different skis with different lengths, but since the difference is 10cm it is considered confirmable. As for any property of a ski, it is necessary to test a significant number of skis to see potential trends.

7 | Conclusion

- There is a clear trend in the results that supports the concept, but further testing is necessary to improve the understanding of its potential.
- A minimum lifting height of the ski is critical. A small increase in lifting height resulted in a significant increase in load, especially on the back end of the ski. It is also important to avoid contact between the entire base of the ski and the moving load cell to prevent significant influence in the area under the curve.
- A spring loading mechanism is necessary to keep the applied load stable. Using a pure clamp mechanism resulted in an increased applied load since the ski has to be elevated slightly from the surface of which it is resting.
- There are clear signs that the concept is able to distinguish skis with different properties.
- The setup is not able to show small deviations in pressure/load like the pressure mats. Instead, it produces a smooth curvature with two peaks, one for the front end and one for the back end of the ski.
- The drawbacks of the OLT setup made it difficult to compare pressure distribution between the concept developed and the pressure mats.
- The prototype is too inaccurate to allow investigation of potential relationships between the load distribution.
- Testing the concept questioned the results from a similar concept, though without the possibility of obtaining important details such as elevation height and loading mechanism.
- The setup is capable of integrating measurements of flex height.
- The peak loads on the front and back end of the ski moves as predicted with increasing load, with clear similarities to the pressure mats used by OLT today.
- Measuring the stiffness of the tip and tail of the ski can be a useful complement to the setup, but further testing is necessary to reveal its potential.

7.1 Recommendations for Further Work

- Two (four in one occasion) different skis were tested in this thesis. It is necessary to test significantly more skis of various flexes to be able to find a way to characterize skis with this setup.

- As this thesis focused on proving and testing main characteristics of the concept and comparing them to the currently used technology, it is necessary to develop a more accurate prototype to fully understand the qualities and possibilities of the concept. This includes a plane surface and more accurate sensors, which allows for minimum lifting of the ski. This requires more resources spent, which means that a discussion on whether or not this is reasonable is necessary.
- Since the classic ski was in contact with the sliding sensor in the area of the "pocket" of the ski, it is necessary to test a skate ski on the OLT setup and compare those results to the results from this setup. This will allow for a comparison of applied loads in the full range of 10kg to full body weight.
- Another possibility is to supplement the pressure mats used today with a setup like the concept developed. Since they have different strengths, a better understanding of a ski could be achieved by using both. Still, an important factor is time and resources. As today's setup is ineffective time wise, it would be undesirable to add on another measurement and setup. Hence, it is necessary to discuss the possibilities.
- Further testing of the stiffness of the tip and tail of the ski is necessary.
- Further attempts on getting in contact with Backström to discuss the findings is an option. Still, it is important to keep in mind that Sweden is one of the biggest competitors in the sport.

Bibliography

[1] Online VD. Skating step[Image on internet]; 2019. [Online; accessed June 22, 2019]. Available from: http://www.visualdictionaryonline.com/sports-games/winter-sports/cross-country-skiing/skating-step.php.

[2] FischerSports. Fischer classic and skate ski. [Image on internet]; 2018. [Online; accessed November 11, 2018]. Available from: https://transfer.fischersports.com/index.php/s/r0vhi9pJWF1XxcO?

[3] FischerSports. Technologies; 2018. [Online; accessed June 8, 2019]. Available from: https://www.fischersports.com/speedmax-skate-cold-medium-273?c=1313.

[4] Madshus. Technology; 2018. [Online; accessed June 8, 2019]. Available from: https://en-no.madshus.com/nordic-skis/propulsion-cold.

[5] NordicSkiRacer. How to have fast skis all the time and in every condition[Image on internet]; 2019. [Online; accessed October 20, 2018]. Available from: http://www.nordicskiracer.com/news.asp?NewsID=15896#.XQ1CKugzY2w.

[6] Breitschädel F. Figures and illustrations from testing by Dr. Breitschädel; 2018.

[7] Colbeck S. The kinetic friction of snow. Journal of Glaciology. 1988;34(116):78–86.

[8] Breitschädel F. Important parameters for the friction of cross country skis on snow; 2007.

[9] Storey C. Stone Grinding and Structuring Cross Country Skis, [Image on internet]; 2008. [Online; accessed November 22, 2018]. Available from: http://www.xcottawa.ca/articles.php?id=1038.

[10] Engineering DAS. The Twists of Strain Gauge Measurements – Part 1, [Image on internet]; 2019. [Online; accessed May 27, 2019]. Available from: https://ueidaq.wordpress.com/2013/08/02/the-twists-of-strain-gauge-measurements-part-1/.

[11] Hoffmann K. Applying the Wheatstone bridge circuit. HBM Germany; 1974.

[12] Tekscan. Pressure Mapping Sensor 5400N from Tekscan. [Image on internet]; 2018. [Online; accessed December 10, 2018]. Available from: https://www.tekscan.com/products-solutions/pressure-mapping-sensors/5400n.

[13] Bäckström M, Dahlen L, Tinnsten M. Essential ski characteristics for cross-country skis performance (P251). In: The Engineering of Sport 7. Springer; 2008. p. 543–549.

[14] Moldestad DA. Some aspects of ski base sliding friction and ski base structure. Fakultet for ingeniørvitenskap og teknologi; 1999.

[15] Eppinger SD, Ulrich KT. Product design and development. McGraw-Hill New York; 1995.

[16] Bowes J. Agile vs Waterfall: Comparing project management methods. [Image on internet]; 2014. [Online; accessed May 21, 2019]. Available from: https://manifesto.co.uk/agile-vs-waterfall-comparing-project-management-methodologies/.

[17] Tutorials RN. Complete Guide for Ultrasonic Sensor HC-SR04 with Arduino, [Image on internet]; 2019. [Online; accessed April 21, 2019]. Available from: https://randomnerdtutorials.com/complete-guide-for-ultrasonic-sensor-hc-sr04/.

[18] Springs SI. Technical information; 2019. [Online; accessed May 29, 2019]. Available from: https://www.industrial-springs.com/13880.

[19] ElecFreaks. Ultrasonic Ranging Module HC-SR04; 2019. [Online; accessed April 21, 2019]. Available from: https://cdn.sparkfun.com/datasheets/Sensors/Proximity/HCSR04.pdf.

[20] Olympiatoppen. Olympiatoppen; 2018. [Online; accessed December 10, 2018]. Available from: https://www.olympiatoppen.no/om_olympiatoppen/page714.html.

[21] no S. VM i 1974: Skirevolusjon og nedtur for de norske fargene; 2019. [Online; accessed June 20, 2019]. Available from: https://www.visitnorway.com/things-to-do/great-outdoors/skiing/cross-country-skiing/.

[22] VisitNorway. Cross-country: A brief history; 2019. [Online; accessed June 20, 2019]. Available from: http://www.skihistorie.no/vm-i-1974-skirevolusjon-og-nedtur-for-de-norske-fargene/.

[23] leksikon SN. Skøytetak; 2019. [Online; accessed June 22, 2019]. Available from: https://snl.no/sk%C3%B8ytetak.

[24] Rivin E. Stiffness and damping in mechanical design. CRC Press; 1999.

[25] Stachowiak GW, Batchelor AW. 10-Fundamentals of Contact Between Solids. Engineering Tribology. 1993;p. 527–556.

[26] Breitschädel F, Haaland N, Espallargas N. A tribological study of UHMWPE ski base treated with nano ski wax and its effects and benefits on performance. Procedia Engineering. 2014;72:267–272.

[27] Lehtovaara A. Kinetic friction between ski and snow. Acta Polytechnica Scandinavica Mechanical Engineering Series. 1989;.

[28] Johnson CD. Process control instrumentation technology. Pearson; 2014.

[29] Bolton W. Mechatronics electrical control systems in mechanical and electrical engineering. Pearson; 2015.

[30] HBM. The Wheatstone Bridge Circuit; 2019. [Online; accessed June 10, 2019]. Available from: https://www.hbm.com/en/7163/wheatstone-bridge-circuit/.

[31] Rainer F, Nachbauer W, Schindelwig K, Kaps P. Effects of ski stiffness on ski performance. 2004;p. 3.

[32] Stapenhurst T. The Benchmarking Book. Elsevier; 2009.

[33] Clausing DP. Total quality development. Mechanical Engineering. 1994;116(3).

[34] Semiconductor A. 24-Bit Analog-to-Digital Converter (ADC) for Weigh Scales; 2019. [Online; accessed April 21, 2019]. Available from: http://www.aviaic.com/Download/hx711F_EN.pdf.pdf.

[35] Zak M. HX711 library; 2019. Available from: https://github.com/gandalf15/HX711/blob/master/HX7

A | Software

A.1 Software Used for Testing

The images below shows the code written in Python on the Raspberry Pi.

```python
import RPi.GPIO as GPIO
from time import sleep
from time import time
import csv
import numpy as np

GPIO.setmode(GPIO.BOARD)
from hx711 import HX711

button = 40

TRIG = 37
ECHO = 38

GPIO.setup(button, GPIO.IN, pull_up_down=GPIO.PUD_UP)

GPIO.setup(TRIG, GPIO.OUT)
GPIO.setup(ECHO, GPIO.IN)

hx = HX711(dout_pin=22, pd_sck_pin=18)
lc = HX711(dout_pin=13, pd_sck_pin=11)

hx_ratio = np.loadtxt('hx_ratio.csv')
lc_ratio = np.loadtxt('lc_ratio.csv')

if (hx_ratio is not None and lc_ratio is not None):
    hx.set_scale_ratio(hx_ratio)
    lc.set_scale_ratio(lc_ratio)
    print('Ratio is set for lc: {ratio}'.format(ratio=lc_ratio))
    print('Ratio is set for hx: {ratio}'.format(ratio=hx_ratio))

distances = []
loads = []
skiloads = []

```

```python
def distanceSensor():
    GPIO.output(TRIG, True)
    sleep(0.11)
    GPIO.output(TRIG, False)

    while GPIO.input(ECHO) == False:
        start = time()

    while GPIO.input(ECHO) == True:
        end = time()

    sig_time = end - start

    distance = (sig_time/0.000058) - float(bindingdistance) + 8
    distances.append(round(distance, 2))


def loadSensor():
    loadreading = round(((hx.get_weight_mean(2)/1000)) + 3.20, 2)
    if loadreading < 0:
        loadreading = 0
    loads.append(loadreading)


def loadSensorSki():
    skiloads.append(round((lc.get_weight_mean(2)/1000), 2))

```

```
calibration = input('Calibration sliding sensor: y/n')

if calibration == 'y':
    err = hx.zero()

    reading = hx.get_raw_data_mean()
    if reading:
        print('Data subtracted by offset but still not converted to units:',
              reading)
    else:

        print('invalid data', reading)

    input('Put known weight on the scale and then press Enter')
    reading = hx.get_data_mean()
    if reading:
        print('Mean value from HX711 subtracted by offset:', reading)
        known_weight_grams = input(
            'Write how many grams it was and press Enter: ')
        try:
            value = float(known_weight_grams)
            print(value, 'grams')
        except ValueError:
            print('Expected integer or float and got:',
                  known_weight_grams)

        ratio = reading / value
        hx.set_scale_ratio(ratio)
        with open('hx_ratio.csv', 'w') as f:
            f.write('%f' % ratio)
        print('Ratio is set for hx: {ratio}'.format(ratio=ratio))
    else:
        raise ValueError('Cannot calculate mean value. Try debug mode. Variable reading:', reading)

```

```
calibration = input('Calibration loaded sensor: y/n')

if calibration == 'y':
    err = lc.zero()

    reading = lc.get_raw_data_mean()
    if reading:
        print('Data subtracted by offset but still not converted to units:',
              reading)
    else:
        print('invalid data', reading)

    input('Put known weight on the scale and then press Enter')
    reading = lc.get_data_mean()
    if reading:
        print('Mean value from HX711 subtracted by offset:', reading)
        known_weight_grams = input(
            'Write how many grams it was and press Enter: ')
        try:
            value = float(known_weight_grams)
            print(value, 'grams')
        except ValueError:
            print('Expected integer or float and got:',
                  known_weight_grams)

        ratio = reading / value
        lc.set_scale_ratio(ratio)
        with open('lc_ratio.csv', 'w') as f:
            f.write('%f' % ratio)

        print('Ratio is set for lc: {ratio}'.format(ratio=ratio))
    else:
        raise ValueError('Cannot calculate mean value. Try debug mode. Variable reading:', reading)

```

```
testloadcell = input('Test sliding load cell: y/n ')

if testloadcell == 'y':
    print('Tap button to print load')
    button_pushed = False
    should_stop = False
    while (1):
        if GPIO.input(button) == 0:
            button_pushed = True
        while button_pushed:
            print(round(hx.get_weight_mean(5), 1))
            sleep(0.5)
            if GPIO.input(button) == 0:
                button_pushed = False
                should_stop = True
                sleep(2)
        if should_stop:
            break


loadsetup = input('Load ski: y/n ')

if loadsetup == 'y':
    print('Tap button to print load')
    button_pushed = False
    should_stop = False
    while (1):
        if GPIO.input(button) == 0:
            button_pushed = True
        while button_pushed:
            print(round(lc.get_weight_mean(5), 1))
            sleep(0.5)
            if GPIO.input(button) == 0:
                button_pushed = False
                should_stop = True
                sleep(2)
        if should_stop:
            break
```

```
IDnumber = input('ski ID-number, ski, test, load (example: 111A.clamp.10kg): ')
bindingdistance = input('Distance from binding to sensor start position (cm): ')

button_pushed = False
should_stop = False

loadski = input('Collect data from load cell on ski: y/n ')
if loadski == 'y':
    print('Tap button to start collecting sensor data. Press button again when sensors reach end.')
    while(1):
        if GPIO.input(button) == 0:
            button_pushed = True
        while button_pushed:
            distanceSensor()
            loadSensor()
            loadSensorSki()
            print('New distance: {distance}'.format(distance=distances[-1]))
            print('New hx load: {m}'.format(m=loads[-1]))
            print('New lc load: {m}'.format(m=skiloads[-1]))
            print()
            sleep(0.1)
            if GPIO.input(button) == 0:
                button_pushed = False
                should_stop = True
                sleep(2)
        if should_stop:
            break

    with open(IDnumber, 'w', newline='') as csvfile:
        fieldnames = ['distance', 'load', 'skiload']
        writer = csv.DictWriter(csvfile, delimiter=',', fieldnames=fieldnames)
        writer.writeheader()
        for i in range(len(distances)):
            writer.writerow({'distance': distances[i], 'load': loads[i], 'skiload': skiloads[i] })
```

```
else:
    print('Tap button to start collecting sensor data. Press button again when sensors reach end.')
    while(1):
        if GPIO.input(button) == 0:
            button_pushed = True
        while button_pushed:
            distanceSensor()
            loadSensor()
            print('New distance: {distance}'.format(distance=distances[-1]))
            print('New hx load: {m}'.format(m=loads[-1]))
            print()
            sleep(0.1)
            if GPIO.input(button) == 0:
                button_pushed = False
                should_stop = True
                sleep(2)
        if should_stop:
            break

    with open(IDnumber, 'w', newline='') as csvfile:
        fieldnames = ['distance', 'load']
        writer = csv.DictWriter(csvfile, delimiter=',', fieldnames=fieldnames)
        writer.writeheader()
        for i in range(len(distances)):
            writer.writerow({'distance': distances[i], 'load': loads[i]})


GPIO.cleanup()
```

A.2 Integral Calculation Software

The following code represents the calculation of the area under the different curves. The trapezoidal rule was used, which is included in the NumPy package.

```
import numpy as np
from numpy import trapz

a, b = np.loadtxt('C:\\Users\schwe\Desktop\Resultfiles\\textfile.txt', unpack=True, delimiter=',')
x = np.array(a)
y = np.array(b)


area = trapz(x, y)
print("area =", area)
```

B | Measurement Data from OLT Setup

B.1 Raw Data from Excel

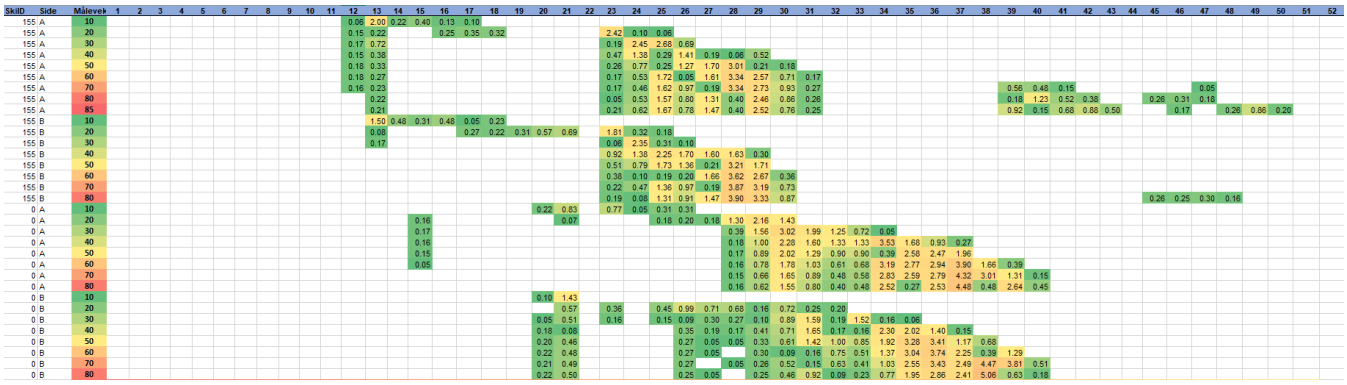

Figure B.1: Raw data from OLT setup measurement for front half of the skis for loads from 10kg to 80kg

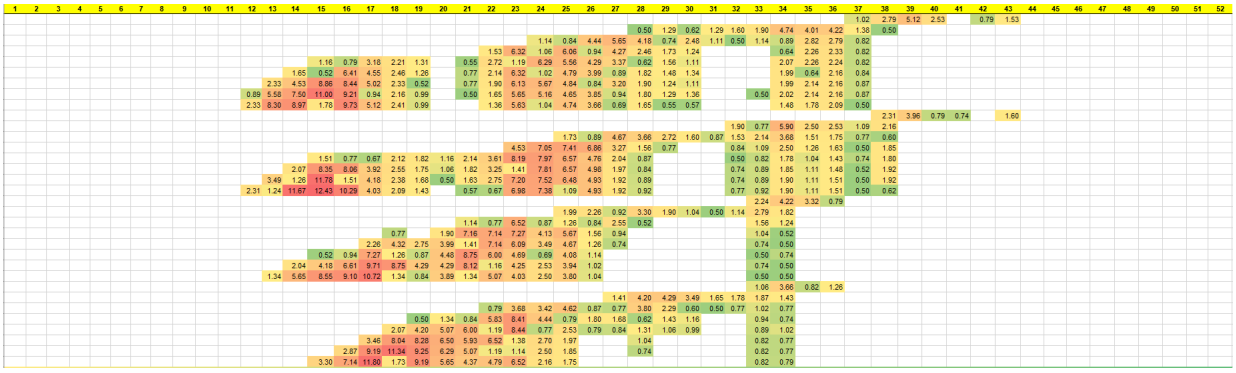

Figure B.2: Raw data from OLT setup measurement for back half of skis for loads from 10kg to 80kg

The data in Figure B.1 and B.2 represents the pressure distribution for the two pairs of skis tested with the OLT setup. There are, in other word, four skis measured. The value in each cell represents the sum of the values from the pressure mat sensors in the direction of the width of the ski.

B.2 Load Distribution Plots For Classic Ski

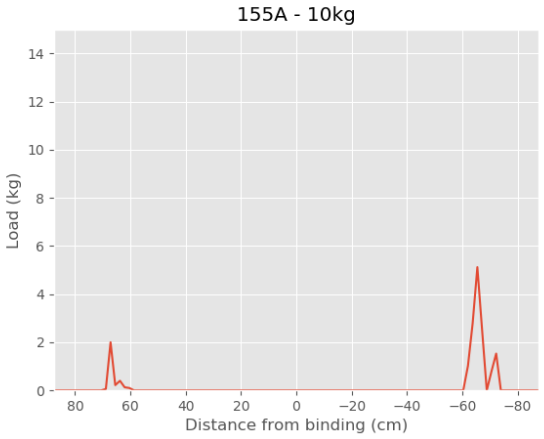

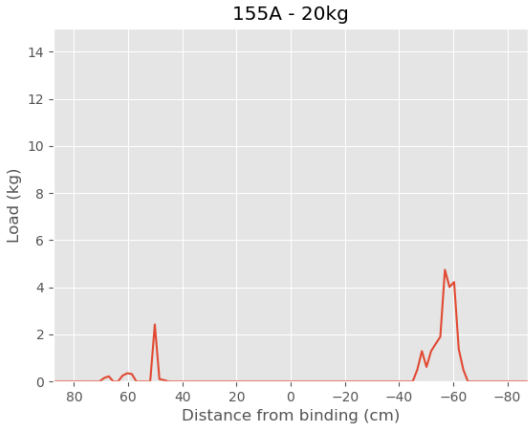

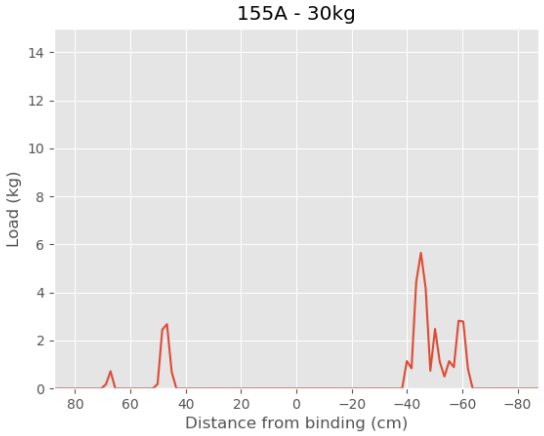

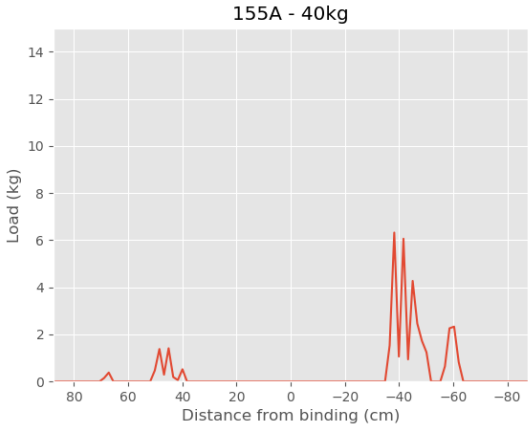

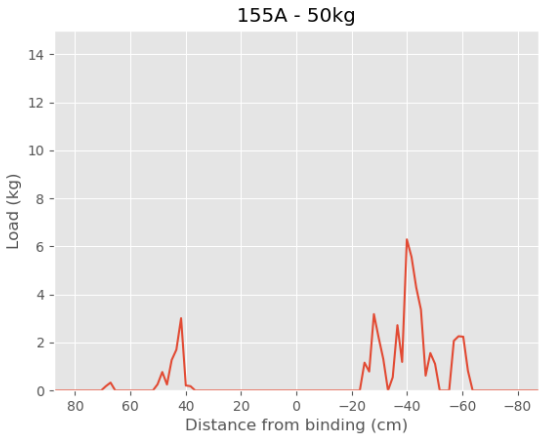

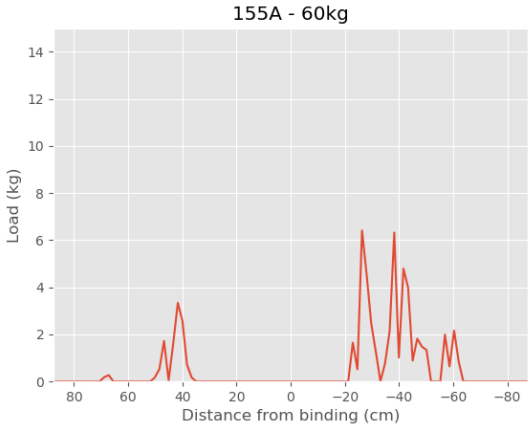

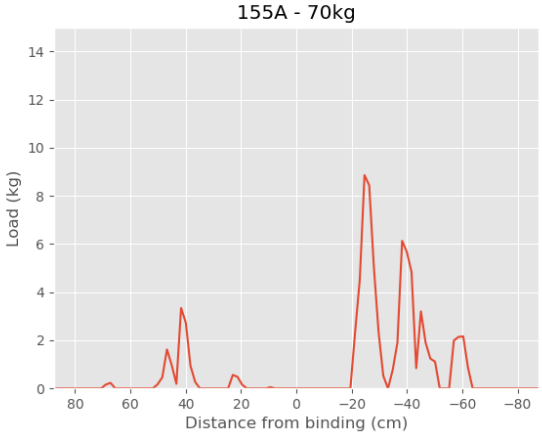
155A - 70kg
Load (kg)
Distance from binding (cm)
14
12
10
8
6
4
2
0
80
60
40
20
0
−20
−40
−60
−80

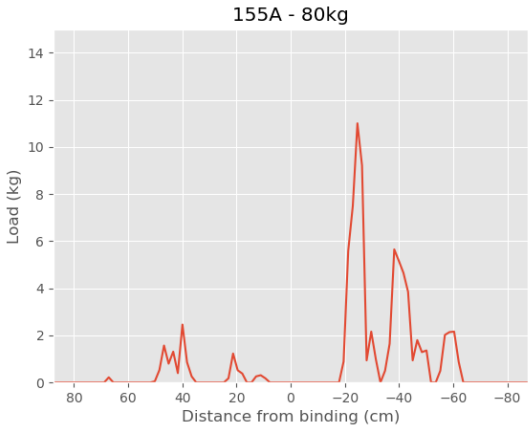
155A - 80kg
Load (kg)
Distance from binding (cm)
14
12
10
8
6
4
2
0
80
60
40
20
0
−20
−40
−60
−80

C | Concept Test Raw Data

The data presented below represents the raw data measurements of the skis. The plots are presented as a scatter to show the data points throughout the measurements.

C.1 Reliability Test

The data below represents the three tests performed to assure repeatability.

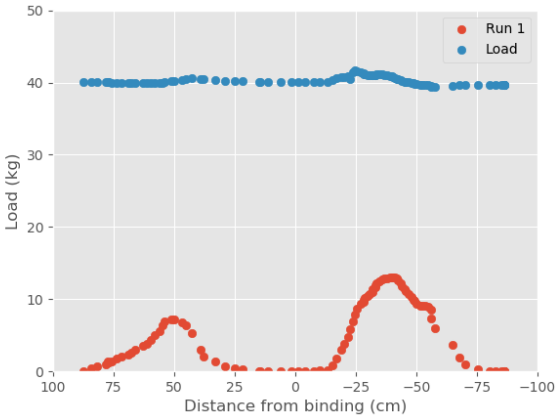

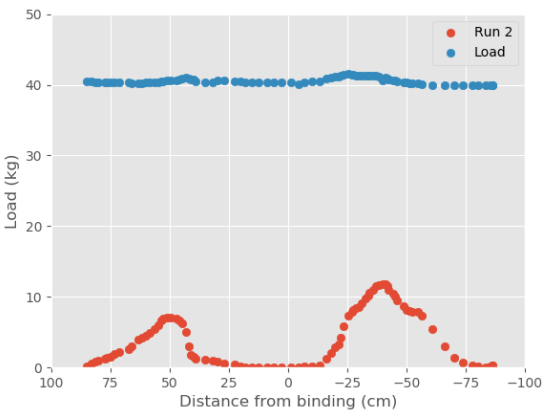

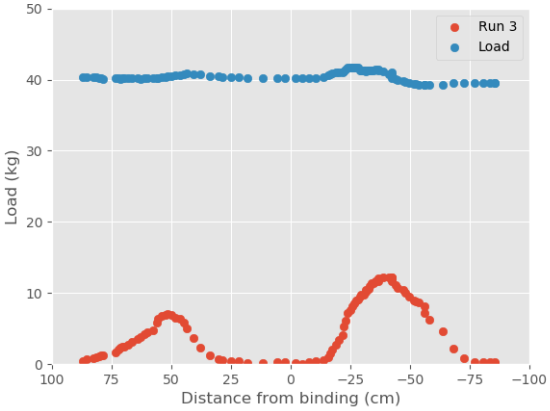

C.2 Reposition of Load

The data below represents the tests performed with a variation in load location. All the tests were performed with the spring setup.

C.2.1 Classic Ski

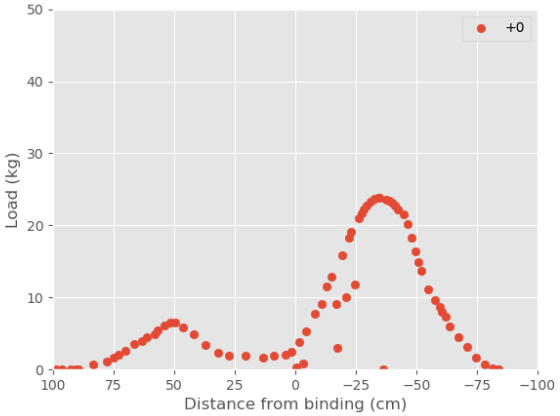

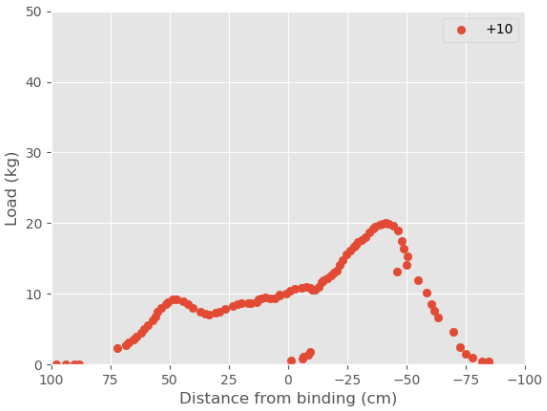

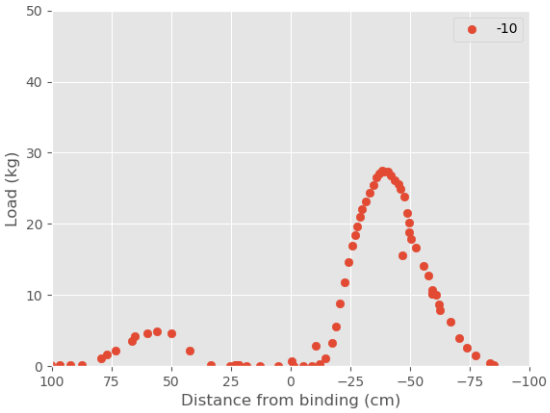

C.2.2 Skate Ski

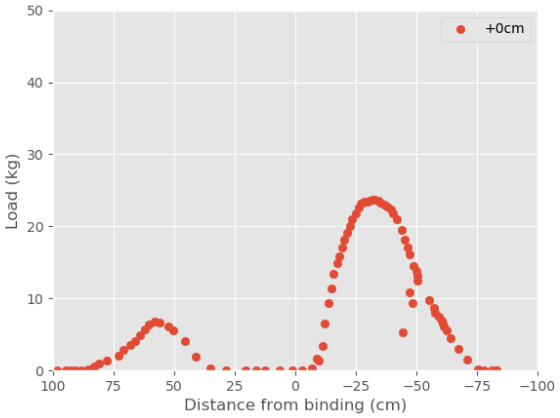

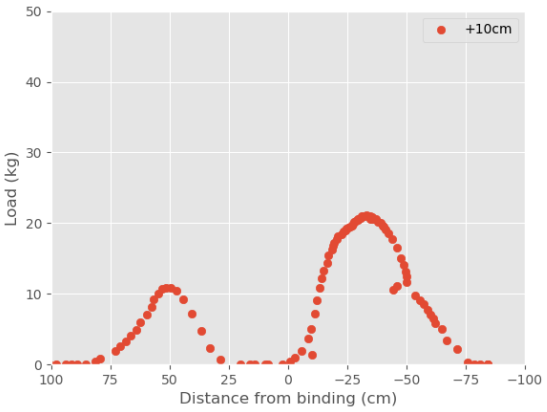

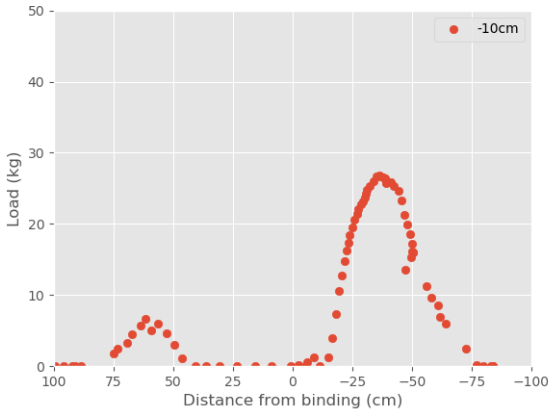

C.3 Test of Lifting Heights

The data below represents the data from the tests performed with increasing lifting height with the clamp setup.

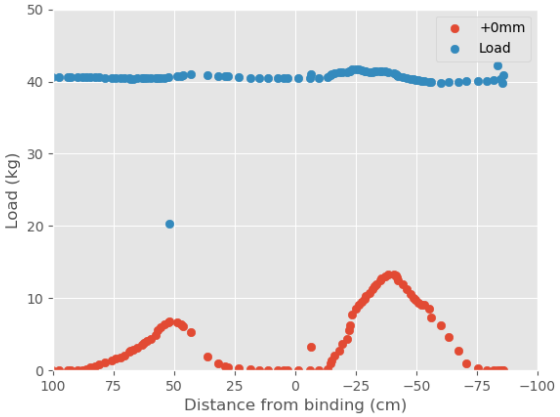

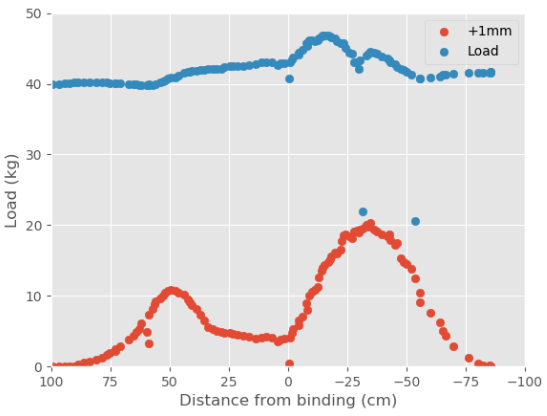

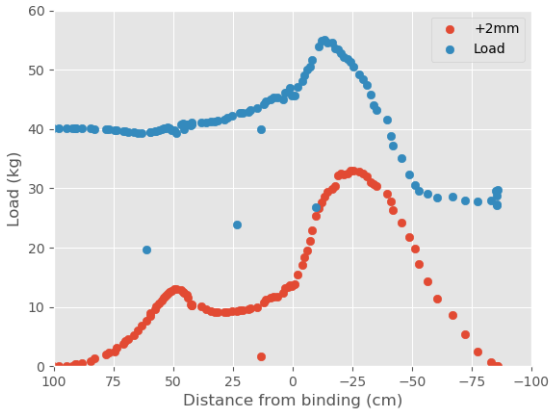

C.4 Clamp Setup

The data below represents the tests performed with an increasing load of 10kg with the clamp setup.

C.4.1 Classic Ski

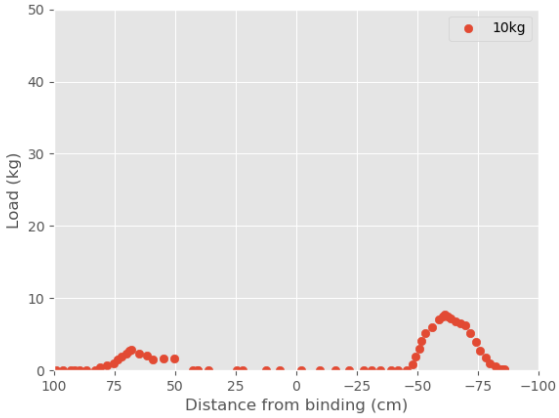

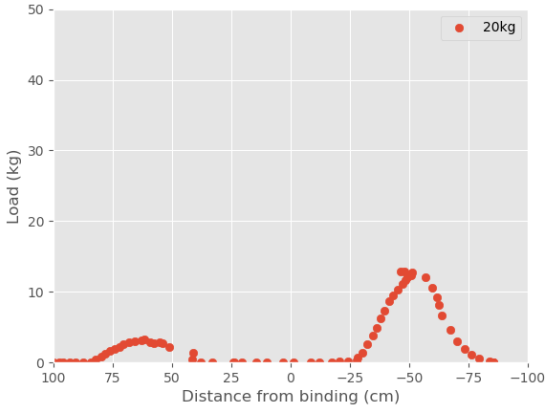

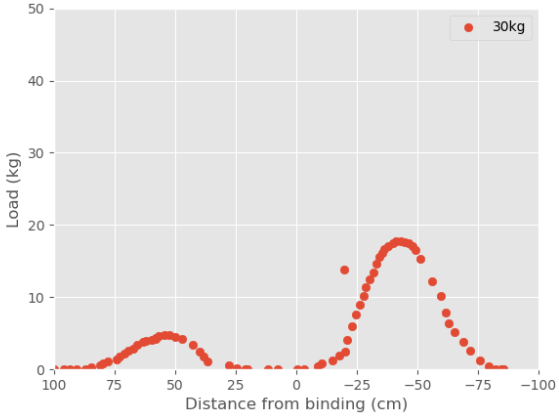

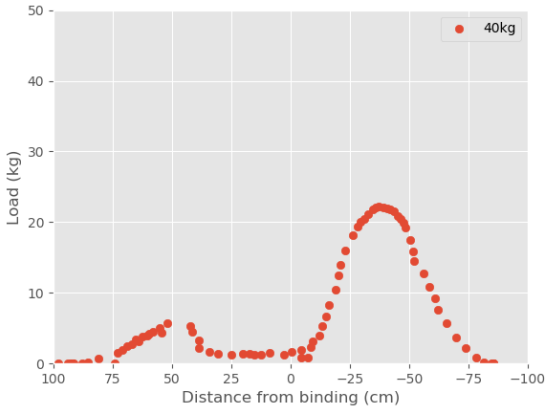

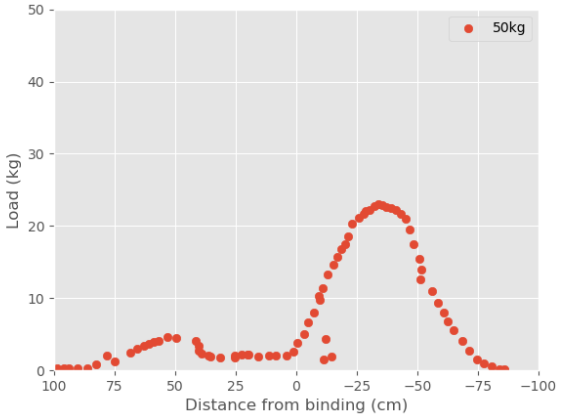

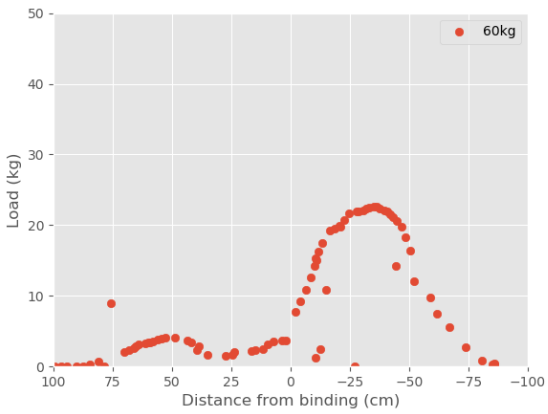

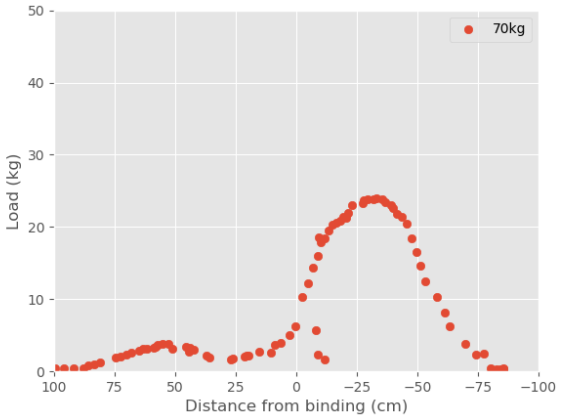

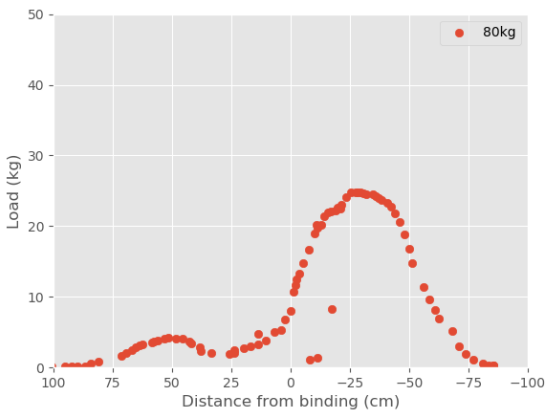

C.4.2 Skate Ski

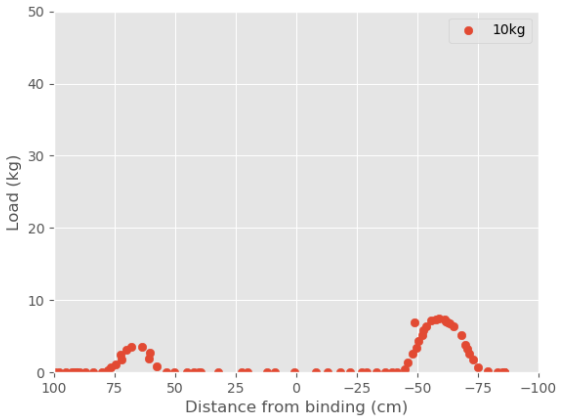

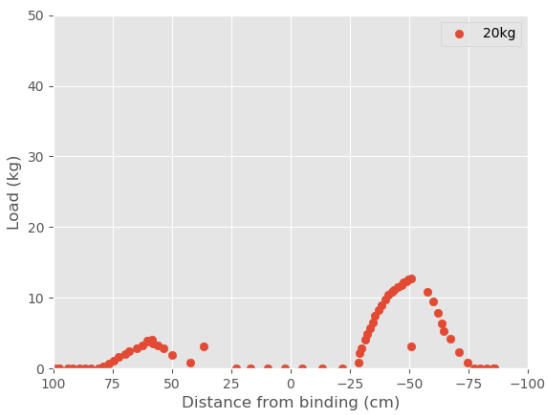

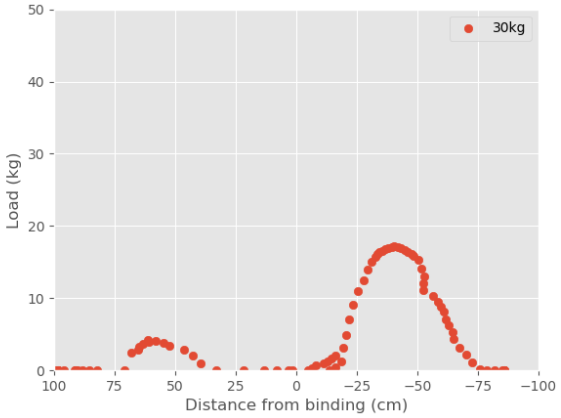
30kg
Load (kg)
Distance from binding (cm)

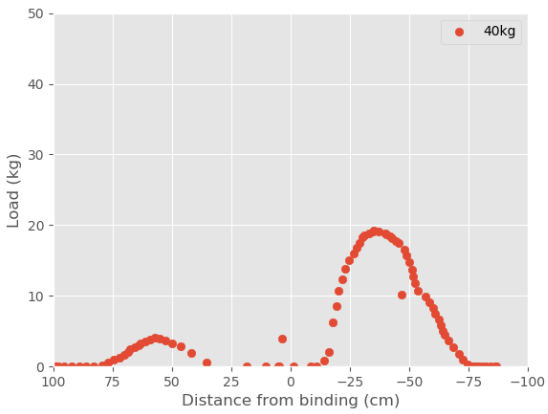
40kg
Load (kg)
Distance from binding (cm)

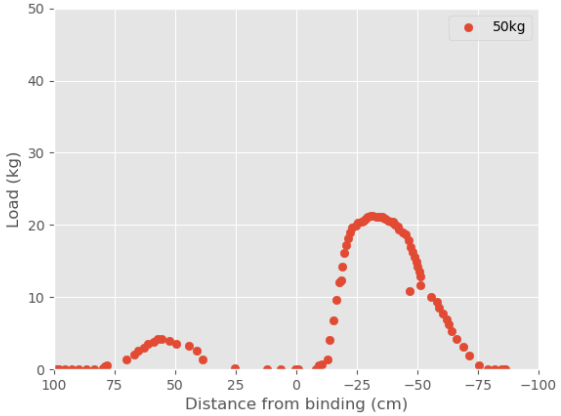
50kg
Load (kg)
Distance from binding (cm)

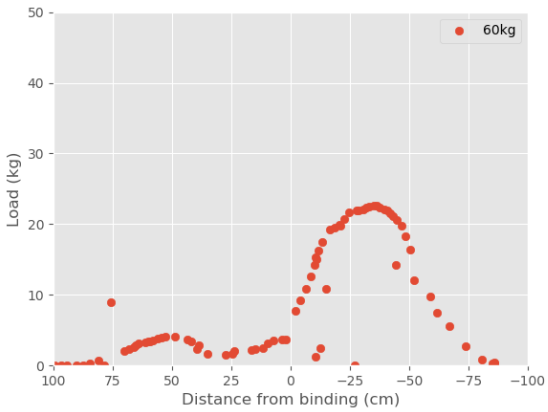
60kg
Load (kg)
Distance from binding (cm)

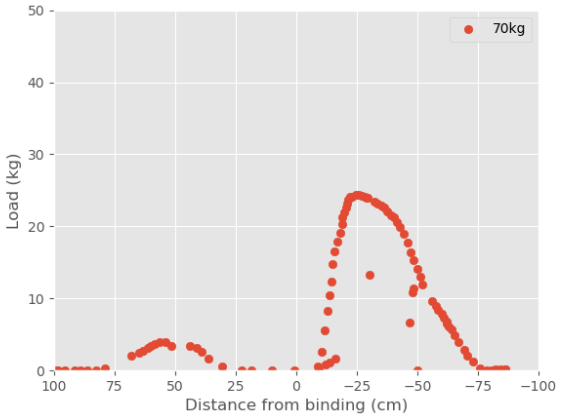
70kg
Load (kg)
Distance from binding (cm)

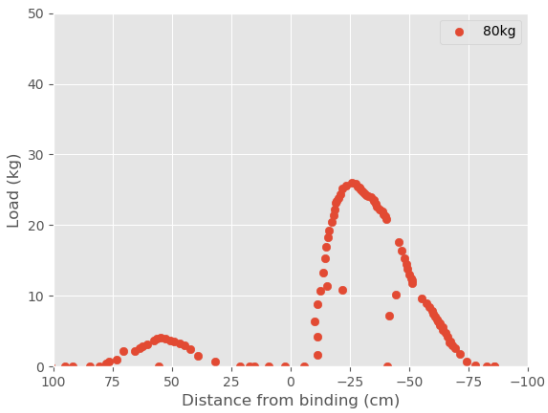
80kg
Load (kg)
Distance from binding (cm)

C.5 Spring Setup

C.5.1 Classic Ski

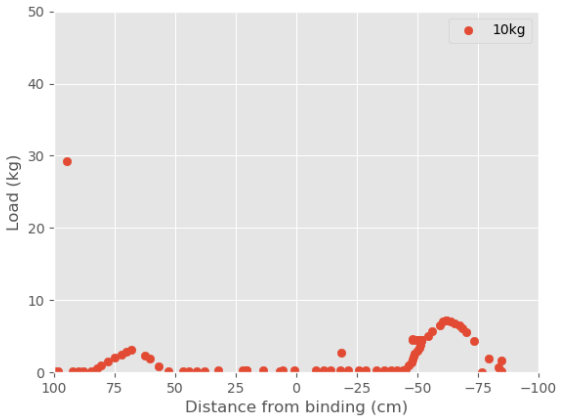

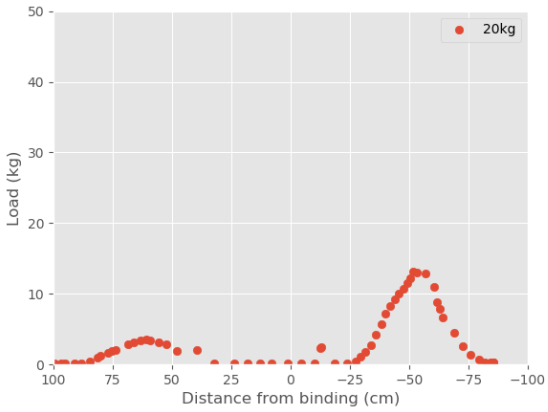

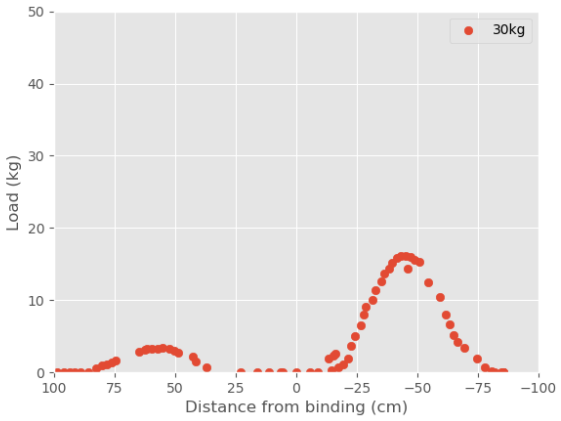

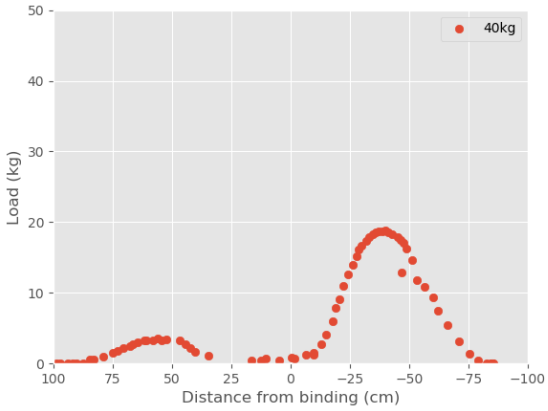

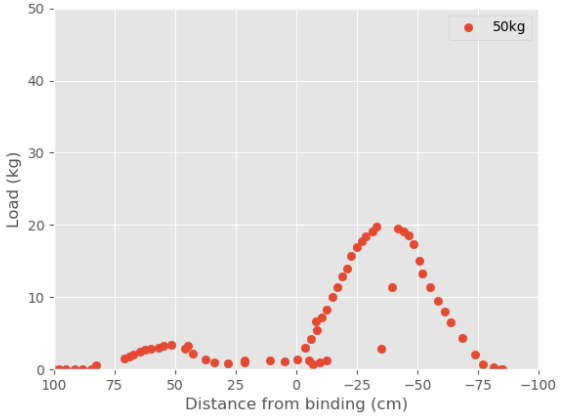

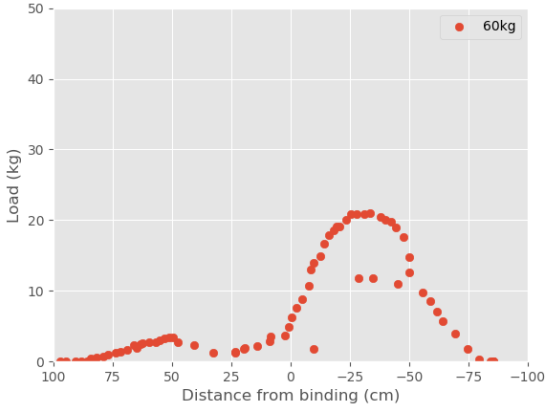

C.6 Spring Setup with Increased Lifting Height

The data below represents the tests with an increased lifting height of approximately 0.4mm.

C.6.1 Classic Ski

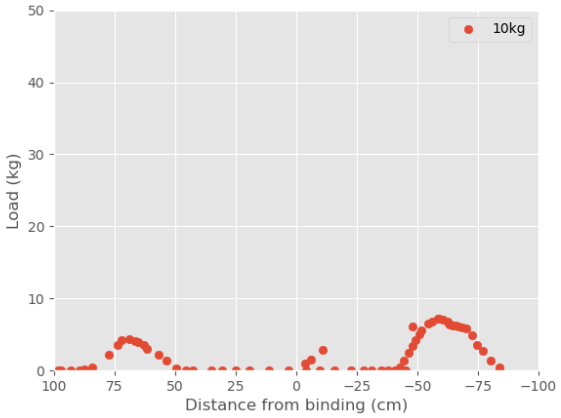

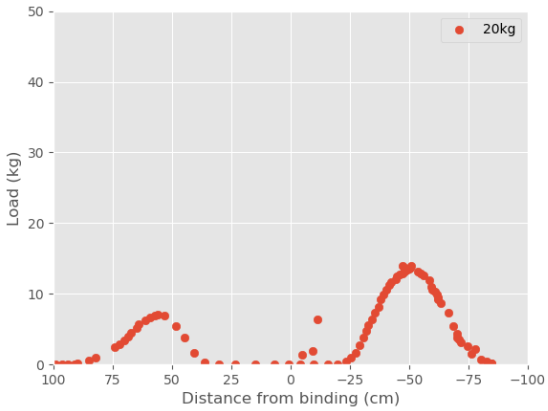

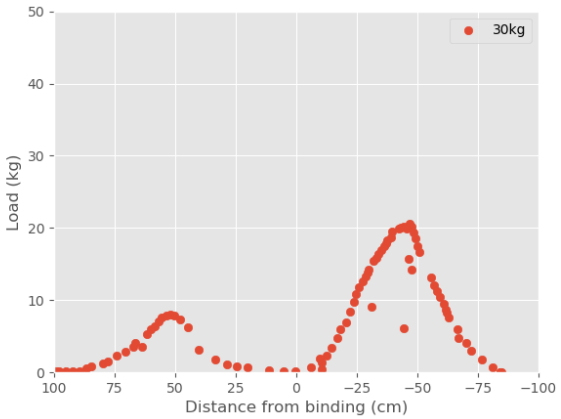

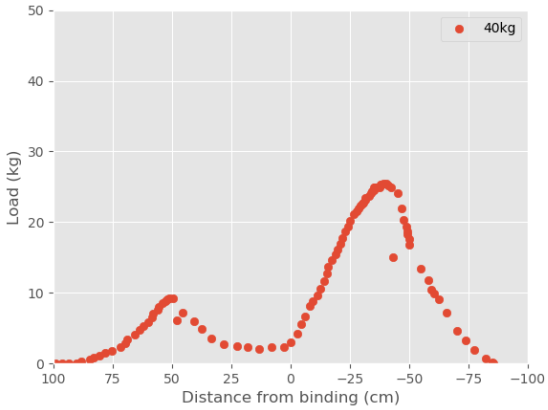

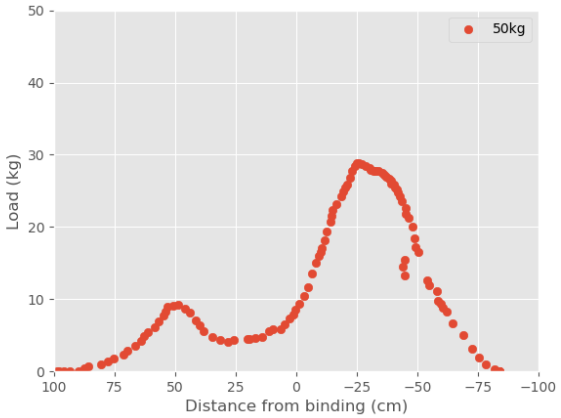

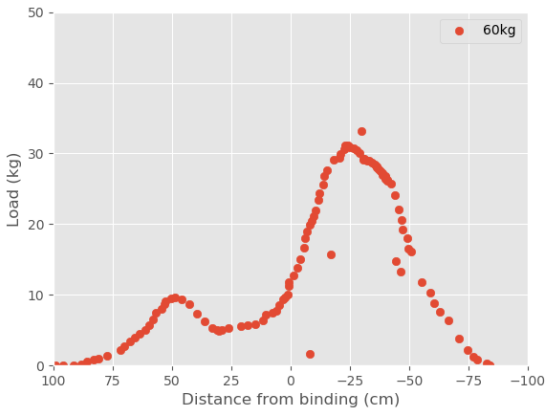

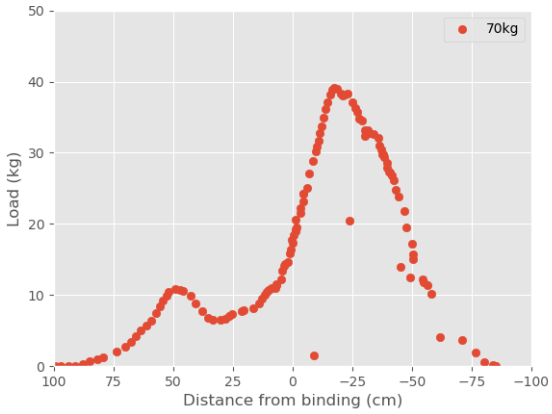

C.6.2 Skate Ski

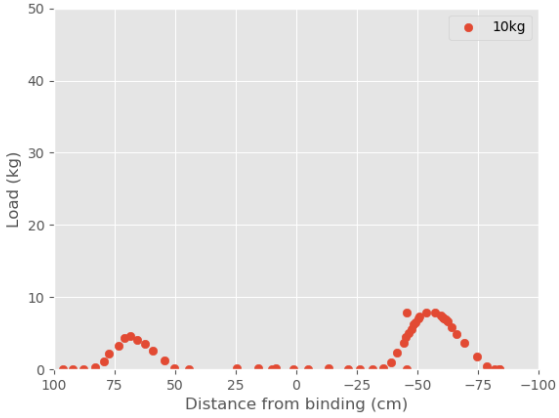

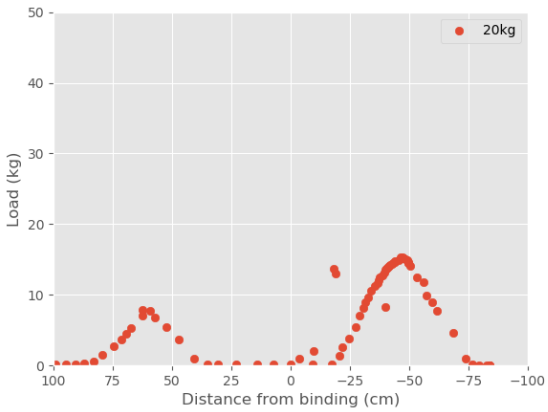

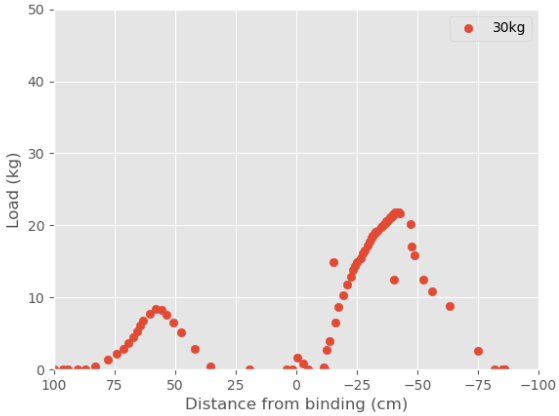

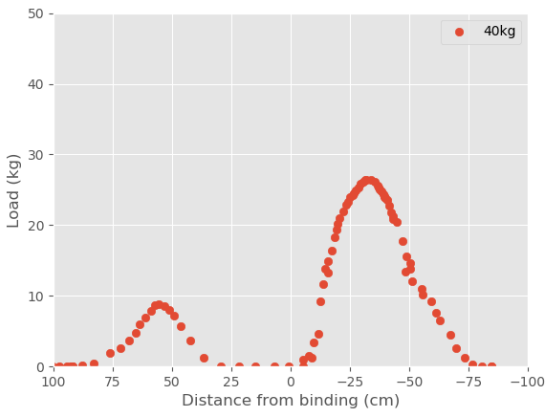

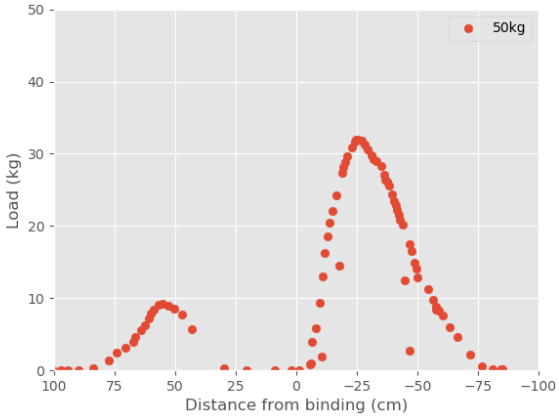

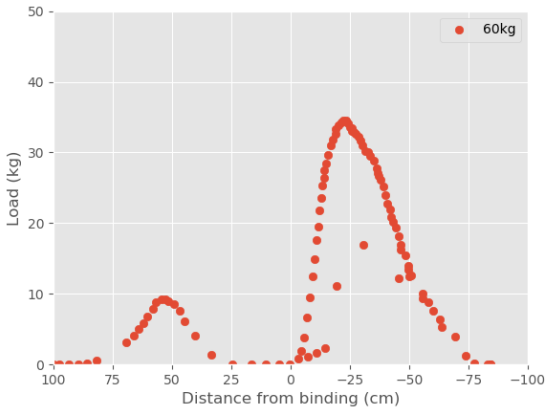

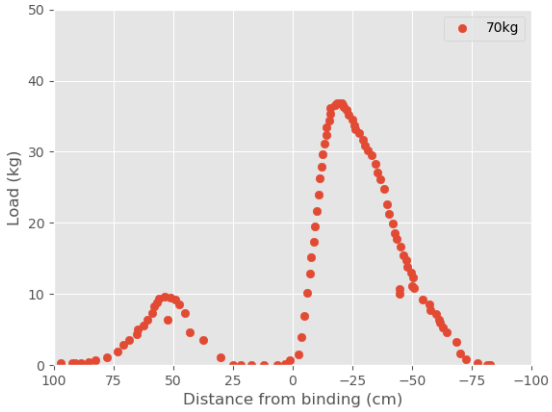

C.7 Spring Setup with Load Location 8cm Behind Binding

The data below represents the tests performed on the classic ski with the load located 8cm behind the binding compared to 14cm for the majority of the other tests. The lifting height is the same as for Section C.6.

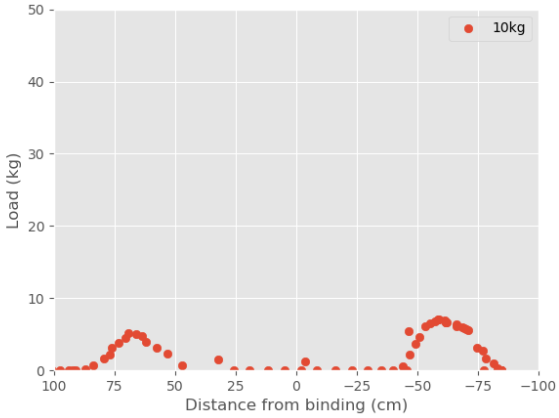

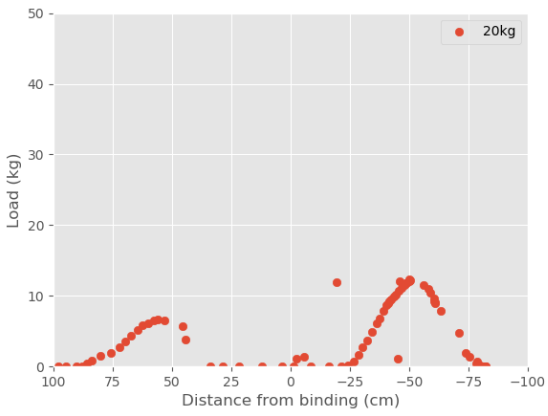

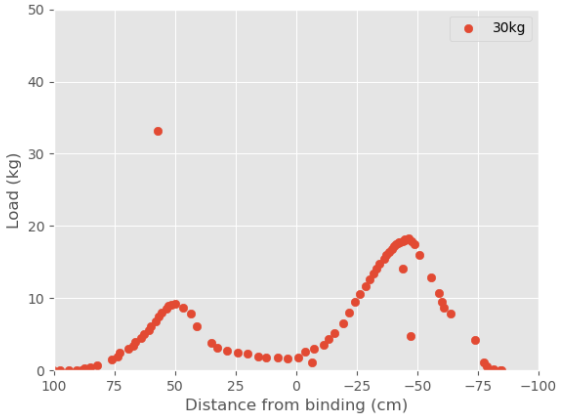
30kg
Load (kg)
Distance from binding (cm)

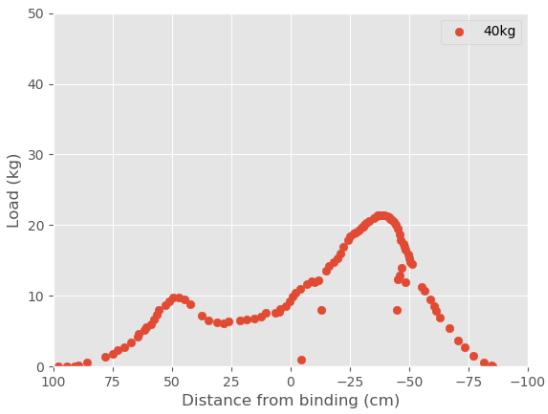
40kg
Load (kg)
Distance from binding (cm)

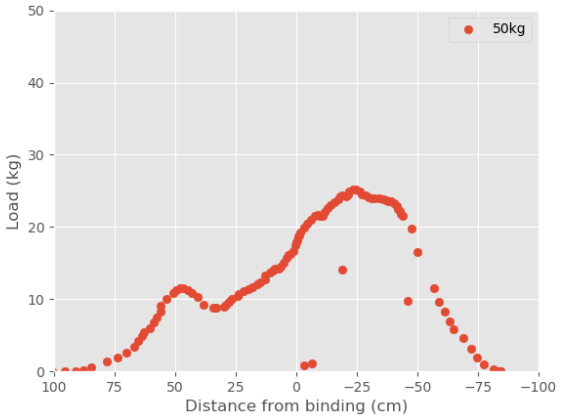
50kg
Load (kg)
Distance from binding (cm)

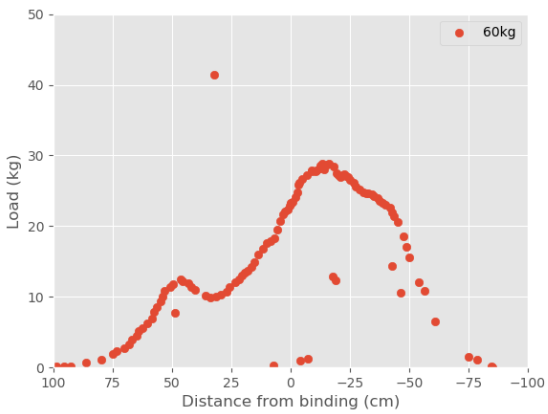
60kg
Load (kg)
Distance from binding (cm)

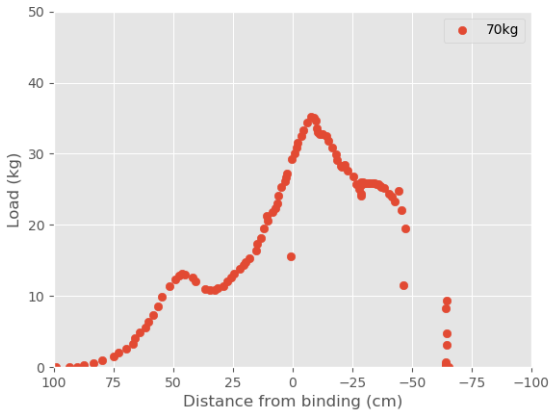
70kg
Load (kg)
Distance from binding (cm)

D | Fritzing

The following represents the wiring of electronics used for the prototype. It is to be noted that one of the load cells represents the S-type load cell.

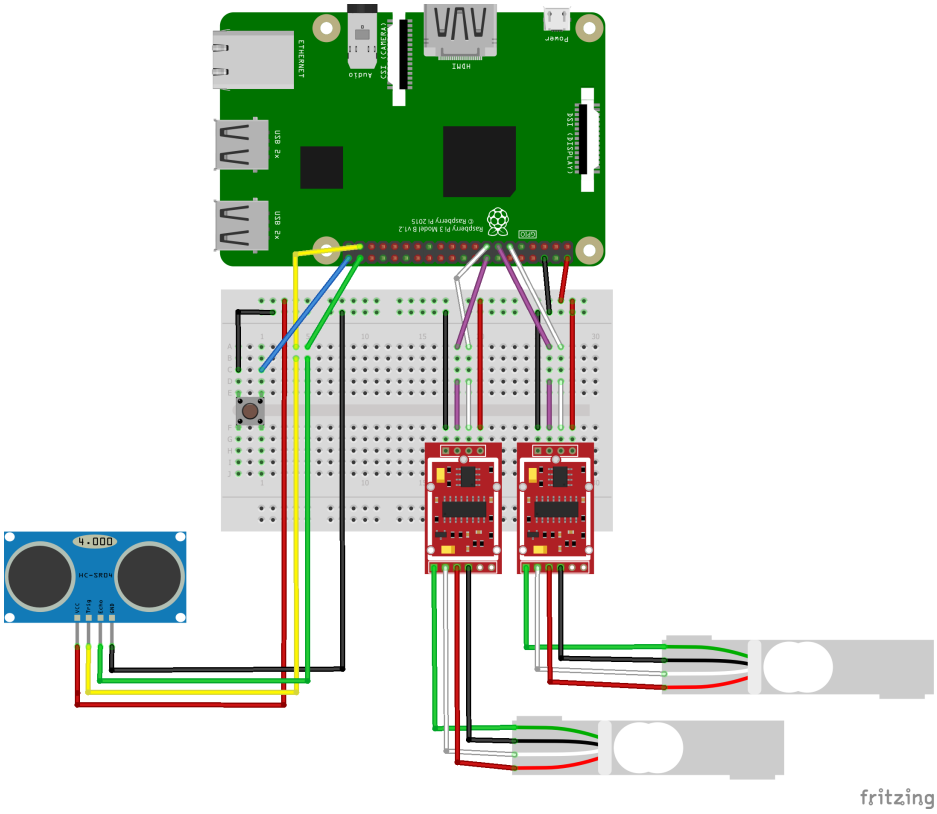

Figure D.1: Wiring schematic

E Test of Sensors

E.1 Distance Sensor

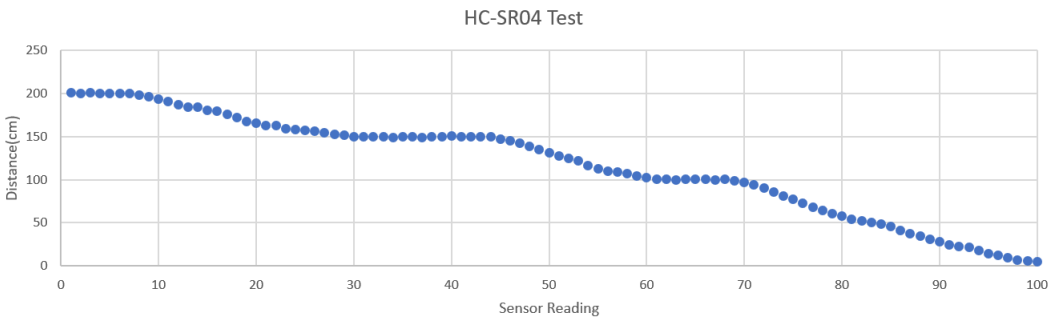

Figure E.1: HC-SR04 distance test

The HC-SR04 sensor was tested by sliding the sensor along a measuring tape close to the wall and holding the sensor in specific positions for about five seconds to see how well the sensor adjusted and to have clear reference points when inspecting the plot. Figure E.1 shows a solid result. When holding the sensor in a specific position, the sensor reading varied in the range of +-0.5cm, which is acceptable.

E.2 Load Cells

Several types of load cells were tested to get a solid grasp on the qualities of the different load cells. The load cells were first calibrated with a calibration load. Thereafter, the load cells were tested with a 5kg and 10kg mass, shown in Figure E.2. To get a better understanding of how the load cells react to a variation in load, the load was removed to see if the output with no load corresponded before and after loading. Looking at the results in Table E.1, all three load cells seem accurate. It is to be noted that calibrating the disc load cell was inaccurate as it was difficult to balance the load on it. This load cell is, therefore, also considered accurate. Looking at the data, it is clear that a small drift is present during all three tests.

Figure E.2: Accurate masses used for testing

Table E.1: Test data

Load cell type	Capacity(kg)	Applied load(kg)	Output(g)	Percent difference
S-type	100	0	-1.1–2.5	-
		5	5001.7-5003.4	0.04
		10	9990.2-9993.2	0.085
		0	-9–11	-
Disc	200	0	7-9	-
		5	5010-5013	0.23
		10	10006-10009	0.075
		0	-20–23	-
Single point	50	0	-20–23	-
		5	4802-4810	3.88
		10	9666-9685	3.25
		0	-33–37	-

F | Concept Images

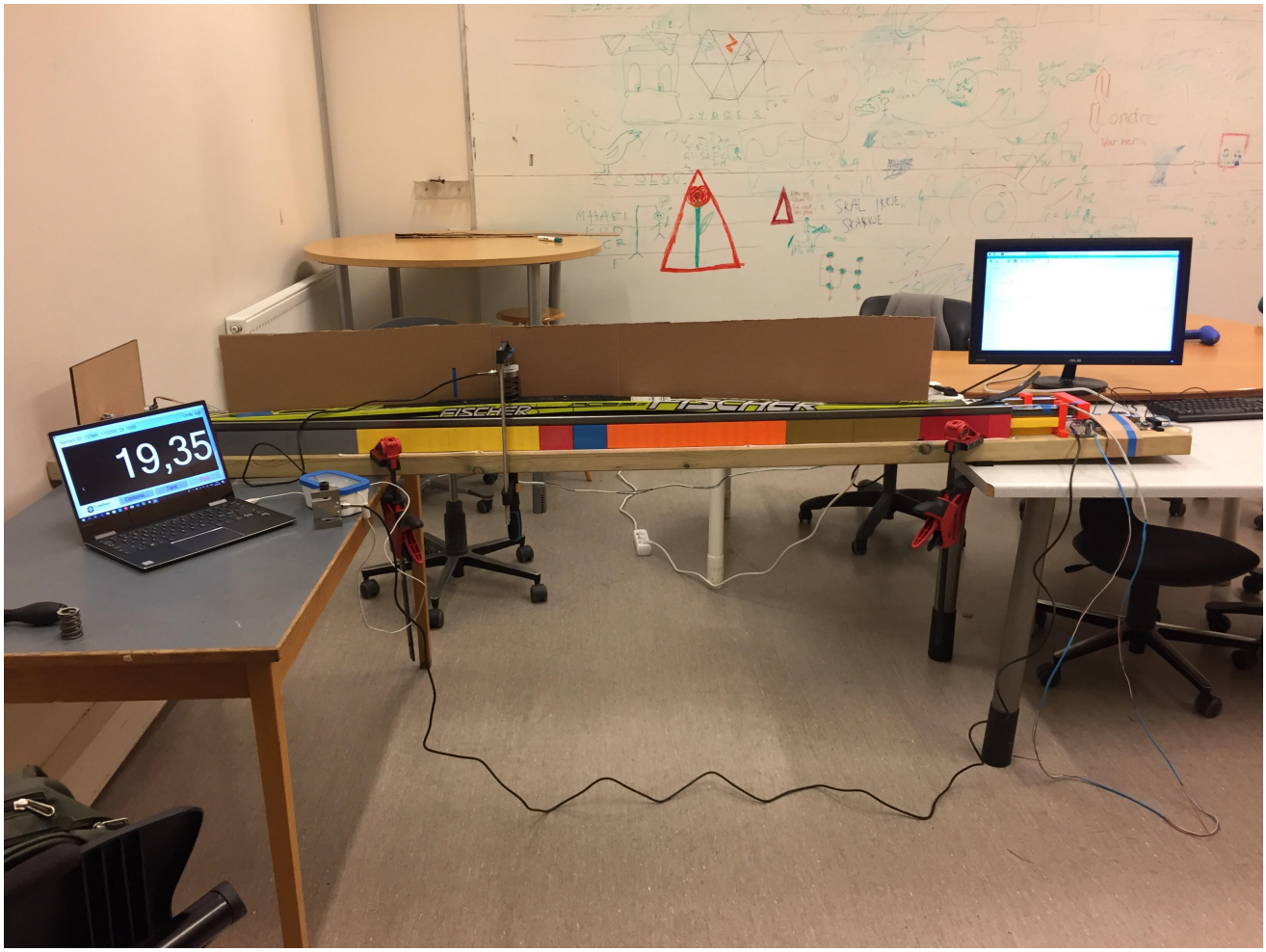

Figure F.1: Side view of the final developed concept with a loaded ski

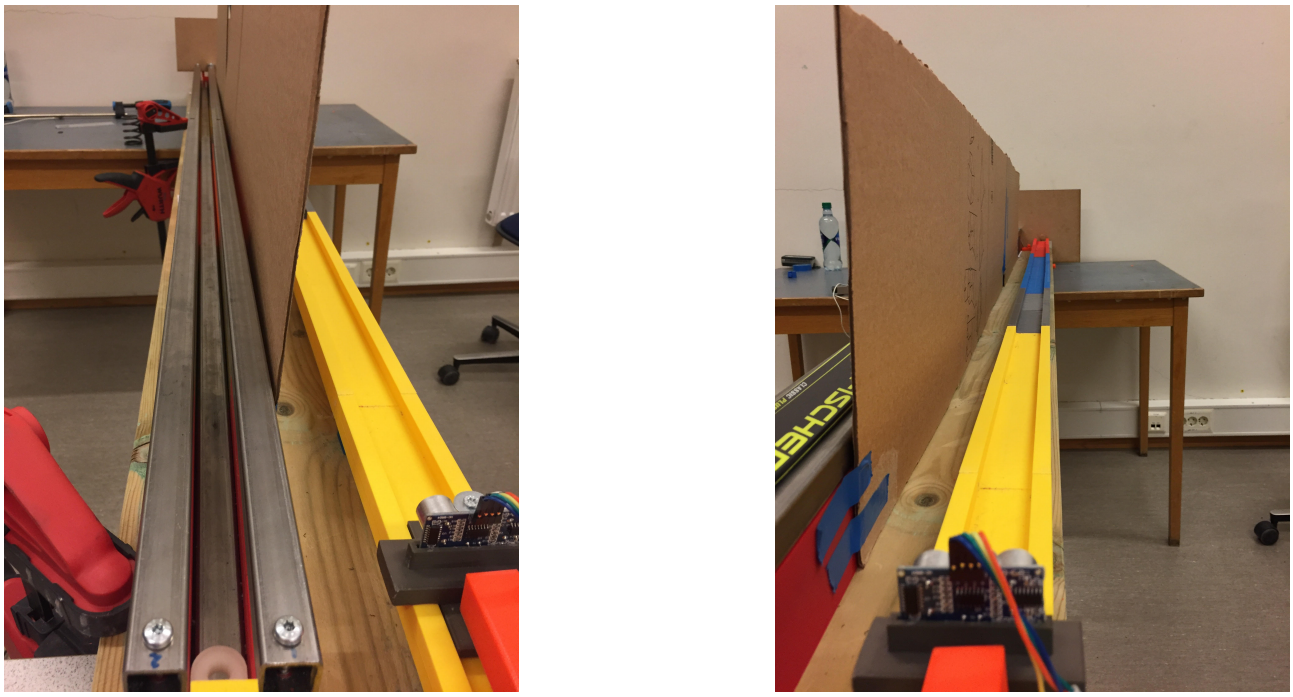

(a) (b)

Figure F.2: Track of sliding load cell (a) and distance sensor (b)

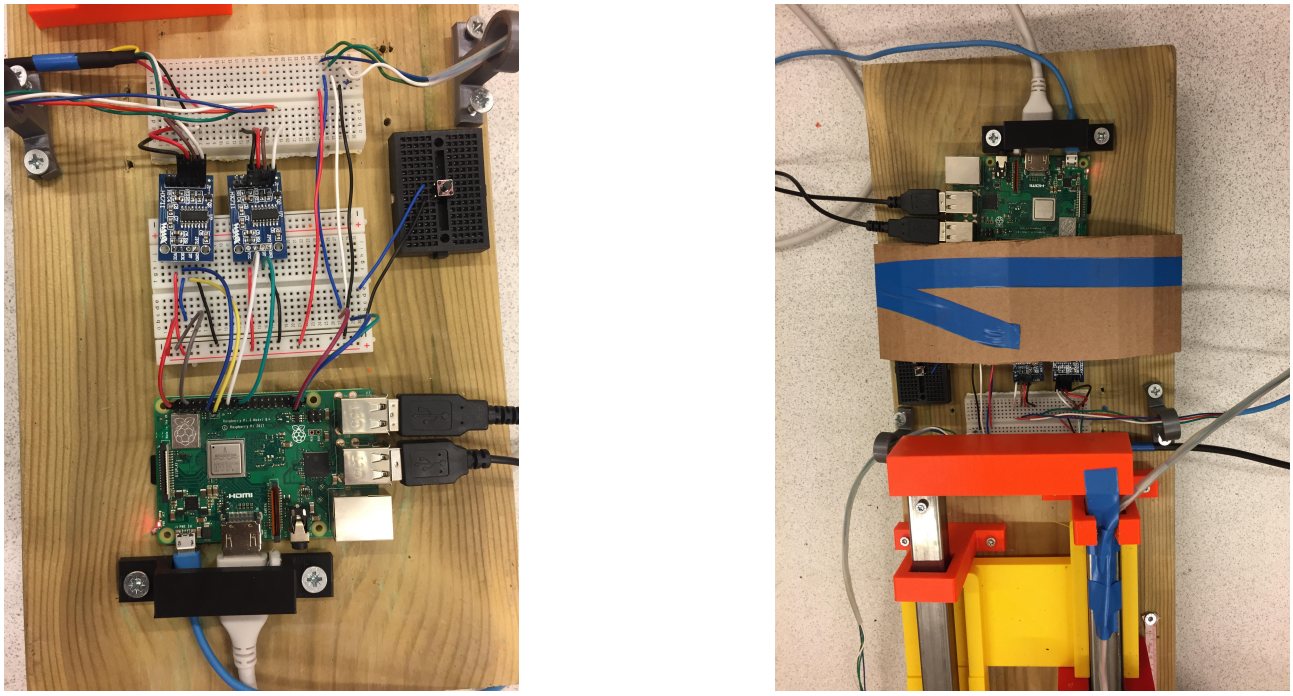

(a) (b)

Figure F.3: Physical wiring (a) and the wiring covered with cardboard (b)

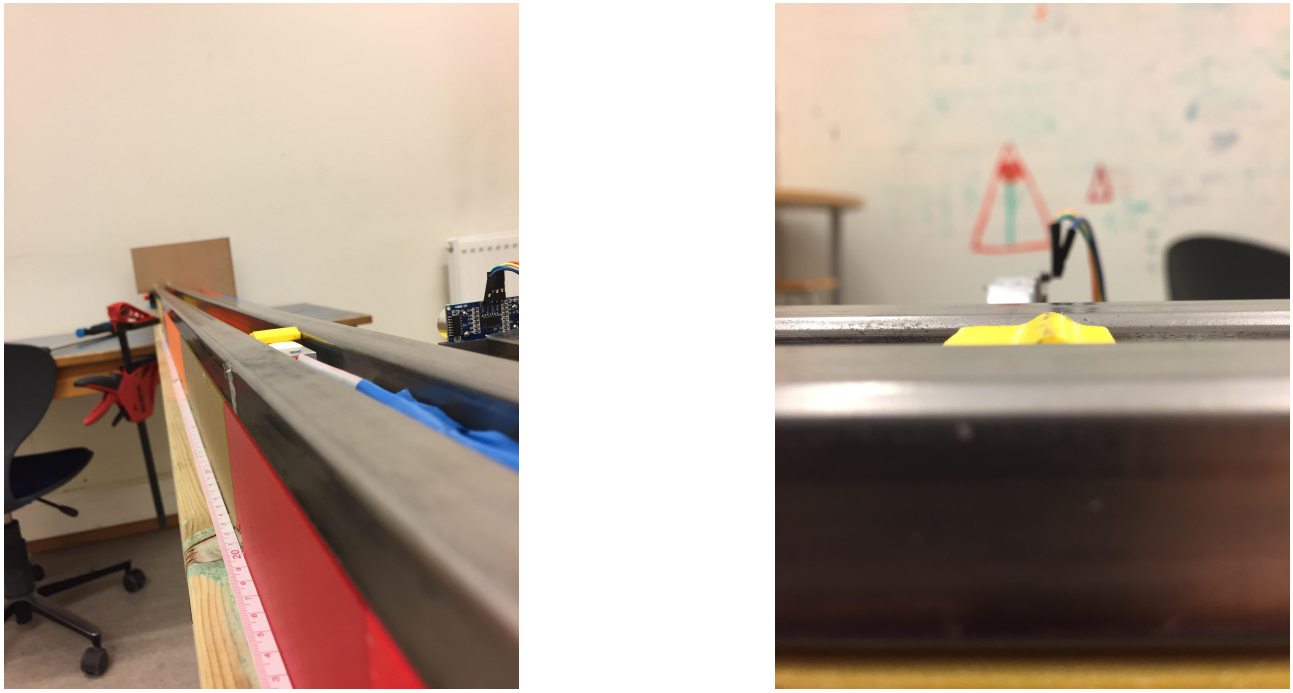

(a) (b)

Figure F.4: Sliding load cell moving along the length of the setup (a) and sideview of the ”lifter” (b)

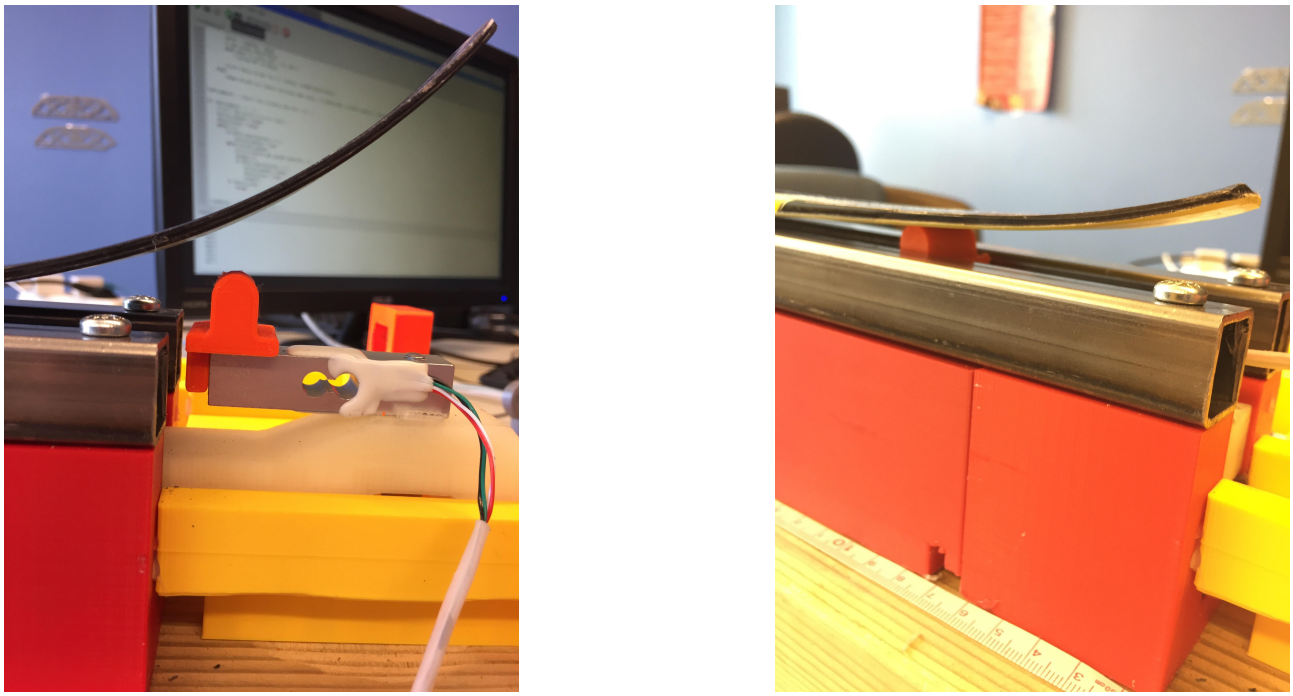

(a) (b)

Figure F.5: 1.5cm lifter used on tip (a) and 1cm lifter used on tail (b)

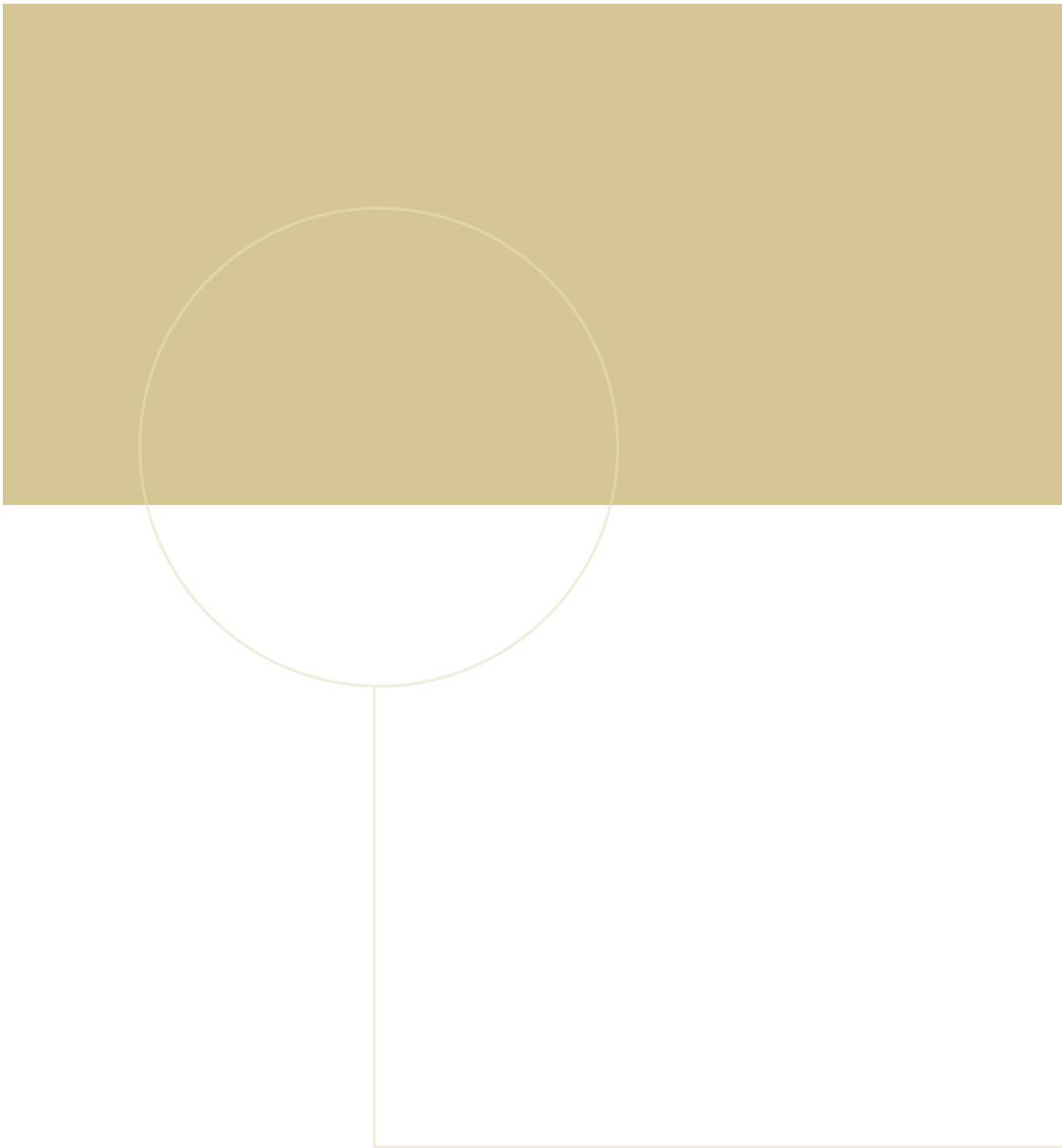

NTNU
Norwegian University of
Science and Technology